UNIVERSITÀ DEGLI STUDI DI MESSINA

Dipartimento di Scienze Chimiche, Biologiche, Farmaceutiche ed Ambientali

DOTTORATO DI RICERCA IN BIOLOGIA APPLICATA E MEDICINA SPERIMENTALE, XXXIV CICLO

Settore scientifico disciplinare: BIO/04

Water content as useful tool for predicting the risk of drought-induced plant mortality

Dottoranda: Elisa Abate

Tutor: Chiar.ma Prof.ssa Patrizia Trifilò

Coordinatore: Chiar.ma Prof.ssa Nunziacarla Spanò

Anno Accademico 2020/2021

Index

Preface

This Thesis provides experimental evidences about the reliability of the relative water content to predict the drought-driven vegetation die-off and die-back.

In the Introduction, I briefly discussed on the effects of global climate changes on plant fitness and survival, focusing on unresolved questions for identifying reliable indicator of plant mortality, a key issue to perform reliable plant mortality risk models and to realize vegetation monitoring programs.

In a first study, I recorded a significant impact of leaf water content and membrane damages on the impairment as well as on the recovery of the leaf hydraulic conductance, the "bottleneck" of plant water transport system. Moreover, in the measured species (i.e., *P. nigra*), a novel negative feedback mechanism linking leaf shrinkage to the leaf hydraulic conductance has emerged. These findings suggested that water content, but also leaf shrinkage, could be used as early indicator of hydraulic failure, a key indicator of whole plant drought resistance. Therefore, in a second study, I tested this hypothesis performing measurements on two Mediterranean native *Salvia* species. Results recorded in this second study led me to checked the impact of leaf hydraulic failure of the two *Salvia* species on whole plant hydraulic conductance as well as on its ability to recover from drought recovery. Then, I performed a fourth study aimed to check if and which plant organ water content is actually a reliable proxy of plant die-off.

The Conclusions chapter provides a general overview and synthesis on the key findings across these studies.

Introduction

Following the proto-industrialization and, mainly, the second industrial revolution, greenhouse gas emissions have increased and have played a decisive role in current global climate change. In fact, the increase in CO_2 emissions in the atmosphere has been particularly relevant since 1950 (Fig. 1) and has been recognized as the main greenhouse gas leading to current climate change (IPCC 2007, 2013).

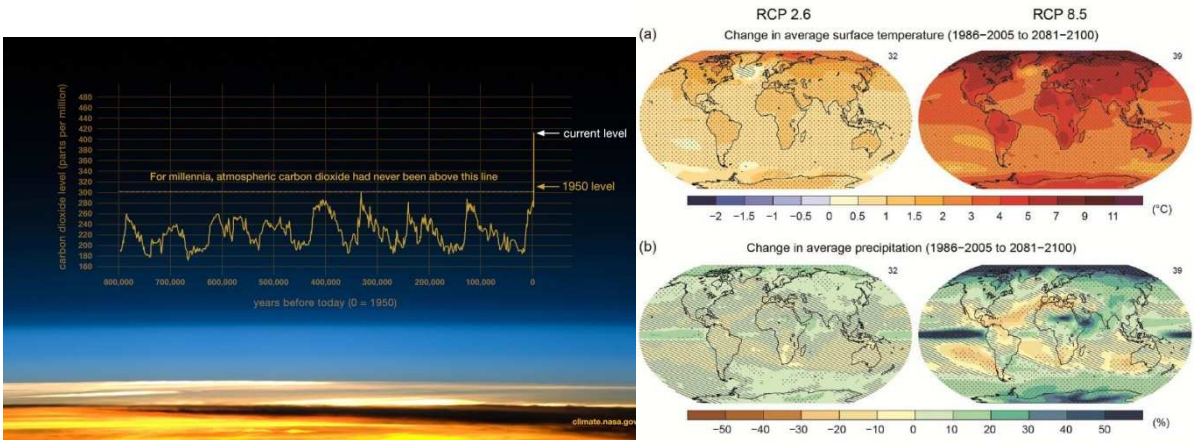

Figure 1: On the left, changes in atmosphere carbon dioxide concentration (Font: https://climate.nasa.gov/). On the right: Climate change projections (Font: IPCC, 2013)

Increase in the average air temperature on continents and oceans on a global scale as well as the consequent widespread melting of snow and ice and raise ocean level are the main impressive (but not the only!) effects attesting the Earth's warming.

As the Earth moves on further warming, increase in frequency and intensity of extreme weather phenomena, including anomalous drought and heat waves events, occurs. This, in turn, is leading to drought-driven plants die-off in different biomes, including the Mediterranean (e.g., Allen et al., 2010; Dai 2013; Adams et al., 2017; Nardini et al., 2017). Rising temperatures and CO_2 levels and changing precipitation patterns affect crop production too (Parry et al., 2004).

The effects of plant mortality are dramatic from an ecological as well as an economic point of view (Anderegg et al., 2013; Meisner et al., 2013; Ma et al., 2012; Reichstein et al., 2013). In fact, considering the roles of forests on global carbon and water cycles, tree mortality may have profound consequences on natural ecosystems and on crops, and are also expected to produce feedbacks to climate change (i.e., Anderegg et al., 2013; Pokhel et al., 2021).

Therefore, it is very urgent not only improving our lacking knowledge on drought-driven plant die-back but also identifying reliable indicators for monitoring the plant fitness and predicting plant mortality risk in order to mitigate the negative effects of drought on forests and crops.

Despite the increasing number of studies on the physiology of plant responses to drought, the mechanisms leading to tree decline and, then, death under prolonged and/or intense water shortage are quite incomplete (Hartmann et al., 2018; McDowell et al., 2019).

As a result of low availability of water in the soil and/or high transpiration rate, plant cells and tissues lose their full turgor (i.e., Bartlett et al., 2012). Thus, in response to water stress and/or increase in temperature, plants commonly reduce gas exchange by stomatal closure in order to limit further water loss (i.e., Bartlett et al., 2016; Rodriguez-Dominiguez et al., 2016; Martin-StPaul et al., 2017). Not at last, rising temperatures leads to exponential increases in vapor pressure deficit (VPD). Different experimental evidences suggests that stomatal conductance decreases under elevated VPD and transpiration increases up to species- specific VPD threshold, leading to a cascade of subsequent negative effects, including carbon assimilation blockage (Gossiord et al., 2020).

Nevertheless, even after stomatal closure, plant water potential continues to decrease because water loss through leaf cuticles, bark and leaky stomata occurs (Cochard, 2019). As a consequence, even in species showing a robust stomatal control for limiting water loss, increase in xylem water potential tension is recorded (Martines-Vilalta and Garcia-Forner, 2016; Albuquerque et al., 2020). When xylem tension exceeds a critical threshold, xylem embolism spreads, on the basis of the air-seeding hypothesis (i.e., Venturas et al., 2017; Nardini et al., 2018). This leads to prevents water transport through the embolized elements, thus reducing plant water transport. Embolism propagation to increasing number of conduits causes the complete blockage of the long-distance water transport system. This dramatic physiological condition is named plant hydraulic failure (McDowell et al., 2008; Brodribb and Cochard, 2009; Choat 2013) and is considered the trigger of plant die-back (Choat et al., 2018).

On the other hand, the drought-driven stomatal closure forces diffusional limitations to CO_2, thus affecting carbon assimilation (Flexas et al., 2006). At severe water stress, metabolic impairment of photosynthesis also occurs likely caused by secondary oxidative stress (i.e., Kaur and Asthir, 2017).

As a consequence, during prolonged drought events, the blockage of carbon assimilation leads to the consumption of stored non-structural carbohydrates (NSC) for maintaining the metabolism. In fact, NSC compounds have a key role in the plant metabolism both for the catabolism as well as

for the anabolism (Hartmann and Trumbore, 2016). However, they play a key role also in the water transport, in the osmoregulation, in the phloem functioning (Tomasella et al., 2020). So, when the storage of NSC decreases below a critical level and photosynthetic carbon gain is inhibited, plant can die for carbon starvation (McDowell et al., 2011).

Not least, global warming leads to the extension of the growing season and acceleration insect cycle life as well as it favors fungi and virus spread. Plants are less able to cope with biotic stress during and/or after drought events. In fact, the drought-driven blockage in carbon gain affects plant ability to synthesize defense compounds too. Furthermore, pests attack frequently damage the water transport system. Overall, this can contribute and/or accelerate the drought driven plant mortality (Griffin-Nolan et al., 2021).

In summary, three main mechanisms driving tree death during drought have been identified: hydraulic failure, carbon starvation and biotic stress (McDowell et al., 2008). An increasing number of studies demonstrated that they are linked each to the other. However, plant water transport impairment is considered the primary pathway for plant mortality during drought events.

Tools for predicting the risk of mortality: what we know?

On the basis of the relevance of hydraulic failure on drought-driven tree mortality, in the last 20 years, great attention has been given to xylem hydraulics (McDowell et al., 2019). By a global analysis on more than 300 species, Choat et al. (2012) have shown that all woody plants converge toward a risky hydraulic behaviour. As a consequence, monitoring loss of xylem hydraulic conductance (K_{xylem}) may be not sufficient to predict the tree die-back and die-off because the loss of K_{xylem} and the knowledge of xylem embolism vulnerability don't determine always robust indicators of drought tolerance in itself (Hammond et al., 2019). Not least : *a*) estimating loss of xylem hydraulic conductivity is very time-expensive and implicates high personnel and plant material costs and *b*) many questions on plant hydraulics remain unresolved, including methodologically doubts for estimating species-specific xylem embolism vulnerability and/or plant ability to recover from drought (Klein et al., 2018; McDowell et al., 2019, Cardoso et al., 2020). Moreover, commonly, the loss of hydraulic conductivity is estimated at stem level as proxy of whole hydraulic pathway (i.e., Choat et al., 2018). By contrast, it is widely recognized that leaf represents a major bottleneck of the soil-plant-atmosphere continuum (Sack and Holbrook, 2006). Significant correlations between leaf hydraulic vulnerability and mean annual precipitation across diverse species' assemblages (Blackman et al., 2014; Nardini and Luglio, 2014) suggest that leaf hydraulic safety plays a critical role in drought tolerance (Fang et al., 2020). In fact, numerous experimental evidences show a tight relationship between leaf water transport efficiency and plant

productivity (i.e., Boer et al., 2016; Brodribb et al., 2005; Scoffoniet al., 2016; Xiong and Nadal, 2020). In other words, leaf hydraulic conductance (K_L) is a major driver of plant hydraulics (Brodribb and Holbrook, 2004; Brodribb et al., 2005; Hochberg et al., 2017; Skelton et al., 2017; Scoffoni et al., 2016; Wang et al., 2018; Xiong and Nadal, 2020). Therefore, monitoring leaf hydraulic decline and/or leaf hydraulics traits may be useful for checking whole plant fitness. At this regard, some studies have documented higher shrinkage before the turgor loss point for species with higher K_L vulnerability (Scoffoni et al., 2014; Trifilò et al., 2016). These results suggests that cell shrinkage might drive the K_L decline during mild dehydration by affecting the extra-xylem water transport pathway. On this view, leaf shrinkage may be used as early indicator of leaf hydraulic failure.

Recently, Martinez-Vilalta et al., (2019) suggested the use of the relative water content (RWC) as reliable indicator of mortality risk (Fig. 2).

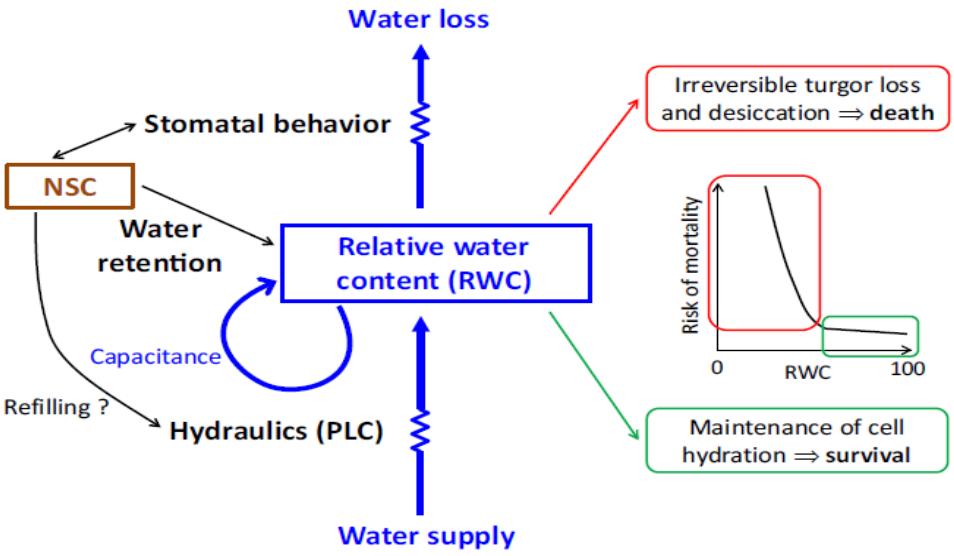

Figure 2: Diagram showing relations between RWC and drought driven plant die-off (Font: Martinez-Vilalta et al., 2019).

In response to water stress, as above discussed, plants adjust their water balance (i.e., water loss/water uptake) by modulating the stomatal opening in order to avoid the risk that high transpiration rates overtake the species-specific sustainable threshold. This physiological response, at short term, permits to maintain RWC value high as a possible (i.e., Lo Gullo et al., 2003; Serrano and Penuelas, 2005). However, similarly to above discussed water potential trend, under chronic drought events, plants dehydration is unavoidable. When relative water content decreases below a specific threshold, plants suffer serious damages that can lead to death (Sapes et al., 2019; Sapes and Sala, 2021). In accordance, John et al. (2018) reported that the leaf RWC threshold

leading to 10% loss of cell rehydration capacity (PLRC) decreases with increasing aridity experienced during the growing season. This result indicates an adaptative role of leaf rehydration capacity for coping with drought. PLRC has been used for decades as a metric of leaf dehydration tolerance. Thus, literature data suggests that also this parameter may be taken into account to monitor plant mortality risk. On the other hand, loss of cell rehydration ability, as a consequence of water shortage, can be affected by leaf cell membrane damages that, in turn, may be useful tool for predicting plant die-off too.

Despite the efforts and increasing studies, nowadays, a reliable and easy-to-measure indicator of mortality risk is still lacking and the gaps in our knowledge lead to shortcoming of tree mortality predictive models (Powell et al., 2013; Fisher et al., 2018; Hood et al., 2018; Schwantes et al., 2018).

Aim of the Thesis

Due to the dramatic effects of current climate change on vegetation survival at global scale, finding mortality risk predictor(s) is fundamental for monitoring plant health and, when needed and possible, performing adequate management actions. In the present Thesis I checked different tools for monitoring the plant die-back and die-off in response to drought.

In detail, on the basis of above discussed *i*) relevance of leaf hydraulic impairment on whole plant hydraulics, *ii*) links between the relative water content and the two main physiological mechanisms leading to plant death (i.e., hydraulic failure and carbon starvation) as well as *iii*) the nexus between leaf hydraulic decline, leaf shrinkage and cell loss of rehydration capability, I performed four different studies aimed to estimate the impact of these parameters on plant die-back in response to drought.

In a first study, I analyzed the dynamic responses of leaf hydraulics in *Populus nigra* L. by measuring leaf hydraulic conductance and the relative contribution of vascular and extra-vascular water pathways to K_L changes under drought and upon recovery. Measurements were done at low and high irradiance taking into account the impact of the relative water content, leaf membrane damages and leaf shrinkage on drought-driven leaf hydraulic conductance decline as well as on its recovery in response to irradiance. Data highlighted the relevance of coordination between water and light availability in modulating the overall K_L response to environmental conditions. Moreover, promising results on the use of the RWC as well as of the cells membrane damage and leaf shrinkage for monitoring the dynamic modulation of K_L (and then plant hydraulic conductance) in response to evaporative water loss and light availability have been recorded.

Thus, a second study aimed to evaluate the predictive power of leaf water content, leaf shrinkage and drought driven leaf damages in two Mediterranean native *Salvia* species has been performed. Results showed that, in the two measured species, not the RWC but the absolute leaf water content and the leaf water potential are reliable parameters for predicting the risk of leaf hydraulic impairment. By contrast, leaf shrinkage showed a poor indicator of dehydration-induced damage when species with succulence syndrome are considered. On the basis of these findings, in a third study, the impact of leaf hydraulic impairment of the two moderate succulent *Salvia* species on the whole plant drought vulnerability was estimated. In this study, I checked possible relations between leaf, stem and root drought-driven water content and/or loss in cell rehydration ability and plant hydraulics. Leaf, stem and root RWC, but also PLRC and REL values were related to loss in plant hydraulic conductance (K_{plant}) in the two *Salvia* species. However, higher correlation values and narrower confidence intervals were recorded in the root. Then, a fourth study aimed to understand if and which plant organ water content (and related parameters) actually can be used to assess mortality risk has been performed on three different species (i.e., *Helianthus annuus* L., *Populus nigra* L. and *Quercus ilex* L.).

Chapter 1

Study 1

The extra-vascular water pathway regulates dynamic leaf hydraulic decline and recovery in *Populus nigra*

Published as: **Trifilò P., Petruzzellis F., Abate E., Nardini A., 2021**. The extra-vascular water pathway regulates dynamic leaf hydraulic decline and recovery in *Populus nigra*. ***Physiologia Plantarum*** 172, 29-40

1. Introduction

Leaf hydraulic conductance (K_L) quantifies the efficiency of water transport at leaf level. K_L is a highly dynamic physiological trait responding to environmental (i.e., light, water availability, temperature, biotic stress) as well as internal (i.e., leaf age, hormones) factors (Trifilò et al., 2003; Sack and Holbrook, 2006; Scoffoni et al., 2008, 2012). This variability allows plants to optimize water supply to mesophyll cells, stomatal aperture and CO_2 uptake under fluctuating conditions (Sack and Holbrook, 2006; Brodribb et al., 2007; Scoffoni et al., 2016). In fact, in terrestrial plants carbon gain is unavoidably coupled to water vapor loss (Brodribb et al., 2016), because CO_2 and H_2O share the same diffusive pathway through stomata. Hence, adequate delivery of liquid water to the transpiring tissues is crucial to maintain hydration and prevent stomatal closure (Tyree and Zimmermann, 2002). Large experimental evidences support the tight relationship between leaf water transport efficiency and plant photosynthetic productivity (i.e., Brodribb et al., 2005; De Boer et al., 2016; Scoffoni et al., 2016: Xiong and Nadal, 2020). This relation is further enhanced by the fact that the leaf hydraulic system presents a major bottleneck of the soil-plant-atmosphere continuum (Sack and Holbrook, 2006).

Water is transported in the leaf through a complex system. Water reaches the leaf lamina mainly via the xylem (or vascular) pathway in the petiole. Then, it flows through the leaf following the vein xylem down to high order veins. From here on, water must cross the bundle sheath and enter in an extra-vascular pathway to reach the evaporation sites. The extra-vascular component, in turn, is composed by different parallel pathways i.e., apoplastic (through the continuum of cell walls), transmembrane (through plasmalemma and tonoplast of sequential cell rows), and symplastic (through plasmodesmata connecting neighbouring cells). Vein architecture and anatomical features of parenchyma can affect both xylem (K_x) and extra-xylem (K_{ox}) hydraulic conductance (i.e., Sack and Frole, 2006; Sack and Scoffoni, 2013; Ohtsuka et al., 2018). Moreover, axial and radial leaf water pathways can operate independently and with similar efficiency (Salleo et al., 2003). For these reasons, dynamic changes of K_L can be caused by different, and not necessarily independent, modifications in one or more components of the leaf water transport system (Nardini and Luglio, 2014; Buckely, 2015; Bartelett et al., 2016; Scoffoni et al., 2017b).

To date, great attention has been paid to the role of leaf xylem embolism as a major factor inducing K_L decline under drought (Nardini et al., 2001, 2003; Brodribb et al., 2007; Scoffoni et al., 2011; Johnson et al., 2012). However, recent studies have proposed that embolism in the vein xylem occurs only at very negative water potential, and in any case well below values inducing stomatal closure (Skelton et al., 2018; Creek et al., 2020). Consistently, some studies have

concluded that drought-induced decline of K_L might be caused by the impairment of the extra-xylem pathway, rather than by xylem embolism (Charra-Vaskou et al., 2012;Scoffoni et al., 2014; Trifilò et al., 2016; Scoffoni et al., 2017a, 2018). These findings suggest that K_{ox} vulnerability might act as a protective mechanism leading to stomatal closure and preventing the drop of water potential to values that might lead to embolism and catastrophic xylem failure (Trifilò et al., 2016; Scoffoni et al., 2017a). A role for K_{ox} in the decline of K_L under drought might also help plants to recover leaf hydraulic capacity more promptly upon rehydration, compared to more costly and uncertain processes of embolism reversal (Trifilò et al., 2003; Johnson et al., 2018).

Besides water availability, irradiance is another major factor influencing both K_L and aperture (Voicu et al., 2008; Blackmann et al., 2009; Nardini et al., 2010, 2012; Scoffoni et al., 2012; Xiong et al., 2018). Previous studies have reported an increase in K_L under high irradiance compared to dark conditions, although not all species respond to light with similar magnitude (Sack et al., 2002; Lo Gullo et al., 2003; Nardini et al., 2005; Tyree et al., 2005; Scoffoni et al., 2008; Sellin et al., 2011; Voicu and Zwiazet, 2011; Guyot et al., 2012; Ohtsuga et al., 2018; Xiong et al., 2018). Light-driven K_L enhancement may help plants to compensate increasing evaporative water loss, thus allowing to maintain gas exchange while avoiding water potential drop and xylem embolism (Cochard et al., 2007; Guyot et al., 2012). K_L response to irradiance is likely caused by modifications in the extra-xylem water pathway, and specifically by up-regulation of aquaporins at the transcriptional or post-translational level. In fact, light-dependent changes of K_L are coupled to changes in transcript abundance of different aquaporin genes (Cochard et al., 2007; Baaziz et al., 2012; Lopez et al., 2013; Minussi et al., 2015; Maurel and Prado, 2017). Also, aquaporins phosphorylation, a key mechanism for water channels regulation, has been reported to occur on daily scale parallel to circadian oscillations of K_L (Prado et al., 2019).

On the basis of the above, K_L emerges as a dynamic trait, that can be modulated in response to evaporative water loss and light availability. Nevertheless, the relative roles of K_x and K_{ox} in mediating K_L decline and recovery under drought, and how these changes are eventually modulated by irradiance, are still poorly investigated. Guyot et al. (2012) reported that light-driven K_L enhancement induced a shift in leaf hydraulic vulnerability to dehydration in 4 different species. However, more recently, Scoffoni et al. (2018) have reported no effects of irradiance on K_L vulnerability to drought in *Arabidopsis thaliana*, even though K_L was responsive to irradiance in well-watered plants. In the present study, we investigated the contribution of the xylem (K_x) and extra-xylem (K_{ox}) water pathways to K_L changes in response to water potential decline, as

well as in the leaf hydraulic recovery in response to re-irrigation. We also quantified how irradiance modifies the trajectories of leaf hydraulic decline and recovery.

1.2. Material and Methods

1.2.1.Plant material and growth conditions

Experiments were performed between May and July 2018 on *Populus nigra* L. plants. In particular, measurements of K_L vulnerability to xylem embolism (see below) were performed on samples collected from five 20-year-old trees growing in the campus of the University of Messina. During the experimental period, trees received only natural precipitation (cumulative rainfall =213 mm). The mean temperature and relative humidity were 23.2 ± 2.8°C and 79 ± 0.8%, respectively (weather station of Torre Faro, Messina, Italy).

Measurements of K_L decline and recovery under drought and re-irrigation were performed on three-year-old saplings provided by a public nursery (Dip. Reg. Azienda Foreste Demaniali, Messina, Sicily, Italy). Plants were grown individually in 4L pots, and regularly irrigated at field capacity until the beginning of the experiment. At the end of April, plants were moved in a greenhouse of the University of Messina (Italy). Here, during the experimental period, the maximum daily photosynthetic photon flux density (PPFD) provided by natural light was 1035 ± 290 μmol s^{-1} m^{-2}, air temperature ranged from 21 ± 4°C to 31 ± 4°C (night/day) and mean relative humidity was 72 ± 4%.

1.2.2. Morpho-anatomical traits

Morpho-anatomical traits were measured in leaves collected from adult plant. Leaf shrinkage during progressive dehydration (Scoffoni et al., 2014) under contrasting irradiance was measured on at least eight leaves per irradiance level. Shoots were cut under water in the morning, transported to the laboratory with their cut basal end immersed in water, and left rehydrating for 2 h. Fully turgid leaves were collected and immediately measured for their fresh weight (FW), leaf area (A_L), leaf thickness (T_L, estimated by averaging values recorded in the bottom, middle, and top thirds of the leaf with a digital calliper, accuracy ± 0.01 mm) and leaf volume (V, estimated as $T_L \times A_L$).

After full-turgor measurements, samples were fixed by their petiole to a bar opposite a fan used to promote dehydration, and were repeatedly measured for the above parameters at different Ψ_L values until turgor loss point (Ψ_{tlp}, see below). Samples were finally dried in an oven for 3 d at 70°C and the above parameter were measured again. To estimate the value of leaf water potential

at different level of dehydration, 15 leaves (different from those used to measure leaf shrinkage) were collected and randomly placed next to leaves used for shrinkage measurements. Two leaves for each level of dehydration were randomly selected to estimate leaf water potential (Ψ_L) with a pressure chamber (3005 Plant Water Status Console, Soilmoisture Equipment Corp., Goleta, CA, USA).

All measurements were performed in samples kept at laboratory irradiance (PPFD<10 μmol m^2s^1) or illuminated with a PPFD > 1200 μmol m^{-2} s^{-1}as provided by a lamp (Dya, APOLLO LED). Similarly to K_L measurements at high irradiance (see below), a transparent plastic container filled with water was put between the leaf surface and the lamp in order to avoid leaf over-heating.

Leaf mass per unit area (LMA) was calculated as DW/A_L, where DW is the leaf dry weight. Leaf density was calculated as the ratio between LMA and leaf thickness. Leaf dry matter content (LDMC) was calculated as: DW/FW.

1.2.3. Measuring leaf hydraulic conductance in response to dehydration and irradiance

Leaf hydraulic conductance (K_L) at different dehydration levels and under contrasting irradiance was measured by the evaporative flux method (EFM, Sack et al., 2002) on samples collected from adult plants (see above). Shoots were sampled in the early morning and rehydrated for at least 4 h to full turgor. Samples were bench-dehydrated and leaves were sampled at different dehydration levels. K_L measurements were performed at laboratory irradiance (low irradiance, LI, i.e., PPFD<10 μmol m^{-2} s^{-1}) or after 30 min exposure at high irradiance (HI, i.e.,PPFD > 1200 μmol m^{-2} s^{-1}) provided by a lamp (see above). All samples were placed next to a fan to promote water loss. Samples at different dehydration levels were cut under water and immediately connected via a peek tubing to a water source resting on a digital balance. Flow readings were recorded at 30 s intervals. At the end of measurements of the steady-state transpiration flow rate (E), the sample was removed from the tubing and leaf water potential (Ψ_L) was immediately measured. K_L was calculated as E/Ψ_L and further normalized by A_L that was recorded at the end of the experiment. To construct vulnerability curves by the EFM, K_L values were plotted against the lowest water potential (i.e., initial or final Ψ_L) experienced by the leaf. All K_L values were standardized to a temperature of 25°C to account for changes in water viscosity.

1.2.4.Estimating leaf xylem and outside-xylem hydraulic vulnerability curves

The vulnerability of leaf xylem hydraulic conductance (K_x) to dehydration was measured by the vacuum pressure method (VPM) (Nardini et al., 2001). Leaves at different dehydration levels,

collected by the same shoots used for estimating K_L by EFM, were cut under water and immediately connected via their petiole to rigid peek tubing that passed through the rubber seal of a 8.0-l PVC vacuum flask into a beaker containing mineral water (Nardini et al., 2007). The beaker rested on a digital balance. Before inserting the leaf in the vacuum chamber, minor veins (fourth order or higher) were severed with a scalpel (12-15 cuts cm^{-2}) in order to bypass he outside-xylem water pathway (Sack et al., 2004, Nardini and Salleo, 2003; Scoffoni et al., 2017b). Flow readings were recorded at 30 s intervals at pressure values of -60, -40, -20 and 0 kPa (with respect to the atmospheric value), induced in the flask by a vacuum pump. The flow (F) was plotted against the pressure (P) and K_L was calculated from the slope of the F-to-P linear relationship. K_x was then scaled by A_L as recorded at the end of the experiment.

Changes in the hydraulic conductance of the extra-vascular pathway (K_{ox}) in response to dehydration, at both low and high irradiance, were estimated as the reciprocal of the difference between K_L measured by EFM along the water potential range tested for each irradiance, and K_x obtained by VPM, following the equation: $K_{ox} = (K_L^{-1}-K_x^{-1})^{-1}$ (Scoffoni et al., 2017b, 2018).

Scoffoni et al. (2017b) have exhaustively discussed the robustness of the "subtraction" method for estimating K_{ox} changes in response to Ψ_L. In the present study, we applied the same experimental procedure not only to construct the vulnerability curve to dehydration, but also to estimate changes of K_L, K_x and K_{ox} in response to re-watering (see below). There is general consensus that EFM can be considered as the most reliable method to estimate K_L decline in response to dehydration at different irradiance levels, mainly because in this method water flows in the leaf lamina similarly to in vivo transpiration (Sack et al., 2002; Guyot et al., 2012). Moreover, measurement of K_x changes in response to Ψ_L, as obtained by VPM, can be considered as reliable on the basis of previous studies that have validated the method (Sack et al., 2004; Nardini et al., 2005; Scoffoni and Sack, 2015; Trifilò et al., 2016; Scoffoni et al., 2017b). Also, there is an overall agreement between K_x vulnerability to dehydration as obtained by VPM, and direct micro-CT observations of leaf xylem embolism (Scoffoni et al., 2017b, 2018). Furthermore, the P_{50} value of K_x as recorded in *P. nigra* in the present study (about -1.9 MPa) was similar to the value recorded by the optical method in the same species (Petruzzellis et al., 2020) (see Results).

1.2.5.Leaf water potential isotherms

Leaf water potential isotherms (or pressure-volume, PV-curves) were measured to estimate: *i*) the leaf water potential at the turgor loss point, Ψ_{tlp}; *ii*) the osmotic potential at full turgor, π_0; *iii*) the bulk modulus of elasticity, ε_{max}; *iv*) the leaf capacitance at full turgor, C_t. PV curves were

measured on 5 leaf samples collected from 5 different potted plants (see above). Leaves were cut under water and allowed to rehydrate for at least 1h before generating PV curves. Leaf water potential (Ψ_L) and leaf water loss were measured at regular intervals during progressive leaf dehydration. Ψ_{tlp} was estimated as the flex point of the relationship between $1/\Psi_L$ and water loss. Moreover, π_0 was calculated by the y-intercept of the linear region of this relationship, and ε_{max} was calculated as $\Delta Pt/(\Delta W/W)$, where ΔPt is the change of turgor pressure and $\Delta W/W$ is the relative change of the leaf water content. Leaf capacitance was also derived from PV curves on the basis of the slope of the relationship between water loss and Ψ_L before Ψ_{tlp} and normalised by A_L. Samples were finally dried in an oven for 3 d at 70°C to obtain their dry weight.

1.2.6. Hydraulic recovery

To estimate changes of K_L, K_x and K_{ox} of plants experiencing Ψ_L values near Ψ_{tlp} and in response to re-irrigation, additional measurements were performed in potted sapling. We decided to set turgor loss point as a critical threshold, because species-specific wilting point corresponds to severe water stress among different species (Bartlett et al., 2016). In detail, 36 potted plants were divided in two groups. Control samples (C) were regularly irrigated at field capacity until the end of the experiment, while a second group of plants was subjected to drought stress (S samples) by suspending irrigation until leaf water potential close to Ψ_{tlp} was recorded in the early morning (i.e., Time 0). At 7.00 am, after checking water potential value, C and S leaves were collected and measured for K_L at LI and HI by EFM, and for K_x by VPM (see above). Similarly, to the procedure used to construct the extra-xylem vulnerability curve, K_{ox} was estimated on the basis of K_L and K_x values. This experimental procedure allowed us to estimate changes in K_L, K_x and K_{ox} in S samples at LI *versus* HI, and in C *versus* S samples. For each C or S plant, we selected leaves close to each other and likely experiencing similar water stress. Immediately after collecting samples at Time 0, C and S plants were irrigated at field capacity and measured 30 min (i.e., at 7.30 am, Rec 30min), 2h (i.e., at 9:00 am, Rec 2h) and 24 h later (i.e., at 7:00 am of the next day, Rec 24h).

1.2.7. Measuring leaf water content and leaf membrane integrity

Measurements of the relative leaf water content (RWC) and leaf membrane integrity were done on the same plants used for measuring K_L recovery from dehydration, collecting samples close to leaves measured for hydraulic recovery. At least 4 leaves were collected at different times from re-irrigation (i.e., Time 0, Rec 30min, Rec 2h, Rec 24h, see above). Their FW was immediately

recorded and then leaves were rehydrated for 24 h with their petiole immersed in a beaker containing deionized water, to obtain turgid weight (TW). Finally, samples were dried in an oven for 3 d at 70°C to measure dry weight (DW). RWC was calculated as: 100* (FW-DW)/(TW-DW). At least 4 leaves were collected at different times from the re-irrigation and used to perform electrolyte leakage test as a proxy of leaf membrane damage (Savi et al., 2016). Leaf discs of 0.7 cm^2 were cut with a razor blade, carefully avoiding major veins, and inserted in a test tube containing 8mL of distilled water. Samples were stirred for 30 min at room temperature. The initial electrical conductivity of the solution (EC_i) was recorded by a conductivity meter (Cond 5, XS instruments, Italy). Samples was then subjected to three freeze-thaw cycles to induce complete membrane disruption, and then processed as above to measure the final electrical conductivity of the solution (EC_f). The relative electrolyte leakage (REL) was calculated as: (EC_i/EC_f) *100.

1.2.8. Estimating leaf water status and gas exchange in response to re-irrigation

To estimate leaf water potential recovery and eventual changes in gas exchange in response to drought and re-irrigation, measurements were performed in 4 C and 4 S plants. Measurements were done at midday on the day when C and S samples were measured for hydraulic conductance (Time 0), as well as 24 h after re-irrigation (Rec 24h). Gas exchange and Ψ_L were measured on a subset of plants different from that used for hydraulic conductance, RWC and REL measurements, but subjected to the same experimental treatment. This subset of samples was irrigated at field capacity not at 7:00 am (as for plants used for the above described measurements) but at 13:30 am (i.e. after gas exchange and water potential measurements). Leaf conductance to water vapour ($g_{L\ midday}$), photosynthetic rate ($A_{n\ midday}$) and leaf water potential ($\Psi_{L\ midday}$) were measured using a portable LCi Analyzer System (ADC Bioscientific Ltd, Herts, UK) and the pressure chamber, respectively.

1.2.9. Statistical analysis

All statistical analyses were performed with the software R (v. 3.6.1, R Core Team, 2019). Differences in leaf shrinkage parameters (i.e. percentage loss of leaf area of a dry leaf and at turgor loss point, PLA_{dry} and PLA_{tlp}, respectively; percentage loss of leaf thickness of a dry leaf and at turgor loss point, PLT_{dry} and PLT_{tlp}, respectively; percentage loss of leaf volume of a dry leaf and at turgor loss point; PLV_{dry} and PLV_{tlp}, respectively) between samples measured at high (HI) and low irradiance (LI) were tested through Student's *t*-tests (α = 0.05) after checking for normality and homoscedasticity assumptions.

Vulnerability curves, showing the decline of hydraulic conductance with decreasing water potential, were analysed using "fitplc" function (Duursma and Choat, 2017). Specifically, one vulnerability curve was fitted separately for K_L and K_{ox} measured on samples under high (HI) and low (LI) irradiance, and for K_x. Differences in P_{50} and P_{80} values (water potential value inducing 50% or 80% loss of hydraulic conductance, respectively) were considered statistically significant when the 95% confidence intervals did not overlap.

Differences in Ψ_L measured just before the re-watering, $g_{Lmidday}$, $A_{nmidday}$ and $\Psi_{L\ midday}$ between well-watered (C) and water stressed (S) samples at different re-irrigation times were tested separately through two-Anova analysis, using "aov" function. Specifically, Ψ_L measured just before the re-irrigation, $g_{Lmidday}$, $A_{nmidday}$ and $\Psi_{L\ midday}$ were the response variables, while group (C *versus* S) and re-irrigation time (Time 0, Rec 30 min, Rec 2h, Rec 24h) and their interaction where the explanatory variables. For statistically significant tests ($P < 0.05$), Tukey HSD post-hoc comparisons test was performed. Normality and homoscedasticity assumptions were checked before the analysis.

Differences in RWC between well-watered (C) and water stressed (S) samples at different re-irrigation times were tested through a Generalised Least Square (GLS) model using "gls" function in nlme package, because the assumption of homoscedasticity was violated. In detail, in this analysis RWC was the response variable, while group (C *versus* S) and re-irrigation time (Time 0, Rec 30 min, Rec 2h, Rec 24h) and their interaction where the explanatory variables. A constant variance function structure (varIdent type) was specified in the model.

Differences in K_L, K_x, K_{ox} and relative electrolyte leakage (REL) measured in well-watered (C) and water stressed (S) samples at different re-irrigation times were tested separately through two-Anova analysis, following procedures described above. Differences between relative values of K_L, K_x and K_{ox} within water stressed (S) samples at different re-irrigation times were tested separately through one-way Anova analysis. Normality and homoscedasticity assumptions were checked before these analyses.

Spearman's rho (ρ) correlation coefficient among K_L and K_{ox} measured on sample under high (HI) and low (LI) irradiance and K_x, REL, RWC and water potential values were calculated using "rcorr" function. For statistically significant correlations ($P< 0.05$), a simple linear regression model was calculated.

1.3. Results

1.3.1. Water relations parameters

The Ψ_{tlp} of *P. nigra* averaged -2.15 ± 0.09 MPa, while π_0 was -1.80 ± 0.05 MPa and mean value of ε_{max} was about 29 MPa. Leaf shrinkage parameters were similar at LI or HI, except for the percentage loss of leaf thickness and leaf volume at the turgor loss point. In fact, both PLT_{tlp} and PLV_{tlp} were significantly higher at LI *versus* HI (Table 1).

Table 1: Mean values ± SD of: leaf structural traits, leaf shrinkage parameters as measured in samples at high irradiance, HI, *versus* low irradiance, LI and PV traits Different letters indicate statistically significant differences between samples at HI *versus* LI. Number of replicas (*n*) are specified.

Structural traits (n=28)	
A_L (cm^2)	23.07 ± 6.57
T_L (mm)	0.20 ± 0.073
V_L (mm^3)	483.39 ± 195.76
LMA ($g\ m^{-2}$)	74.42 ± 9.22
LDMC ($mg\ g^{-1}$)	305.26 ± 33.07
Leafdensity ($g\ cm^{-3}$)	0.37 ± 0.07
Shrinkage parameters	
PLA_{dry} (%) LI	15.76 ± 1.45 (*n*=16)
PLA_{dry} (%) HI	17.62 ± 2.87 (*n*=12)
PLA_{tlp} (%) LI	1.98 ± 0.84 (*n*=16)
PLA_{tlp} (%) HI	1.81 ± 0.81 (*n*=12)
PLT_{dry} (%) LI	53.54 ± 12.16 (*n*=16)
PLT_{dry} (%) HI	49.43 ± 15.99 (*n*=12)
PLT_{tlp} (%) LI	27.99 ± 8.01**a** (*n*=16)
PLT_{tlp} (%) HI	16.91 ± 7.40**b**(*n*=12)
PLV_{dry} (%) LI	58.92 ± 9.39 (*n*=16)
PLV_{dry} (%) HI	57.56 ± 14.61 (*n*=12)
PLV_{tlp} (%) LI	27.93 ± 7.52**a** (*n*=16)
PLV_{tlp} (%) HI	18.36 ± 7.30**b**(*n*=12)
PV traits (n=5)	
$-\Psi_{tlp}$ (MPa)	2.15 ± 0.09
$-\pi_o$ (MPa)	1.80 ± 0.05
ε_{max} (MPa)	28.56 ± 3.09
C_t($mmol\ m^{-2}MPa^{-1}$)	337.10 ± 46.40

Notes: A_L: leaf area, T_L: leaf thickness and V_L: leaf volume, as measured at full turgor; LMA: leaf mass per area; LDMC: leaf dry matter content; leaf density); PLA_{dry} and PLA_{tlp}: percentage loss of leaf area of a dry leaf and at turgor loss point, respectively; PLT_{dry} and PLT_{tlp}: percentage loss of leaf thickness of a dry leaf and at turgor loss point, respectively; PLV_{dry} and PLV_{tlp}: percentage loss of leaf volume of a dry leaf and at turgor loss point, respectively; Ψ_{tlp}: leaf water potential at turgor loss point; π_o: osmotic potential at full turgor; ε_{max}: bulk modulus of elasticity; C_t: leaf capacitance at full turgor.

1.3.2. *Leaf hydraulic decline in response to dehydration*

P. nigra showed higher K_L vulnerability to dehydration at HI compared to LI (Fig. 1, Table S1). P_{50} was about -1.3MPaat HI and -2.4 MPa at LI. The shift in vulnerability to dehydration at HI *versus* LI was clearly induced by a light-driven shift in maximum K_L, and this in turn was due to modifications occurring in the extra-vascular pathway. Indeed, the xylem water potential inducing 50% loss of K_{ox} was significantly less negative at high irradiance compared to low irradiance (Fig. 1, Table S1). The P_{50} of K_x was about-1.9 MPa, i.e., statistically similar to the water potential inducing 50% loss of K_{ox} at LI, but more negative than P_{50} for K_{ox} at HI (Table S1).

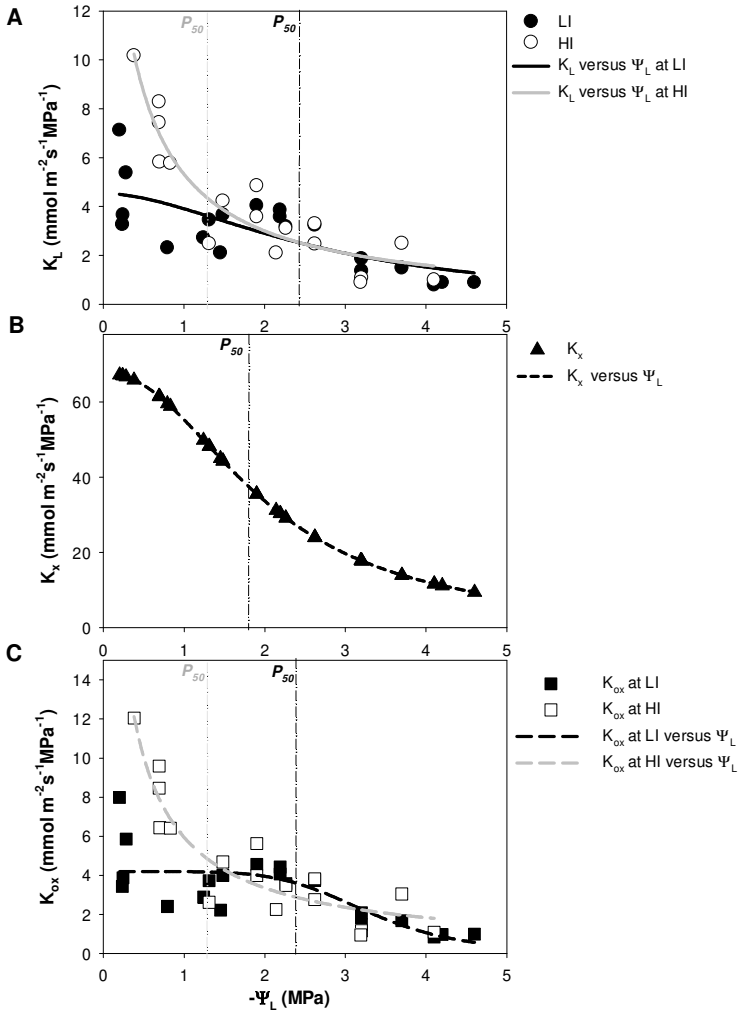

Figure 1: (**A**) Decline of leaf hydraulic conductance (K_L) with decreasing leaf water potential (Ψ_L) as measured in *P. nigra* samples under low (LI) and high (HI) irradiance (black and white circle symbols and black and grey lines, respectively); (**B**) vulnerability of xylem water pathway (K_x, black triangles and short-dashed lines) to dehydration and (**C**) vulnerability of the extra- xylem water pathway (K_{ox}) under low (LI) and high (HI) irradiance (black and white square symbols and black and grey long-dashed lines, respectively). K_{ox} values have been estimated as the reciprocal of the difference between $K_L$values (as obtained by evaporative flux method, along the water potential range tested for each species) and $K_x$values (as obtained by vacuum pump method), following Equation: $K_{ox} = (K_L^{-1} - K_x^{-1})^{-1}$ (Scoffoni et al. 2017b). All curves were fitted to the data with three-parameter logistic functions: $y = a/[1 + (x/x_0)^b]$. Black and grey dash-dotted lines indicate the leaf water potential values inducing 50% (P_{50}) loss of hydraulic conductance at low and high irradiance, respectively.

1.3.3. Leaf hydraulic recovery

Turgor loss (S samples at Time 0) did not affect the ability of *P. nigra* leaves to recover Ψ_L and RWC within 30min after re-irrigation at field capacity (Fig. 2, Table S2).

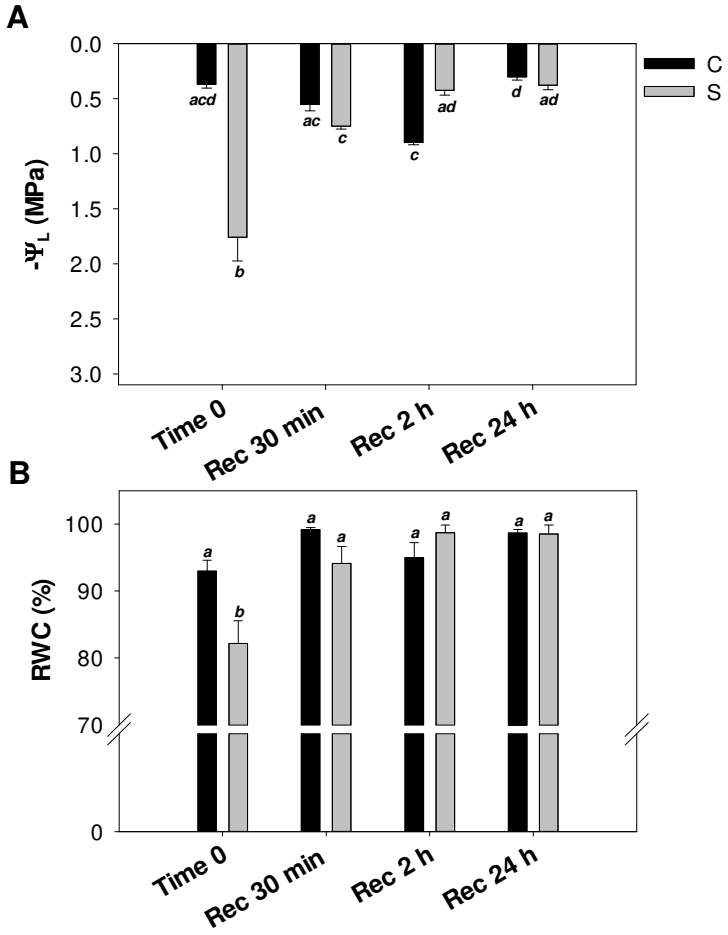

Figure 2: Mean values ± SEM of (**A**) the leaf water potential (Ψ_L) and (**B**) the relative water content (RWC) as measured in well-watered (C, black columns) and water stressed (S, grey columns) plants of *P. nigra*. Samples were measured just before the re-irrigation (i.e., Time 0) as well as 30 min, 2 h and 24 h the re-irrigation (i.e., Rec 30 min, Rec 2h, Rec 24 h, respectively). Different letters indicate statistically significant differences between groups.

In accordance, since Rec 30min, S plants showed Ψ_L and RWC values statistically similar to C samples. Despite the recovery of leaf water status, no recovery in gas exchange was recorded (Fig. 3). At Rec 24h, stomatal conductance and photosynthetic rates in S plants were statistically similar to values recorded, in the same plants, at Time 0 and about 75% lower than values recorded in well-watered plants (Fig. 3, Table S3).

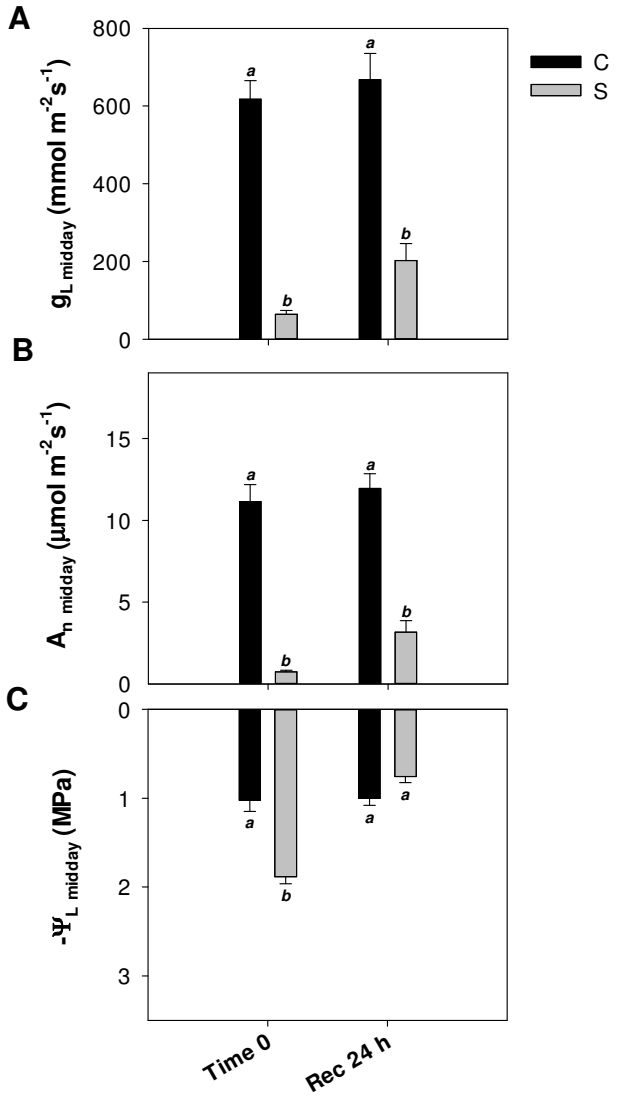

Figure 3: Mean values ± SEM of (**A**) stomatal conductance to water vapour ($g_{L\ midday}$), (**B**) photosynthetic rate ($A_{n\ midday}$) and (**C**) leaf water potential ($\Psi_{L\ midday}$), as recorded in well-watered (C, dark columns) and water stressed (S, grey columns) plants of *P. nigra*. Samples were measured at midday the day in which S samples experiencing, in the morning, values of Ψ_L near the turgor loss point (i.e., Time 0) and 24 h after the re-irrigation (i.e., Rec 24 h). Different letters indicate statistically significant differences between groups.

Well-watered samples showed an increase of K_L and K_{ox} in response to irradiance, but no changes in K_L, K_x and K_{ox} were recorded in response to time of re-irrigation (Table S4). On this basis, the mean values of K_L, K_x and K_{ox}, as recorded in C samples at LI and at HI, was considered as a reference point (i.e., maximum value) and changes of K_L, K_x and K_{ox}, as recorded in S samples, were estimated as relative values (i.e., by dividing each hydraulic conductance value measured in S samples by the mean value of hydraulic conductance as recorded in C leaves, at the same time after re-watering and irradiance treatment).

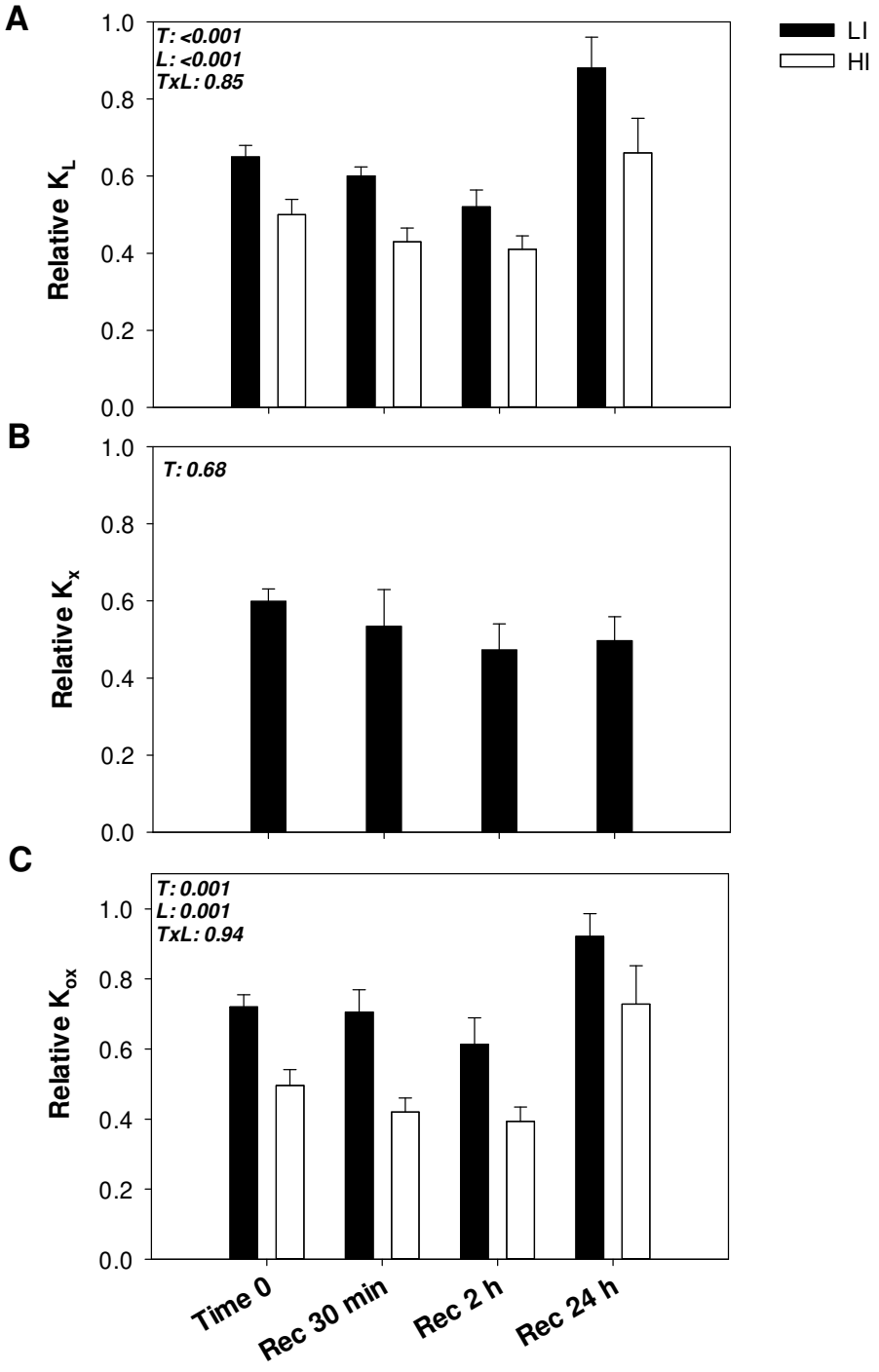

Figure 4: Mean values ± SEM of (**A**) the relative leaf hydraulic conductance (K_L), (**B**) relative xylem hydraulic conductance (K_x) and (**C**) relative extra-xylem hydraulic conductance (K_{ox}) as recorded in water stressed plants at low (LI, black columns) and high (HI, white columns) irradiance respect to value recorded in well-watered samples. Samples were measured just before the re-irrigation (i.e., Time 0) as well as 30 min, 2 h and 24 h the re-irrigation (i.e., Rec 30 min, Rec 2h, Rec 24 h, respectively). *P* values as resulted by two-way Anova of relative K_L and K_{ox} by time after re-irrigation (T, i.e., Time 0, Rec 30min, Rec 2h, Rec 24h) and irradiance (L, i.e., LI: low irradiance, HI: high irradiance) and results of one way Anova of relative K_x are reported.

Water stress significantly affected leaf water transport capacity at HI, and the recorded decrease of K_L in S samples at Time 0 was induced by relevant impairment in the xylem as well as in extra-xylem water pathways (Fig. 4). At Time 0, the relative K_L at LI was about 0.6. However, 24h after re-watering, a significant recovery of K_L was detected at both LI and HI. It can be noted that, despite the recovery, the relative K_L value at HI remained significantly lower than the value recorded at LI (Fig.4, Table S5). The recovery of K_L was paralleled by a recovery of K_{ox}. In accordance, while no recovery in K_x values was recorded in response to re-irrigation, the relative K_{ox} at LI was about 0.7 at Time 0 and significantly increased up to 0.9 at Rec 24h. Similarly, to the relative K_L trend, at Rec 24h the relative K_{ox} values were significantly lower at HI *versus* LI.
Water stress induced a leaf membrane damage of about 20%. This damage was partially repaired only 24h after re-irrigation (Fig. 5, Table S6).

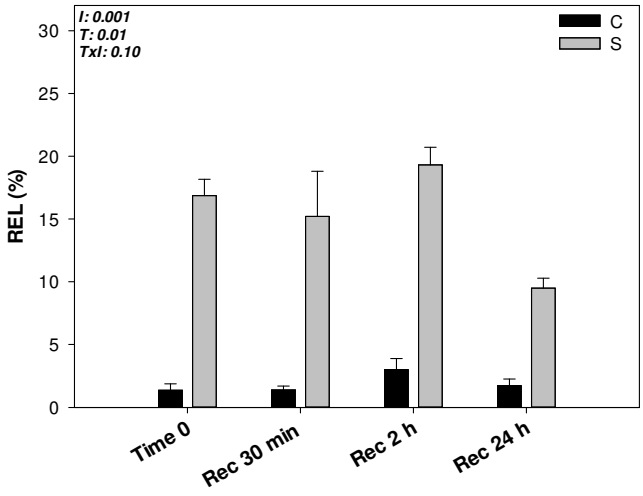

Figure 5: Mean values ± SEM of the relative leaf membrane electrolyte leakage (REL) as recorded in well-watered (C, solid columns) and in water stressed (S, striped columns) plants of *P. nigra*. Samples were collected just before the re-irrigation (i.e., Time 0) as well as 30 min, 2 h and 24 h the re-irrigation (i.e., Rec 30 min, Rec 2h, Rec 24 h, respectively). *P* values as resulted by two way Anova of REL values by irrigation treatment (I, well-watered *versus* water-stressed plants) and time after re-irrigation (T, i.e., Time 0, Rec 30min, Rec 2h, Rec 24h) are reported.

1.3.4.Correlations

Negative correlations were recorded between K_L, K_x and K_{ox} values and REL (Fig. 6, Table S7). It can be noted that correlations were more robust between REL and hydraulic conductance values (i.e., K_L and K_{ox}) at HI than at LI.

1.4. Discussion

In this study we investigated the role of the xylem and the extra-xylem water pathways in driving leaf hydraulic decline during dehydration, as well as the leaf hydraulic recovery in response to re-irrigation, both at high and low irradiance. Data on leaf shrinkage during dehydration and shifts of K_L and relative P_{50} at HI *versus* LI highlighted a fine coordination between leaf water economy and light availability. K_{ox} drove the initial decline of K_L at HI, as well as the short-term hydraulic recovery after re-irrigation. However, despite the recovery of K_L (and K_{ox}), the leaf ability to respond to irradiance remained partially impaired even 24h after re-irrigation, as a likely outcome of drought-induced membrane damage, only partially recovered over short-term.

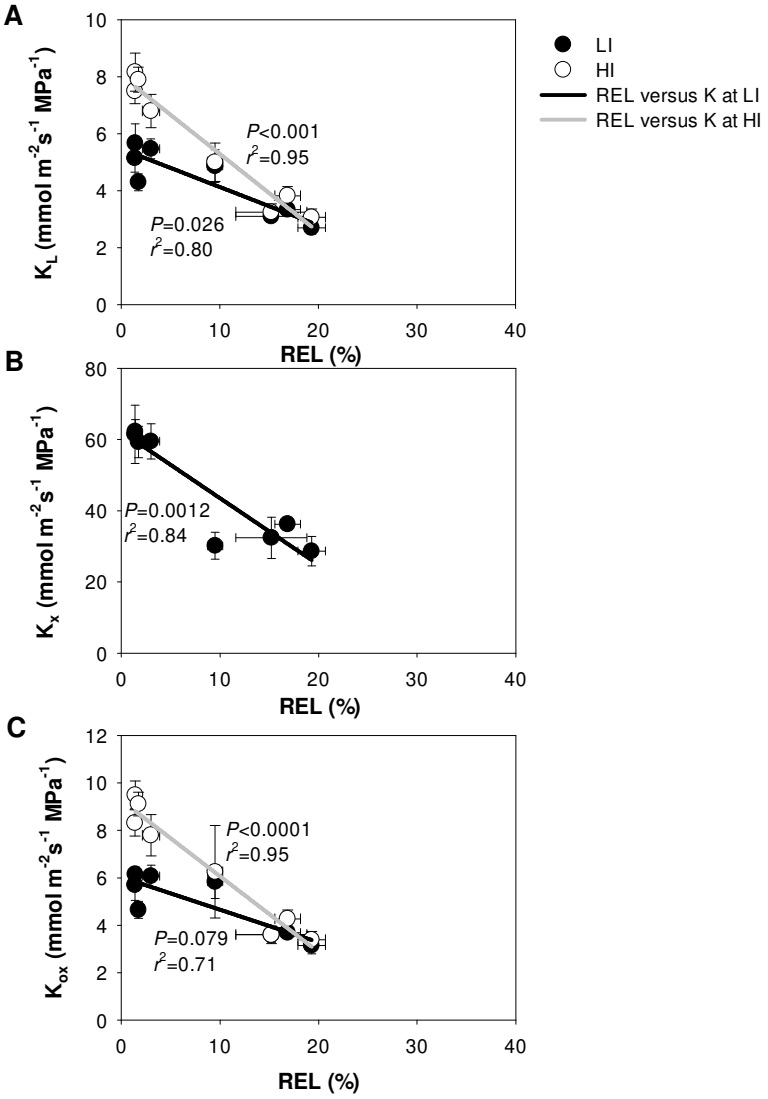

Figure 6: Relationships between the mean values ± SEM of (**A**) leaf (K_L), (**B**) xylem (K_x) and (**C**) extra-xylem (K_{ox}) hydraulic conductance and the relative leaf membrane electrolyte leakage (REL) as recorded at low (LI) and high (HI) irradiance (black and white circles, respectively). Black and grey lines indicate relationships statistically different as recorded at LI and HI, respectively. Coefficient of determination (r^2) and *P* values are reported.

1.4.1. K_L decline to dehydration in response to low versus high irradiance

Both K_L and K_{ox} increased in response to irradiance. The increase of K_L as well as of K_{ox} at HI was detectable until Ψ_L ~ -1.0 MPa, but it disappeared in more severely dehydrated leaves. This induced an irradiance-driven shift in P_{50} and P_{80} values of K_L and K_{ox}. The increase of K_L at HI *versus* LI was clearly driven by K_{ox} enhancement, suggesting that cell membrane permeability, possibly modulated by aquaporins, increased with irradiance (Maurel et al., 2008; Kim and Steudle, 2009), and declined upon excessive water loss (Kim and Steudle, 2007; Guyot et al., 2012). At low irradiance and in well hydrated leaves, the leaf xylem hydraulic resistance (R_x= 1/K_x) made up about 20% of the whole leaf hydraulic resistance (R_L= 1/K_L), while at high irradiance R_x and R_{ox} (R_{ox}= 1/K_{ox}) contributed equally to the whole leaf hydraulic resistance. Hence, in dark-adapted leaves the major hydraulic resistance to water flow was represented by the extra-xylem water pathway (about 80%). However, when well hydrated leaves were illuminated, a shift in the hydraulic resistance partitioning was recorded. Higher and substantial R_{ox} with respect to R_x, as recorded at LI, supports the hydraulic segmentation hypothesis (Tyree and Ewers, 1991; Scoffoni et al., 2016) at leaf level. Reduced R_{ox} at HI did not change this protective mechanism in *P. nigra*. Indeed, the P_{50} of K_{ox} at HI was significantly lower than that of K_x. As a consequence, the loss of 50% of the extra-xylem hydraulic conductance induced a decrease of K_x by less than 30%. This, in turn, confirms the hypothesis that a "mesophyll sacrifice" might allow plants to prevent xylem embolism formation (Scoffoni et al., 2014, 2017a, 2017b, 2018; Trifilò et al., 2016). In summary, our results suggest that high vulnerability of the extra-xylem water pathway at HI actually protects xylem from embolism build-up under active transpiration. This feature, coupled to lower leaf shrinkage at HI (see comments below), might function as a fine signal to induce stomatal closure in order to limit further and stronger K_L reductions. Indeed, in our *P. nigra* plants, a strong stomata closure was recorded at water potential values inducing loss of both K_{ox} and turgor.

Our findings are in partial disagreement with recent studies showing that no xylem embolism occurs before the turgor loss point (Charra-Vaskou et al., 2012; Delzon and Cochard, 2014; Bouche et al., 2016; Brodribb et al., 2016; Scoffoni et al., 2017a, 2017b; Cardoso et al., 2018; Scoffoni et al., 2018). Indeed, in *P. nigra* Ψ_{tlp} was very close to the P_{50} for K_x value. The occurrence of 50% decrease in xylem hydraulic conductance, coupled with turgor loss, apparently induced a strong reduction of stomatal aperture. However, our data do not allow to disentangle the actual contribution of these two mechanisms to the induction of stomatal closure.

Increased K_L in response to irradiance has been recorded in different species (i.e., Lo Gullo et al., 2003; Nardini et al., 2005; Tyree et al., 2005; Scoffoni et al., 2008; Sellin et al., 2011; Xiong et al., 2018). This physiological response might provide a functional advantage by improving water supply to well illuminated leaves. This, in turn, would favour maintenance of mesophyll hydration, thus enhancing photosynthetic rates (i.e., Cochard et al., 2007; Scoffoni et al., 2018). On the other hand, K_L light enhancement may make the leaf more vulnerable to dehydration, as reported by Guyot et al. (2012) in 4 woody species and confirmed in this study for *P. nigra*. Recently, Scoffoni et al. (2018) reported that despite the K_L increase recorded at high irradiance in well-watered leaves of *Arabidopsis thaliana*, no shift in K_L vulnerability to dehydration was detected at low *versus* high irradiance. Data reported by Scoffoni et al. (2018) suggest that, in some species, the K_L light enhancement may confer only functional advantages to some species, without additional 'costs' in terms of hydraulic vulnerability. This may be particularly advantageous for short-lived species (Scoffoni et al., 2018). But this was not the case in 3 woody evergreens (Guoyt et al., 2012), one annual herbaceous (i.e., *Helianthus annuus* L., Guyot et al., 2012) and one deciduous tree (*P. nigra*, present study). The relative advantages, costs, and related trade-offs of light-induced K_L enhancement require further testing at anatomical, molecular and physiological levels.

1.4.2. Leaf shrinkage at low versus high irradiance and its effect on leaf hydraulics

The shrinkage of drought-stressed leaves has been reported to occur on both a daily and seasonal basis (Ogaya and Peñuelas, 2006; Seelig et al., 2015). However, to the best of our knowledge, our data represent the first report of significantly lower PLT_{tlp} and PLV_{tlp} when samples are dehydrated at high *versus* low irradiance. The control of the extra-xylem water pathway via leaf shrinkage, as a function of water and light availability, represents a still relatively unexplored connection between leaf hydraulic conductance and gas exchange (Flexas et al., 2013; Xiong et al., 2017; Scoffoni et al., 2018; Xiong et al., 2018; Xiong and Nadal, 2020). Recently, Harayama et al. (2019) reported that species with lower major vein density showed higher loss of K_L induced by aquaporin inhibition, and suggested a species-specific trade-off between xylem and extra-xylem water pathways to optimize the ratio between the efficiency of the leaf hydraulic conductance to the carbon cost of leaf construction. Moreover, Muries et al. (2019) suggested the possibility for leaves to regulate the water reallocations and/or retentions by modulating the cell-to-cell hydraulic conductance and, then, a trade-off between leaf capacitance and conductance. Our findings suggest a novel negative feedback mechanism linking leaf shrinkage to the leaf hydraulic

conductance. As far as water and light are available, plants showing light-driven K_L enhancement can improve their leaf water transport capacity, maintaining stomata open and maximizing CO_2 uptake. At low water potential but high irradiance, cells shrinkage occurs likely induced by high transpiration rates. If water vapour loss cannot be supported by liquid water delivery, both cell shrinkage and damage to leaf membrane integrity occur (i.e., Cruz de Carvalho, 2008; Kaur and Asthir, 2017), leading to loss of cell-to-cell connectivity. This "shrinking message" may act as a nearly signal inducing aquaporin gating and stomatal closure, preventing further water loss and drop of xylem pressure that would trigger air seeding and embolism. Aquaporins are typically activated/expressed in response to light, favouring higher rate of water inflow to sustain higher transpiration (Chaumont and Tyerman, 2014; Maurel and Prado 2017). Moreover, high irradiance can induce aquaporin inhibition by ROS production (Maurel et al., 2008; Kim and Steudle ,2009).

1.4.3. Leaf hydraulic recovery

When *P. nigra* plants were subjected to a drought treatment bringing leaf water potential to the turgor loss point, relative water content dropped to about 80% leading to strong decrease of gas exchange as well as a significant impairment of the xylem and extra-xylem water pathways, especially at high irradiance. It can be noted that the decline of K_L, K_x and K_{ox} recorded in potted samples was similar to values recorded on adult plants so suggesting that measured adult tress and potted plants showed similar hydraulic responses. Twenty-four hours after re-watering, a significant (but not complete) recovery of leaf hydraulic conductance was recorded. This recovery was clearly induced by a recovery of the extra-xylem water pathway. Moreover, robust negative correlations were recorded between whole leaf as well as extra-xylem hydraulic conductance and leaf membrane integrity, especially at high irradiance, highlighting the relevant role of membrane integrity in regulating leaf hydraulic efficiency and light-mediated K_L regulation. To the best of our knowledge, this is the first study demonstrating the relevance of K_{ox} not only in leaf hydraulic vulnerability, but also in the short-time hydraulic recovery. In the past, the decline and recovery of K_L have been attributed to changes of K_x (Trifilò et al., 2003; Johnson et al., 2009; Laur and Hacke, 2014), but it has been suggested that some of the techniques originally used to detect embolism in leaf veins (e.g., dye perfusion) might be prone to artefacts.

Despite the recovery of K_L driven by K_{ox}, no short-term recovery of gas exchange was recorded. Hydraulic conductance and gas exchange rates are known to be correlated, as only an efficient water transport can guarantee adequate cell hydration under active transpiration (Brodribb et al., 2016). Recovery in transpiration rates of drought-stressed plants typically occurs after re-watering,

upon full recovery of K_L (Blackmanet al., 2009; Li et al., 2016; Skelton et al., 2017; Trueba et al., 2019). In this study, despite leaf water potential and RWC of S plants being statistically similar to values recorded in C plants within 30min after the re-irrigation, no increase in $g_{L\ midday}$ (and $A_{n\ midday}$) was recorded. These results are consistent with the hypothesis that leaf membrane damages and limited K_{ox} recovery might inhibit stomatal re-opening after a drought event (Trueba et al., 2019).

1.5. Conclusions

This study is the first attempt to check *in planta* the roles of K_x and K_{ox} in driving K_L dynamics in response to water availability and irradiance. Robust and clear evidence on the role of K_{ox} (as a function of the leaf membrane integrity) on leaf hydraulic vulnerability and its recovery ability has been provided. Our data provide new insights into the very fine coordination between water and light availability as well as between gas exchange and leaf hydraulic conductance. Present findings reveal that xylem and cell-to-cell water movement represent a very complex system where each pathway influence, directly or indirectly, the other one.

1.6. Supplementary Material

Table S1: Leaf water potential values inducing 50% (P_{50}) and 80% (P_{80}) loss of the whole leaf (K_L), leaf xylem (K_x) and leaf extra-xylem (K_{ox}) hydraulic conductance as recorded in *P. nigra* at low (LI) and high (HI) irradiance.

		P_{50} (MPa)	2.5% CI (MPa)	97.5% CI (MPa)	P_{80} (MPa)	2.5% CI (MPa)	97.5% CI (MPa)
K_L	**LI**	-2.41	-1.69	-3.01	-4.27	-3.4	-4.94
K_L	**HI**	-1.33	-0.61	-1.66	-2.94	-2.53	-3.4
K_x		-1.86	-1.81	-1.91	-3.4	-3.28	-3.49
K_{ox}	**LI**	-2.37	-1.66	-3.23	-4.94	-4.23	-9.64
K_{ox}	**HI**	-1.27	-0.47	-1.64	-2.89	-2.46	-3.5

Table S2: (**A**) Summary of GLS model. Relative water content (RWC) was the response variable, and irrigation treatment (I, i.e., well-watered *versus* water-stressed plants), time after re-irrigation (T, Time 0, Rec 30min, Rec 2h, Rec 24 h) and their interaction were the explanatory variables. Degrees of freedom (Df), Chi squared (Chisq) and P values are reported. (**B**) Results of a two way Anova of the leaf water potential (Ψ_L) values by irrigation treatment (I, i.e., well watered *versus* water stressed-plants) and time after re-irrigation (T, Time 0, Rec 30min, Rec 2h, Rec 24 h). Degrees of freedom (Df), Sum of squares (Sum sq), Mean sum of squares (Mean sq), *F* and *P* values are reported.

Table S2A						
		Df	**Chisq**	***P***		
RWC	**I**	1	0,001	0,97		
	T	3	5,928	0,11		
	IxT	3	10,805	0,005		
Table S2B						
		Df	**Sum sq**	**Mean sq**	***F***	***P***
Ψ_L	**I**	1	1,649	1,6488	106,4	< 0.001
	T	3	4,778	1,5928	102,8	< 0.001
	IxT	3	9,307	3,1025	200,3	< 0.001
	Residuals	55	0,852	0,0155		

Table S3: Results of two way Anova analyses of the leaf water potential ($\Psi_{L\ midday}$), stomatal conductance to leaf water vapor ($g_{L\ midday}$) and photosynthesis rate ($A_{n\ midday}$) by irrigation treatment (I, i.e. well-watered *versus* water-stressed plants) and time after re-irrigation (T, i.e. Time 0, Rec 24 h). Degrees of freedom (Df), Sum of squares (Sum sq), Mean sum of squares (Mean sq), *F* and *P* values are reported.

		Df	**Sum sq**	**Mean sq**	***F***	***P***
$g_{L\ midday}$	**I**	1	930633	930633	43,962	<0.001
	T	1	35532	35532	1,679	0,22
	IxT	1	2494	2494	0,118	0,74
	Residuals	12	254027	21169		
		Df	**Sum sq**	**Mean sq**	***F***	***P***
$A_{n\ midday}$	**I**	1	234,39	234,39	16,518	0,001
	T	1	10,51	10,51	0,741	0,41
	IxT	1	4,09	4,09	0,288	0,60
	Residuals	12	170,28	14,19		
		Df	**Sum sq**	**Mean sq**	***F***	***P***
$\Psi_{L\ midday}$	**I**	1	0,285	0,285	6,469	0,001
	T	1	0,992	0,992	22,496	0,03
	IxT	1	0,924	0,924	20,958	0,002
	Residuals	8	0,352	0,044		

Table S4: Mean values ± SEM and results of:(**A**) and (**B**) a two way Anova results of the leaf hydraulic conductance (K_L) and extra-xylem hydraulic conductance (K_{ox}) by time after re-irrigation (T, i.e. Time 0, Rec 30min, Rec 2h, Rec 24h) and irradiance (L, i.e. LI: low irradiance, HI: high irradiance) and (**C**) one way Anova results of the xylem hydraulic conductance K_x, as measured in well-watered (C) and treated (S) samples of *P. nigra*. Degrees of freedom (Df), Sum of squares (Sum sq). Mean sum of squares (Mean sq), *F* and *P* values are reported.

A) K_L

		C						
T	**L**	**Mean ± SEM**			**Df**	**Sum sq**	**Mean sq**	***F***	***P***
Time 0	LI	5.15 ± 0.49		**T**	3	2.89	0.96	0.846	0.483
	HI	7.25 ± 0.44		**L**	1	42.34	42.34	37.15	<0.001
Rec 30 min	LI	5.67 ± 0.68		**Tx L**	3	5.37	1.79	1.571	0.225
	HI	8.17 ± 0.67		**Residuals**	22	25.07	1.14		
Rec 2 h	LI	5.47 ± 0.35							
	HI	6.80 ± 0.59							
Rec 24 h	LI	4.30 ± 0.30							
	HI	7.90 ± 0.44							

B) K_{ox}

		C						
T	**L**	**Mean ± SEM**			**Df**	**Sum sq**	**Mean sq**	***F***	***P***
Time 0	LI	5.70 ± 0.65		**T**	3	4.4	1.47	0.736	0.542
	HI	8.31 ± 0.55		**L**	1	66.78	66.78	33.51	<0.001
Rec 30 min	LI	6.15 ± 0.30		**Tx L**	3	8.01	2.67	1.339	0.287
	HI	9.49 ± 0.59		**Residuals**	22	43.84	1.99		
Rec 2 h	LI	6.07 ± 0.46							
	HI	7.79 ± 0.87							
Rec 24 h	LI	4.65 ± 0.36							
	HI	9.11 ± 0.50							

C) K_x

	C							
T		**Mean ± SEM**		**Df**	**Sum sq**	**Mean sq**	***F***	***P***
Time 0		61.48 ± 8.23	**T**	3	25	8.34	0.068	0.976
Rec 30 min		62.25 ± 3.40	**Residuals**	12	1476	123.01		
Rec 2 h		59.50 ± 4.94						
Rec 24 h		59.35 ± 4.40						

A) K_L

S								
T	**I**	**Mean ± SEM**		**Df**	**Sum sq**	**Mean sq**	***F***	***P***
Time 0	LI	3.33 ± 0.16	**T**	3	19.73	6.58	8.62	<0.001
	HI	3.82 ± 0.32	**L**	1	0.64	0.64	0.85	0.37
Rec 30 min	LI	3.10 ± 0.12	**Tx L**	3	0.18	0.06	0.08	0.97
	HI	3.24 ± 0.29	**Residuals**	24	18.30	0.76		
Rec 2 h	LI	2.70 ± 0.23						
	HI	3.07 ± 0.29						
Rec 24 h	LI	4.86 ± 0.50						
	HI	5.00 ± 0.44						

B) K_{ox}

S								
T	**I**	**Mean ± SEM**		**Df**	**Sum sq**	**Mean sq**	***F***	***P***
Time 0	LI	3.69 ± 0.16	**T**	3	37.59	12.53	8.82	<0.001
	HI	4.27 ± 0.36	**L**	1	0.83	0.83	0.59	0.45
Rec 30 min	LI	3.60 ± 0.33	**Tx L**	3	0.36	0.12	0.09	0.97
	HI	3.63 ± 0.36	**Residuals**	24	34.10	1.42		
Rec 2 h	LI	3.14 ± 0.36						
	HI	3.39 ± 0.34						
Rec 24 h	LI	5.83 ± 0.75						
	HI	6.27 ± 0.88						

C) K_x

S								
T		**Mean ± SEM**		**Df**	**Sum sq**	**Mean sq**	***F***	***P***
Time 0		36.25 ± 1.62	**T**	3	126.9	42.3	0.327	0.806
Rec 30 min		32.42 ± 5.79	**Residuals**	12	1552.8	129.4		
Rec 2 h		28.67 ± 4.17						
Rec 24 h		30.16 ± 3.77						

Table S5: Results of a two way Anova of relative (**A**)leaf hydraulic conductance (K_L) and (**B**) relative extra-xylem hydraulic conductance (K_{ox}) by time after re-irrigation (T) and irradiance treatment (L) and results of (**C**) one way Anova of relative xylem hydraulic conductance (K_x) at different time after re-irrigation as the recorded in S samples of *P. nigra*. Degrees of freedom (Df), Sum of squares (Sum sq), Mean sum of squares (Mean sq), *F* and *P* values are reported.

A) Relative K_L					
	Df	**Sum sq**	**Mean sq**	***F***	***P***
T	3	0.44	0.15	9.55	<0.001
L	1	0.21	0.21	13.74	<0.001
Tx L	3	0.01	0.00	0.26	0.85
Residuals	24	0.37	0.02		
B) Relative K_{ox}					
	Df	**Sum sq**	**Mean sq**	***F***	***P***
T	3	0.47	0.16	7.00	<0.001
L	1	0.42	0.42	19.02	<0.001
Tx L	3	0.01	0.00	0.13	0.94
Residuals	24	0.54	0.02		
C) Relative K_x					
	Df	**Sum sq**	**Mean sq**	***F***	***P***
T	3	0.05	0.02	0.52	0.68
Residuals	17	0.51	0.03		

Table S6: Results of a two way Anova of the relative leaf membrane electrolyte leakage (REL) values by irrigation treatment (I, well watered *versus* water-stressed plants) and time after re- irrigation (T, i.e. Time 0, Rec 30min, Rec 2h, Rec 24h). Degrees of freedom (Df), Sum of squares (Sum sq), Mean sum of squares (Mean sq), *F* and *P* values are reported.

Table S6					
	Df	**Sum sq**	**Mean sq**	***F***	***P***
I	1	1579,3	1579,3	103,788	<0.001
T	3	190,2	63,4	4,166	0,01
TxI	3	104,2	34,7	2,282	0,10
Residuals	29	441,3	15,2		

Table S7: Correlation matrix. Spearman's rank correlation coefficients (ρ) and *P* values are reported.

	K_L at LI	K_L at HI	K_x	K_{ox} at LI	K_{ox} at HI	REL	RWC	Ψ_L
K_L at LI		0.83	0.83	0.98	0.83	-0.81	0.17	-0.05
K_L at HI	0.01		0.86	0.79	1.00	-0.90	0.29	-0.38
K_x	0.01	0.01		0.71	0.86	-0.86	0.00	-0.02
K_{ox} at LI	<0.001	0.02	0.05		0.79	-0.71	0.24	-0.02
K_{ox} at HI	0.01	<0.001	0.01	0.02		-0.90	0.29	-0.38
REL	0.01	<0.001	0.01	0.05	<0.001		-0.10	0.48
RWC	0.69	0.49	1.00	0.57	0.49	0.82		-0.36
Ψ_L	0.91	0.35	0.96	0.96	0.35	0.23	0.39	

Chapter 2

Study 2

Too dry to survive: leaf hydraulic failure in two *Salvia* species can be predicted on the basis of water content

Published as: **Abate E., Nardini A., Petruzzellis F., Trifilò P., 2021**. Too dry to survive: Leaf hydraulic failure in two *Salvia* species can be predicted on the basis of water content. ***Plant Physiology and Biochemistry*** 166, 215-224.

2. Introduction

Water availability is a common limiting factor for terrestrial plants growing in arid and semi-arid regions. However, global warming is expected to expose plants of several different biomes to increased risk of die-off induced by anomalous drought and heat waves (i.e., Eamus et al., 2013; Allen et al., 2015; Brodribb et al., 2019). In fact, increased air temperature and VPD are expected to exacerbate drought impacts at a global scale, even for biomes generally not water-limited (Allen et al., 2010). The impacts of species-specific die-off on biodiversity and ecosystem services are potentially dramatic, and are predicted to worsen in the next future (Anderegg et al., 2013; IPCC, 2019).

Plant responses to drought are complex, and involve the coordination of different and still not well understood physiological mechanisms. There is current consensus that plant hydraulics play a critical role in setting species-specific tolerance to drought (McDowell et al., 2019). In fact, hydraulic failure has been recognized as a major correlate of drought-driven plant death (Hartmann et al., 2013; Rowland et al., 2015; Adams et al., 2017; Choat et al., 2018), and a loss of plant hydraulic conductivity (PLC) of 90% is considered a point of no return leading to plant death (Urli et al., 2013; Trifilò et al., 2015; Hammond et al., 2019). However, a number of relevant questions on correlations between hydraulic traits and plant resistance/resilience to drought remain unresolved (Cardoso et al., 2020). Most importantly, easy-to-measure and reliable indicators of drought-driven mortality risk are still largely lacking (Anderegg et al., 2019; Sapes et al., 2019; Stocker et al., 2019).

Recently, the relative water content (RWC) has been suggested as a simple indicator of plant mortality risk, due to its multiple correlations with plant hydraulics, stomatal aperture and carbon uptake (Martinez-Vilalta et al., 2019). Sapes et al. (2019) have reported good correlations between plant water content, loss of hydraulic conductivity and carbohydrate depletion in *Pinus ponderosa* samples. Stem RWC was useful for predicting loss of hydraulic conductivity in some tree species (Rosner et al., 2019), but Mantova et al. (2021) pointed out that this might only apply to woody angiosperms, and not to conifers.

In the present study, we investigated the robustness of leaf water content as a proxy for predicting the occurrence of hydraulic failure in two native Mediterranean species, *Salvia ceratophylloides* Ard. and *Salvia officinalis* L. Climate change is expected to be exacerbated in the Mediterranean region where summer warming rates are apparently 20-40% higher than the global mean value (Mariotti et al., 2015; Lionello and Scarascia, 2018; Raymond et al., 2019). This, in turn, may affect typical biodiversity richness of the Mediterranean biome (i.e., Cowling et al., 2015; Rundel

et al., 2016; Buira et al., 2021), increasing the extinction risk of different endemic species (Sala et al., 2000; Underwood et al., 2009; Cramer et al., 2018; Tramblay et al., 2020). On this view, checking possible indicators of hydraulic failure on native Mediterranean species is very relevant for improving the reliability of predictive models of Mediterranean vegetation responses to novel climate conditions.

Our study has been focused on leaf hydraulic conductance (K_L) as a major driver of plant hydraulics (Brodribb and Holbrook, 2004; Brodribb et al., 2005; Hochberg et al., 2017; Skelton et al., 2017; Scoffoni et al., 2016; Wang et al., 2018; Xiong and Nadal, 2020). Moreover, significant correlations have been reported between leaf hydraulic vulnerability and mean annual precipitation across diverse species' assemblages (Blackmann et al., 2014; Nardini and Luglio, 2014), suggesting that leaf hydraulic safety plays a critical role in drought tolerance (Fang et al., 2020). Leaf hydraulic vulnerability to water stress has been originally attributed to the occurrence of xylem embolism, which was considered as the major cause of K_L decline under drought (i.e., Nardini et al., 2003; Scoffoni et al., 2011; Johnson et al., 2012). However, recent findings have outlined the relevance of the outside-xylem pathways in controlling K_L changes during dehydration (Trifilò et al., 2016, Scoffoni et al., 2017; 2018), as well as post-drought recovery (Trifilò et al., 2021). Some studies have documented a trade-off between leaf hydraulic vulnerability and the leaf shrinkage that is typically observed during dehydration: higher shrinkage before the turgor loss point was reported for species with higher K_L vulnerability (Scoffoni et al., 2014; Trifilò et al., 2016). These results suggest that cell shrinkage might drive the K_L decline during mild dehydration by affecting the extra-xylem water transport pathway. This, in turn, may trigger stomatal closure and protect K_x from xylem embolism spread (Scoffoni et al., 2014, 2017a; Trifilò et al., 2016; 2021).

In this view, a reliable indicator of the risk of leaf hydraulic damage like leaf shrinkage (Scoffoni et al., 2014; Trifilò et al., 2016) and/or RWC thresholds (Trueba et al., 2019) may actually well quantify the risk of leaf hydraulic failure. In accordance, John et al. (2018) reported species-specific RWC thresholds for loss of leaf rehydration capacity, as a possible indicator of dehydration tolerance.

We compared the leaf hydraulic vulnerability to drought of two *Salvia* species to check if leaf water content and/or leaf shrinkage may be reliable proxies of incipient leaf hydraulic failure. We specifically tested the following hypotheses: 1) different *Salvia* species display similar critical RWC dehydration thresholds for leaf hydraulic failure; 2) leaf hydraulic failure leads to loss of

leaf rehydration capacity; 3) leaf shrinkage before the turgor loss can be used as an early diagnostic tool to predict K_L impairment.

2.1 Materials and Methods

2.1.1. Plant material and growth conditions

Experiments have been performed on 8-month-old plants of *S. ceratophylloides* and *S. officinalis*. *S. ceratophylloides* (*Sc*) is a rare perennial herbaceous species, endemic in southern Italy (Crisafulli et al., 2010). To the best of our knowledge, no data on hydraulics and water relations of this species are available in the literature. *S. officinalis* (*So*) is a Mediterranean-native perennial species, widely naturalized even outside its original habitat (Pignatti, 2002). Previous studies have analysed some of the functional bases of drought tolerance of this species (Raimondo et al., 2015; Savi et al., 2016).

In October 2019, seeds provided by the Botanical garden of the University of Messina were fully immersed in water for 24 hours, and then planted in greenhouse trays. After emergence of at least two developing leaves, seedlings were transferred in 3.4L pots filled with forest topsoil collected from Colli San Rizzo (Messina, Italy). Seedlings were grown in a greenhouse until the beginning of May 2020. The greenhouse received only natural light, with maximum daily values of photosynthetic photon flux density (PPFD) averaging 810 ± 260 μmol s^{-1} m^{-2}, air temperature ranging from 21 ± 2 °C to 17 ± 2 °C (day/night), and air relative humidity of 55 ± 3%. During the growth period plants were regularly irrigated to field capacity on a daily basis. At the beginning of May, 15 samples per species were transferred in a garden of the Department CHIBIOFARAM, University of Messina. All measurements were performed in June 2020.

2.1.2. Pressure-volume (PV) curves and capacitance measurements

Leaf water potential at the turgor loss point (Ψ_{tlp}), osmotic potential at full turgor (π_0), bulk modulus of elasticity (ε) and leaf capacitance at full turgor were calculated based on leaf water potential isotherms measured at the beginning of June in well-watered plants. Leaves were collected from 5 different plants per species, and water potential isotherms were obtained following the procedure described by Tyree and Hammel (1972). Ψ_{tlp} was estimated as the flex point of the relationship between 1/leaf water potential (Ψ_L) and the water loss; π_0 was calculated by the y-intercept of the linear region of this relationship; ε was calculated as: $\Delta Pt/(\Delta W/W)$ where ΔPt is the change of turgor pressure and $\Delta W/W$ is the relative change of the leaf water content.

Leaf capacitance before (C_{ft}) and at Ψ_{tlp} (C_{tlp}) was estimated by PV curves analysis as well as by the fast rehydration kinetic method (FRM, Nardini et al., 2012) because *i*) differences in leaf capacitance may be obtained between different techniques (Blackmann and Brodribb, 2010; Trifilò et al., 2016) and *ii*) changes in capacitance value before and at the turgor loss point have been reported in some species (Trifilò et al., 2016). On the basis of PV curves, leaf capacitance was calculated from the slope of the relationship between the water loss and Ψ_L before and after the turgor loss (i.e., $C_{ft,PV}$ and $C_{tlp,PV,}$ respectively) and normalised by leaf area (A_L). Leaf images were acquired with a scanner (HP Scanjet G4050, USA) and A_L was measured with the software ImageJ (http://imagej.nih.gov/ij/). Dry weight (DW) was obtained after oven-drying leaves for 3 days at 70°C.

For the leaf rehydration kinetic method, twelve leaves per species were cut under water and rehydrated for at least 1 hour. Leaves were then dehydrated on the bench to Ψ_L values corresponding to about 50% of species-specific Ψ_{tlp} (n=6), or to Ψ_{tlp} (n=6). More in detail, before estimating their initial Ψ_L, samples were wrapped in plastic film, weighed to record their initial weight (W_i) and inserted in the pressure chamber to estimate their water potential. Once the balance pressure was reached, the cut section of the petiole was covered with deionised water and the pressure inside the chamber was released at a rate of 0.015 MPa s^{-1} down to atmospheric value, thus allowing leaf rehydration. At the end of pressure relaxation, the excess water was adsorbed with a filter paper and the leaf was left inside the chamber for 5 min at atmospheric pressure to allow equilibration of water content and Ψ_L. Ψ_L was measured again (i.e., final Ψ_L) and the leaf was weighed to obtain its final weight (W_f). Leaf capacitance in the turgor range ($C_{ft,FRM}$) or to Ψ_{tlp} ($C_{tlp,FRM}$) was calculated as ($W_f - W_0$)/ (initial Ψ_L– final Ψ_L) and normalised by A_L.

2.1.3. Estimating the leaf relative water content and leaf rehydration capacity during dehydration.

To check the rehydration time and avoid artefacts induced by over-hydration phenomena, we measured the time course of rehydration in both species during preliminary experiments. Ten leaves per species at different levels of dehydration were measured for their fresh weight (FW) and then rehydrated with petioles immersed in deionized water. Their weight was then measured each hour for 8 consecutive hours and 24 hours later. Samples were finally oven-dried to obtain DW. The saturated water content (SWC) was reached within 5-8 hours in both species and no further significant increase in leaf water content was recorded (Fig. S1B, D). For this reason, the turgid weight (TW) of measured samples was recorded after 8-12 hours of rehydration.

Measurements of the relative leaf water content (RWC) and percentage loss of leaf rehydration capacity (PLRC) during dehydration were performed on samples collected from well-watered plants. Shoots were cut under water, rehydrated for about 1 hour to full turgor, and bench-dehydrated for time interval ranging from 5 min to 48 hours. During the rehydration and following bench-dehydration, shoots were maintained in a black plastic bag with a piece of wet filter paper inside, for at least 30 min in order to stop transpiration and favour the equilibration of water potential values across all leaves. At different dehydration levels, leaves were collected and their FW was immediately recorded. Leaves were then rehydrated for > 8 hours with their petiole immersed in a beaker containing deionized water, and finally oven-dried to obtain heir DW. For each leaf, we calculated RWC as:

RWC = 100*[(FW-DW)/DW]/SWC

and PLRC as:

PLRC = 100*100-[(TW-DW)/ DW]/SWC

where SWC is the saturated water content (g g^{-1}) of leaves at Ψ_L<-0.5 MPa. RWC is frequently estimated as: (FW-DW)/(TW-DW). However, at species-specific water content values, cells lose their rehydration ability and this produces over estimation of RWC values. In accordance, when overcoming species-specific thresholds, we recorded discrepancies between the values obtained applying the two different formulas (Supplementary Fig.1A,C).

In order to estimate possible relationships between RWC, PLRC, leaf water potential, cell membrane damage and leaf hydraulic conductance values during the dehydration, additional leaves adjacent to those measured for RWC and PLRC, were also collected during the bench-dehydration and used for experiments described below.

Leaves measured for RWC were used also for estimating the leaf mass per unit area (LMA) (see below).

2.1.4. Estimating leaf hydraulic conductance changes during dehydration

Leaf hydraulic conductance (K_L) was measured using the rehydration kinetic method (RKM) (Brodribb and Holbrook, 2003). Leaves were sampled at different dehydration levels from the same shoots used for estimating RWC and PLRC (see above). One leaf was sampled and used to estimate the initial water potential (Ψ_i). A second adjacent leaf was detached with the petiole immersed in 10 mM KCl solution filtered at 0.2 μm, and left rehydrating for 30-90 s before measuring the final leaf water potential (Ψ_f). Leaf hydraulic conductance was then calculated as:

$K_L = C*t^{-1} * \ln(\Psi_i/\Psi_f)$

where C is the leaf capacitance, t is the rehydration time. Because differences in leaf capacitance were recorded between PV and FRM methods (see above), we used values measured by the FRM because they more closely resemble the fast water exchange occurring during leaf transpiration, opposed to slow water release during bench dehydration (Blackmann and Brodribb, 2011). All K_L measurements were performed at normal laboratory irradiance (PPFD<10 μmol m^{-2} s^{-1}) and normalised at 20 °C.

2.1.5. Leaf hydraulic conductance response to irradiance

Light-driven changes in K_L have been recorded in different species (i.e., Scoffoni et al., 2008; Xiong et al., 2018), and in some cases can lead to changes in leaf hydraulic vulnerability (Guyot et al., 2012; Trifilò et al., 2021). To check this possible effect in our study species, measurements of K_L were performed at laboratory irradiance or after 30 min illumination by a LED light source (Dya, APOLLO LED) providing a PPFD of 1200 μmol m^{-2} s^{-1}. Measurements were performed the evaporative flux method (EFM, Sack et al., 2002). Well-watered leaves (i.e., Ψ_L>-0.5 MPa) were cut under water and connected to rigid peek tubing connected to a beaker containing water. The beaker rested on a digital balance and flow readings were recorded at 30s intervals at atmospheric pressure. Leaves were maintained next to a fan to promote water loss and, to avoid leaf over-heating during measurements at high irradiance, a transparent plastic container filled with water was placed between the leaf surface and the lamp.

Measurements were performed only in well-watered samples, and not repeated in dehydrating leaves because no K_L changes were recorded in response to irradiance (see Results).

2.1.6. Leaf cell membrane integrity

Electrolyte leakage measurements were done to obtain insights into eventual cell membrane damage induced by leaf dehydration (Trifilò et al., 2021). Measurements were performed on leaf samples collected from bench-dehydrated shoots at different dehydration levels and already used to measure RWC, PLRC, Ψ_L and K_L (see above). Leaf discs of about 0.5 cm^2 were cut with a razor blade and inserted in a test tube containing 8 mL of distilled water. Samples were stirred for 30 min at room temperature and the initial electrical conductivity of the solution (EC_i) was recorded by a conductivity meter (Cond 5, XS instruments, Italy). Samples were then subjected to three freeze-thaw cycles (i.e., T = -20 ^oC, +20 ^oC) to induce complete membrane disruption and processed as above to measure the final electrical conductivity of the solution (EC_f). The relative electrolyte leakage (REL) was calculated as (EC_i/EC_f) *100.

2.1.7. Minimum cuticular conductance

Minimum leaf conductance to water vapor (g_{min}) was measured in 6 leaves per species, by measuring the minimum transpiration rate divided by mole fraction vapour pressure deficit and two times the mean projected leaf area (John et al., 2018). In detail, leaves were first hydrated for >8 hours. After recording their turgid weight and leaf area, they were suspended by their petioles over a fan for at least 2 hours to induce stomatal closure. During this dehydration time leaves were weighed at 15min intervals and, finally, the leaf area was measured again and leaves were oven-dried for 3 days at 70°C to obtain DW. Room temperature and relative humidity were recorded at 30s intervals using a thermohygrometer (Velleman, Gavere, Belgium).

2.1.8. Structural traits

Samples measured for RWC were used also for estimating the leaf mass per unit area (LMA) calculated as DW/A_L. Leaf shrinkage during progressive dehydration (Scoffoni et al., 2014; Trifilò et al., 2016) was measured on 15 leaves per species. Shoots were cut under water and left rehydrating for about 1 hour. Fully turgid leaves were collected and immediately measured for their FW, A_L and leaf thickness (T_L, estimated by averaging values recorded in the bottom, middle, and top thirds of the leaf with a digital calliper, accuracy ± 0.01 mm). Leaf volume (V) was estimated as: $T_L \times A_L$. Samples were then fixed by their petiole to a bar opposite to a fan to favour dehydration and repeatedly measured for the above parameters at different Ψ_L values until turgor loss point was reached. They were finally oven-dried, and the above parameters were measured again. The leaf water potential at different levels of dehydration was measured on leaf samples (different from those used to measure leaf shrinkage) randomly placed next to leaves used for shrinkage measurements. Two leaves for each level of dehydration were randomly selected to estimate leaf water potential (Ψ_L) with a pressure chamber (3005 Plant Water Status Console, Soilmoisture Equipment Corp., Goleta, CA, USA).

Samples measured for leaf shrinkage traits were used also to estimate leaf succulence and leaf density as:

Leaf succulence = SWC/A_L

Leaf density = LMA/T_L

2.1.9. Statistical analysis

To test possible differences among *Sc* and *So* in leaf structural traits, water storage traits, and data obtained by PV analysis and shrinkage traits, a t-test ($\alpha = 0.05$) was performed after checking for normality assumption. To test the differences among species (*Sc* and *So*) and the effects of cell turgor (i.e., before and after turgor loss point) on leaf capacitance as well as the effects of irradiance (low *versus* high irradiance) as measured by the EFM a two-way ANOVA test was performed. For statistically significant tests ($p < 0.05$), a Tukey's post hoc test using Holm-Sidak p-values correction was carried out to perform pairwise comparisons. Simple linear regressions were used to determine the relationships between REL to RWC, REL to Ψ_L, PLRC to REL, K_L to REL and REL to water content for each species independently. Lines were fitted for leaves with REL > 15% for *Sc* and > 18% for *So* (i.e., REL values recorded in well watered samples). All previous analyses were run using SigmaStat 2.0 (SPSS, Inc., Chicago, IL, USA) statistics package. The relationship between RWC and Ψ_L, PLRC and Ψ_L, and between PLRC and RWC in each species were assessed using "fitplc" package for R software (R Core Team, 2020). Specifically, a sigmoidal model was fitted and Ψ values and associated 95% confidence intervals (C.I.s) corresponding to RWC equal to 50% (P_{RWC50}), PLRC equal to 10% and 50% (RWC_{PLRC10} and $RWC_{PLRC50,}$ respectively) and RWC values and associated 95% C.I.s corresponding to PLRC values of 10 and 50% (RWC_{PLRC10} and $RWC_{PLRC50,}$ respectively) were calculated. Using the same framework, we calculated Ψ and RWC values and associated 95% C.I.s corresponding to 10%, 50% and 88% loss of K_L in each species (P_{10}, P_{50}, P_{88}, RWC_{KL10}, RWC_{KL50}, RWC_{KL88}, respectively) as well as PLRC and associated 95% C.I.s corresponding to 10% and 50% loss of K_L in each species (i.e., $PLRC_{KL10}$ and$PLRC_{K50L}$). At last, leaf water content values and associated 95% C.I.s corresponding to PLRC of 10% and 50% and to loss of K_L of 10, 50% and 88% were also calculated. Differences of each of the above mentioned parameters between *Sc* and *So* were considered as statistically significant when the 95% C.I.s did not overlap.

2.2. Results

Compared to *S. ceratophylloides, S. officinalis* had higher values of leaf surface area (17 *versus* 10 cm^2), leaf volume (1.2 *versus* 0.6 cm^3), leaf thickness (0.8 *versus* 0.6 mm), LMA (80 *versus* 56 g m^{-2}) and leaf density (0.13 *versus* 0.07 g cm^{-3}) (Table 1). By contrast, *Sc* showed significantly higher leaf succulence (35 *versus* 25 mg cm^{-2}), SWC (5.2 *versus* 3.4 g g^{-1}) and g_{min} (8.3± 0.5 *versus* 3.2 ± 0.8 mmol $m^{-2}s^{-}1$) than *So*.

Leaf capacitance values before and after turgor loss, as obtained by PV curve analysis (i.e. $C_{ft, PV}$ and $C_{tlp, PV}$), were substantially higher than values obtained by the fast rehydration kinetic method

(i.e. $C_{ft,FRM}$ and $C_{tlp,FRM}$, Table 1). Nevertheless, the two techniques showed a similar trend, in that leaf capacitance was similar in the two species, independent on the method (i.e., about 0.22 mol $m^{-2}s^{-1}$ $MPa^{-1}$by FRM and about 1.5 mol $m^{-2}s^{-1}$ MPa^{-1} by PV curve analysis). An increase in leaf capacitance was recorded at the turgor loss point in both species and by both methods (Table 1). It can be noted that at the turgor loss point, *Sc* showed values of leaf capacitance about 2 times higher than *So* (i.e.,0.67 *versus* 0.38 mol m^{-2} MPa^{-1} by FRM and 9.9 *versus* 4 mol m^{-2} MPa^{-1} by PV analysis, respectively). *So* showed significantly lower Ψ_{tlp} (-1.9 *versus* -1.5 MPa) and π_o (-1.5 *versus* -1.2 MPa), and higher ε_{max} (28 *versus* 17 MPa) compared to *Sc*, but similar RWC_{tlp} values were recorded in the two species.

At turgor loss point and in dry leaf samples, the percentage loss of leaf thickness and leaf volume were significantly higher in *Sc* compared to *So* (Table 1), while no significant difference in percentage loss of leaf area (PLA) value was recorded.

The two study species showed an increase in PLRC and relative electrolyte leakage (REL) in response to dehydration (i.e., at more negative Ψ_L and lower RWC values, Fig. 1). However, the RWC values inducing 10% loss of rehydration capacity (i.e., RWC_{PLRC10}), taken as a proxy of critical dehydration threshold (John et al., 2018), were different in the two species. In fact, RWC_{PLRC10} was about 55% in *S. ceratophylloides* and about 70 % in *S. officinalis* (Figs. 1B, H, Supplementary Table 1). Moreover, differences were recorded also in terms of RWC values inducing 50% loss of rehydration capability (RWC_{PLRC50}). This parameter was about 17% in *Sc* and 27% in *So* (Figs. 1B, H, Supplementary Table S1). Differences in Ψ_L values inducing 10% and 50% loss of rehydration capacity were recorded in *Sc* and *So* too (Figs. 1C, I, Supplementary Table S1). The increase in PLRC during dehydration was likely induced by increasing cell membrane damage, as positive correlations between PLRC and REL were recorded in both species (Figs 1F, N). It can be noted that an increase in REL in response to dehydration occurred at similar Ψ_L values (about -1.3 MPa, Figs. 1E, M) but at different relative water content (i.e., RWC~70% and 85% in *Sc* and *So*, respectively, Figs. 1D, L). Irradiance did not affect K_L in the two species (Table 2). *Sc* and *So* showed a similar leaf hydraulic vulnerability in response to dehydration if Ψ_L values were taken into account (Fig. 2A, E, Supplementary Table 1). In fact, similar water potential value inducing 50% and 88% loss of K_L was recorded in the two *Salvia* species (i.e., P_{50} ~ -2.0 MPa, P_{88}~ -3.2 MPa, Fig. 2A, E, Supplementary Table 1). By contrast, values of RWC inducing 50% and 88% loss of K_L (i.e., RWC_{KL50} and RWC_{KL50}, respectively) were different. In particular, RWC_{KL50} was about 35% for *S. ceratophylloides* and 65% for S.

officinalis and RWC_{KL88} was about 15% for *S. ceratophylloides* and 40% for S. *officinalis* (Fig. 2B, F, Supplementary Table 1).

Table 1: Mean values ± SD of leaf structural traits, water storage traits, PV traits and leaf shrinkage traits as measured in *S. ceratophylloides* and *S. officinalis* plants. Number of replicas (n) are specified and *P* values are reported. Different letters indicate statistically significant leaf capacitance values through a two-way Anova analysis (S: species, M: method, SxM: Species x Method). A_L: leaf area, V_L: leaf volume; T_L: leaf thickness; LMA: leaf mass area; SWC: leaf saturated water content; $C_{ft,\ FRKM}$ and $C_{tlp,\ FRM}$: leaf capacitance at full turgor and at turgor loss point, respectively, estimated by fast rehydration kinetic method; $C_{ft,\ PV}$ and $C_{tlp,\ PV}$: leaf capacitance at full turgor and at turgor loss point, respectively, estimated by PV curve analysis; g_{min}: minimum cuticular conductance; Ψ_{tlp}: leaf water potential at turgor loss point; π_o: osmotic potential at full turgor; ε_{max}: bulk modulus of elasticity; RWC_{tlp}: relative water content at turgor loss point; PLT_{tlp} and PLT_{dry}: percentage loss of leaf thickness at turgor loss point and of a dry leaf, respectively; PLA_{tlp} and PLA_{dry}: percentage loss of leaf area at turgor loss point and of a dry leaf, respectively; PLV_{tlp} and PLV_{dry}: percentage loss of leaf volume at turgor loss point and of a dry leaf, respectively.

	S. ceratophylloides	***S. officinalis***	***P* value**
Leaf structural traits			
A_L, cm^2 (*n*=50)	9.3 ± 4.9	17.0 ± 7.4	**<0.001**
V_L, cm^3 (*n*=15)	0.58 ± 0.19	1.22 +0.33	**<0.001**
T_L, mm (*n*=15)	0.58 ± 0.08	0.79 ± 0.07	**<0.001**
LMA, g m^{-2} (*n*=50)	55.6 ± 14.2	79.5 ± 16.5	**<0.001**
Leaf density, g cm^{-3} (*n*=15)	0.07 ± 0.01	0.13 ± 0.02	**<0.001**
Water storage traits			
Leaf succulence, mg cm^{-2} (*n*=15)	35.3 ± 7.9	25.2 ± 5.7	**<0.001**
SWC, g g^{-1} (*n*=7)	5.2 ± 0.6	3.4 ± 0.3	**<0.001**
$C_{ft,\ FRM}$ mmol $m^{-2}MPa^{-1}$ (*n*=6)	0.216 ± 0.093a	0.215 ± 0.080a	**S:0.012 M: <0.001**
$C_{tlp,\ FRM}$	0.667 ± 0.166 b	0.383 ± 0.078c	**SxM: 0.012**
$C_{ft,\ PV}$ mmol $m^{-2}MPa^{-1}$ (*n*=5)	2.049 ± 0.564a	1.033 ± 381.2a	**S:<0.001 M: <0.001**
$C_{tlp,\ PV}$	9.941 ± 1.865b	3.984 ± 1.643c	**SxM: <0.001**
$g_{min,}$ mmol $m^{-2}s^{-1}$(*n*=5)	8.3 ± 0.5	3.2 ± 0.8	**<0.001**
PV traits (*n*=5)			
Ψ_{tlp} (MPa)	1.48 ± 0.04	1.87 ± 0.14	**0.02**
π_0 (MPa)	1.19 ± 0.03	1.52 ± 0.16	**0.008**
ε_{max} (MPa)	17.20 ± 3.8	27.8 ± 1.6	**<0.01**
RWC_{tlp}(%)	74.5 ± 6.9	74.70 ± 5.4	0.975
Shrinkage traits (*n*=15)			
PTL_{tlp}, %	21.65 ± 9.39	10.64 ± 4.56	**<0.001**
PLA_{tlp}, %	6.89 ± 2.65	6.43 ± 2.56	0.777
PLV_{tlp}, %	21.5 ± 11.5	14.07 ± 5.7	**0.005**
PTL_{dry}, %	50.20 ± 7.10	26.11 ± 7.18	**<0.001**
PLA_{dry}, %	48.54 ± 5.98	45.21 ± 4.33	0.054
PLV_{dry}, %	74.67 ± 7.98	60.86 ± 5.52	**<0.001**

A 50% loss of K_L was recorded at different PLRC values ($PLRC_{KL50}$). The $PLRC_{KL50}$ was about 30% in *Sc* and 10% in *So* (Fig. 2C, G, Supplementary Table 1). Moreover, a tight correlation between K_L and REL was recorded in both species (Fig. 2D, H).

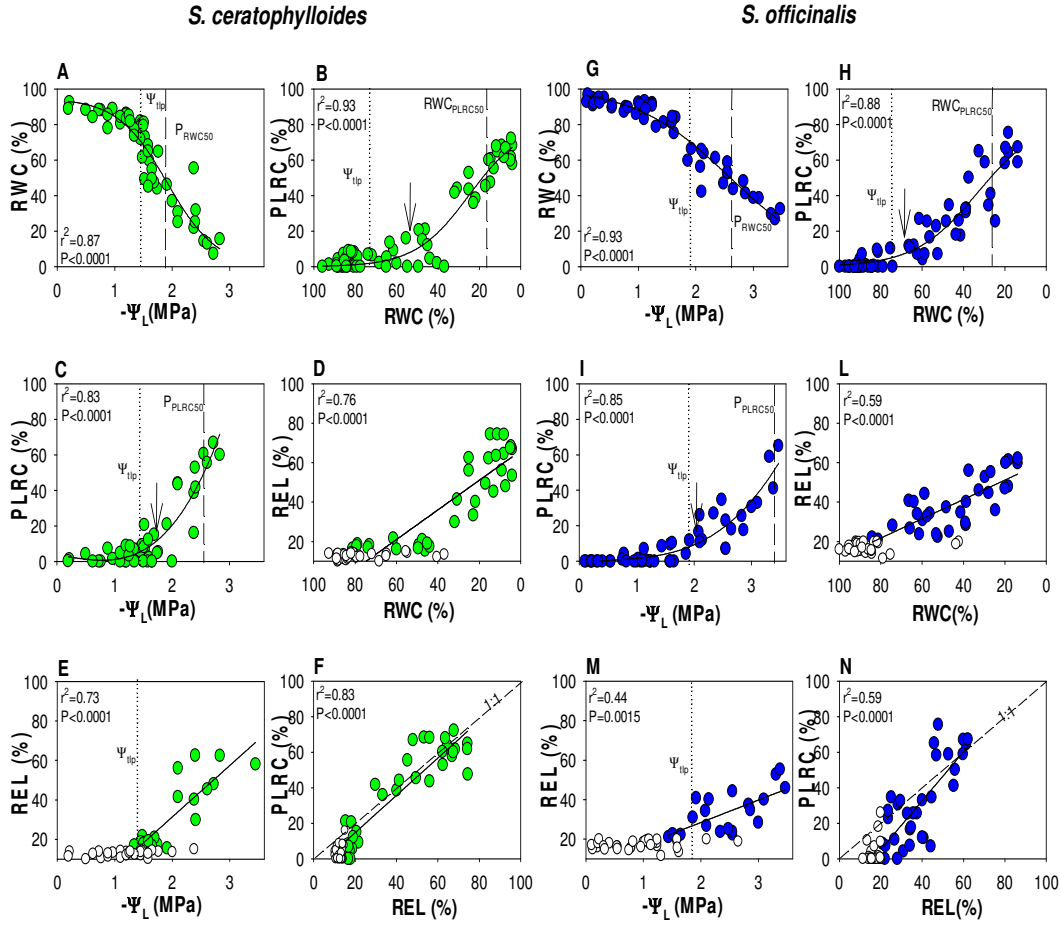

Figure 1: Decline of relative water content RWC (**A**, **G**), percentage loss of leaf rehydration capacity PLRC (**C**, **I**) and relative electrolyte leakage REL (**E**, **M**) with decreasing leaf water potential (Ψ_L); decline of PLRC (**B**, **H**) and REL (**D**, **L**) with decreasing RWC; relationships between PLRC and REL (**F**, **N**) as measured in *S. ceratophylloides* (green circles)and *S. officinalis* (blue circles). Best fitted regression curves are designed by dark line. White symbols indicate data not included in the regression. Fitted regression are as follows: A): RWC = 94.83/(1+exp(-(Ψ_L-1.91)/-0.43)); B): PLRC = 80.6/(1+exp(-(RWC-24.99)/-13)); C) PLRC = 3.5-4.43*Ψ_L-2.37*Ψ_L^2+4.4*Ψ_L^3; D) REL= 66.1-0.75*RWC; E) REL= -20.8+26.1 *Ψ_L; F) PLRC: = -6.3+1.05*REL; G) RWC = 101.2/(1+exp(-(Ψ_L -2.58)/-0.83)); H) PLRC = 83.57/(1+exp(-(RWC-33.14)/-15.1)); I) PLRC= -1.3+4.81*Ψ_L -3.95*Ψ_L^2+2.1*Ψ_L^3; L) REL= 60.9-0.49*RWC; M) REL= 5.6+11.4*Ψ_L; N) PLRC= -22.45+1.38*REL. r^2 and *P* value of each regression are reported. Dotted lines indicate the leaf water potential at turgor loss point (Ψ_{tlp}). Arrows in B), C), H), I) indicate the PLRC thresholds. Long dashed lines in B) and H) indicate the RWC value inducing 50 % PLRC (RWC_{PLRC50}). Long dashed lines in C) and I) indicate the Ψ_L value inducing 50 % PLRC (P_{PLRC50}). Short dashed lines in F) and N) indicate the 1:1 relationship.

Table 2: Mean values ± SD (*n*=5) of leaf hydraulic conductance (K_L) as measured in the two *Salvi*a species at low and high irradiance (LI and HI, respectively) by the evaporative flux method (EFM). *P* values as result of a two-way ANOVA by species (S), and irradiance (I) are given.

	S. ceratophylloides K_L **(mmol $m^{-1}s^{-1}MPa^{-1}$)**		***S. officinalis*** K_L **(mmol $m^{-1}s^{-1}MPa^{-1}$)**		***P* value**
	LI	**HI**	**LI**	**HI**	
EFM	21.7 ± 2.8	20.9 ± 6.1	17.9 ± 1.9	16.9 ± 2.3	**S**: **0.045** I: 0.871 SxM: 0.987

The study species showed different leaf saturated water content, i.e., 5.2 ± 0.6 g g^{-1} in *Sc versus* 3.4 ± 0.3 g g^{-1} in *So* (Table 1). This difference led to leaf hydraulic impairment occurring at different RWC but at similar absolute water content values (Fig. 3). Indeed, the increase in REL occurred at a leaf water content of about 2.9 g g^{-1} and, even more surprisingly, the most commonly used hydraulic conductance loss thresholds (i.e., 10%, 50% and 88% loss of K_L) were recorded at the same water content in *Sc versus So* (i.e., about 2.9 g g^{-1},1.8 g g^{-1} and 1.3 g g^{-1}, respectively, Fig. 3, Supplementary Table 1).

2.3. Discussion

Our data reveal that similar leaf water content thresholds induce similar leaf hydraulic impairment in two *Salvia* species, suggesting that leaf water content (but not RWC) might be a useful warning proxy for leaf hydraulic failure. Indeed, in contrast to our working hypothesis, *Sc* and S*o* showed different RWC thresholds for leaf hydraulic failure, but similar leaf water content values leading to leaf hydraulic decline during dehydration and cell membrane damage. Moreover, the lack of any K_L decline until the turgor loss point in *Sc*, despite consistent leaf shrinkage, provide new insights into the relations between leaf shrinkage and leaf hydraulic vulnerability. In fact, this result and the tight and linear correlation between K_L impairment and REL as recorded in *Sc* and *So,* strongly suggest that K_L decline is driven by leaf cell membrane damages, regardless of the amount ofleaf shrinkage. Thus, leaf shrinkage alone does not always predict t K_{ox} impairment, as previous studies had suggested (Trifilò et al., 2016; Scoffoni et al., 2017a). In this view, cell membrane damage, but not leaf shrinkage, may offer a more useful tool for monitoring the risk of K_L decline under drought.

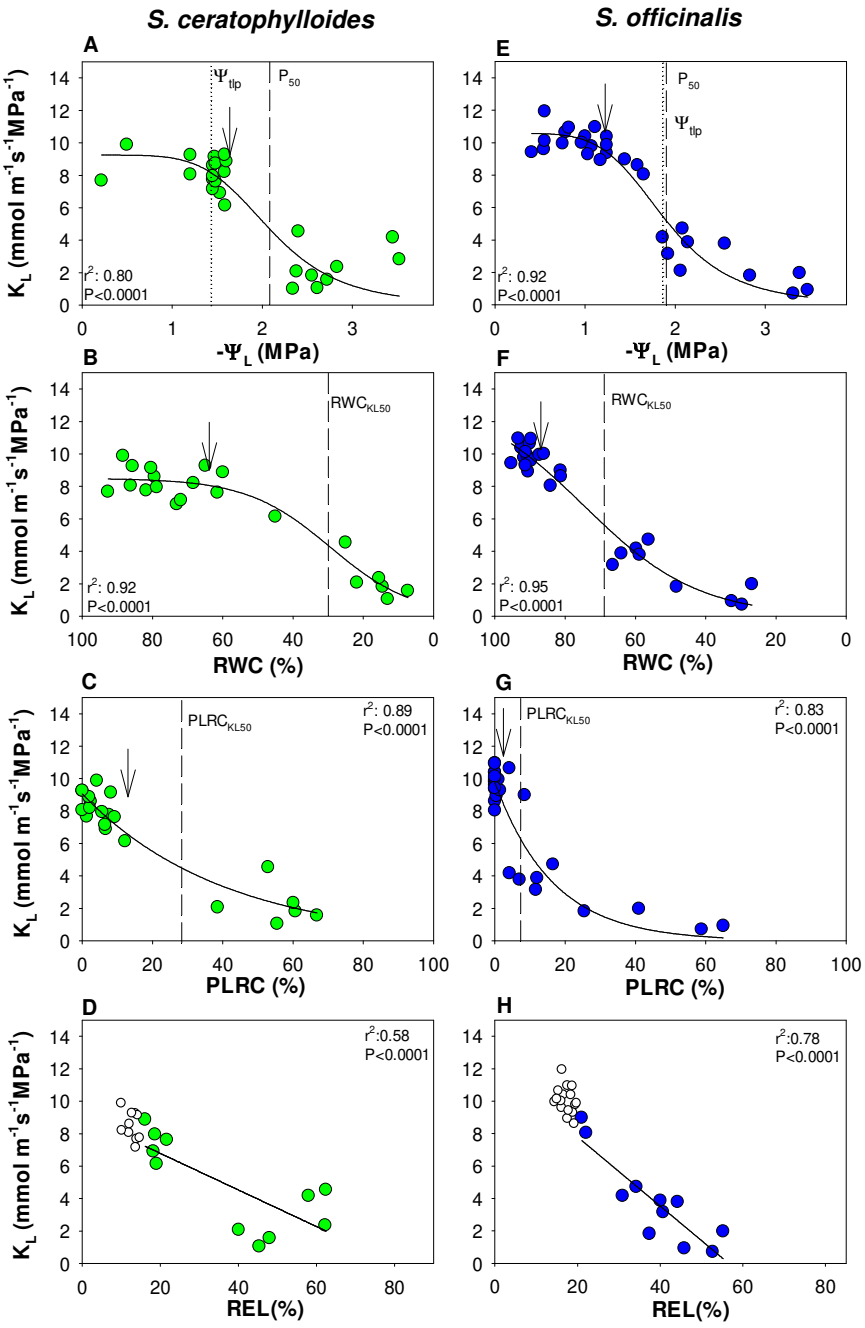

Figure 2: Decline of leaf hydraulic conductance (K_L) as a function of the leaf water potential Ψ_L (**A**, **E**), and the relative water content (**B**, **F**); relationships between K_L and percentage loss of leaf rehydration capacity PLRC (**C**, **G**) and relative electrolyte leakage REL (**D**, **H**) as measured in *S. ceratophylloides* (green circles) and *S. officinalis* (blue circles). Best fitted regression curve is designed by dark line. White symbols indicate values not included in the regression. Fitted regression are as follows: A) $K_L = 9.24/[1 + (\Psi_L /2.09)^{5.29}]$; B) $K_L = 8.5/(1+\exp(-(RWC-29.4)/11.9))$; C) $K_L = 9.05*\exp(-0.02*PLRC)$; D) $K_L = 9.04-0.11*REL$; E) $K_L = 10.6/[1 + (\Psi_L /1.88)^{4.98}]$; F) $K_L = 13.6/(1+\exp(-(RWC-74.6)/16.3))$; G) $K_L = 9.77*\exp(-0.06*PLRC)$; H) $K_L = 12.05-0.21*REL$. r^2 and *P* value of each regression are reported. Dotted lines indicate the leaf water potential at turgor loss point (Ψ_{tlp}). Arrows in A), B), E), F) indicate K_L thresholds. Long dashed lines in A) and E) indicate the Ψ_L value inducing 50% loss of K_L (P_{50}), in B) and F) indicate the RWC value inducing 50% loss of K_L (RWC_{KL50}) and in C) and G) indicate the PLRC value inducing 50% loss of K_L ($PLRC_{KL50}$).

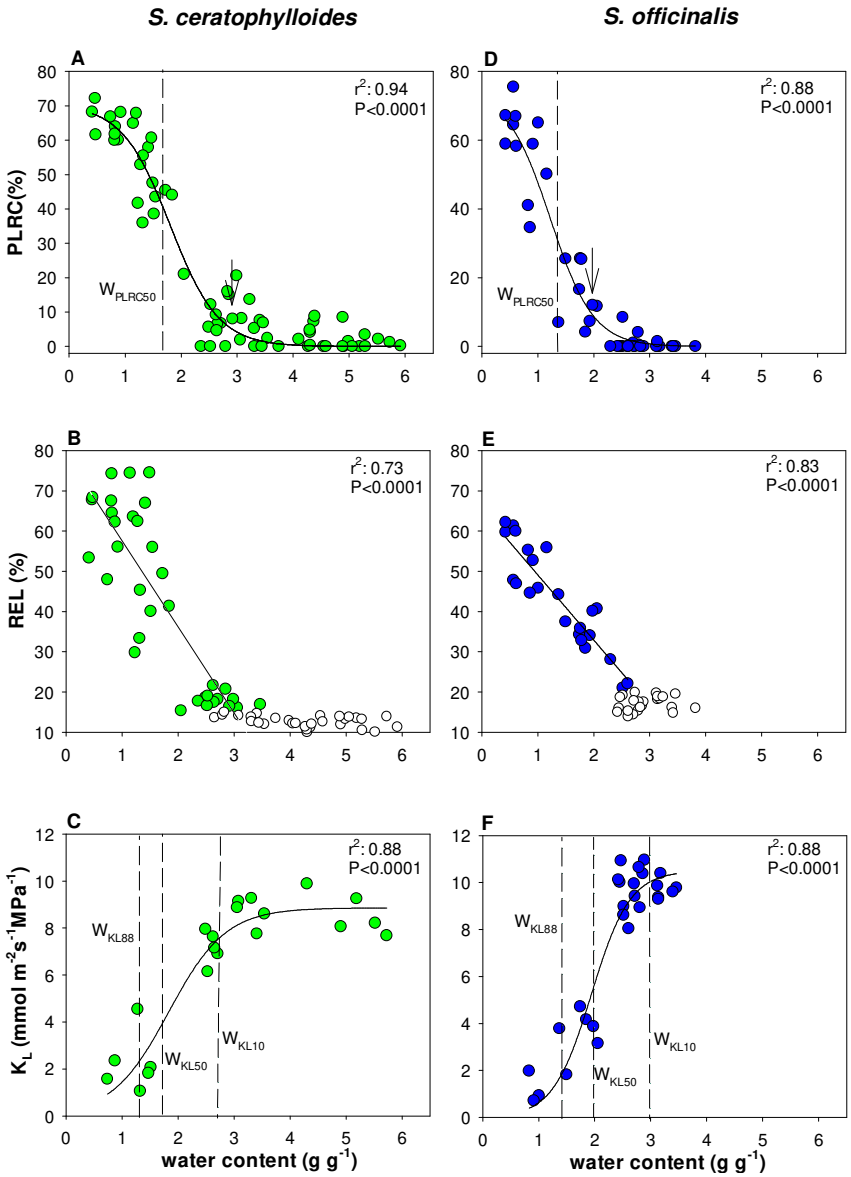

Figure 3: Relationships between water content (W) and percentage loss of leaf rehydration capacity, PLRC (**A**, **D**), relative electrolyte leakage, REL (**B**, **E**) and leaf hydraulic conductance K_L (**C**, **F**) as measured in *S. ceratophylloides* (green circles) and *S. officinalis* (blue circles). Best fitted regression curve is designed by dark line. White symbols indicate not included in the regression. Fitted regression are as follows: A) PLRC = 68.3/(1+exp(-(W-2.04)/-0.41)); B) REL=78.9-21.4*W; C) K_L=8.8/(1+exp(-(W-1.8)/0.5)); D) PLRC = 74.3/(1+exp(-(W-1.22)/-0.38)); E) REL= 65.3-16.2*W; F) K_L= 10.5/(1+exp(-(W-1.9)/0.34)). r^2 and *P* value of each regression are reported. Arrows in A) and D) indicate PLRC thresholds. Long dashed lines in A) and D) indicate the water content inducing 50% loss of PLRC value (W_{PLRC50}), in C) and F) indicate the water content value inducing 10% (W_{KL10}), 50% (W_{KL50}) and 88(W_{KL88}) loss of K_L.

2.3.1. Leaf water storage and its relationships with leaf hydraulic vulnerability

Sc and *So* showed different water-use strategies, as indicated by significantly different leaf water relation parameters. In *Sc*, the relatively low modulus of elasticity, coupled to high SWC and leaf capacitance, allowed maintaining relatively high cell water content during the first steps of

dehydration with respect to *So*. This behaviour apparently delayed leaf hydraulic impairment caused by turgor loss. After the turgor loss point, the increase in leaf capacitance recorded in *Sc* increased the water loss per unit change in water potential, thus inducing a more rapid drop in RWC compared to *So*. Water relations of *So* have been described in previous studies, highlighting the drought tolerance strategy of the species (Raimondo et al., 2015; Savi et al., 2016). Lower Ψ_{tlp} and π_o values, and higher bulk ε_{max} of *So* compared to *Sc*, would confirm such a drought tolerance strategy (Bartlett et al., 2012; Tombesi et al., 2014). It should be noted that higher cell wall rigidity causes sharper drop of Ψ_L per unit water loss (i.e., Tyree and Hammel, 1972; Bartlett et al., 2012), leading to higher RWC_{tlp} (Salleo, 1983). However, likely because of similar values of leaf capacitance before the turgor loss and about 0.4 MPa lower Ψ_{tlp} as recorded in *So versus Sc*, the RWC_{tlp} was similar in the two species. These contrasting water use strategies are consistent with recorded differences in terms of leaf succulence, which was higher in *Sc* compared to *So*. Moreover, differences between the two species were recorded in terms of leaf capacitance at the turgor loss point: it was two-fold higher in *Sc* than in *So*. Succulence syndrome is common for species living in semi-arid habitats, where the occurrence of dry periods is balanced by rain events and water inputs from fog or dew that can supplement the low precipitations (Ogburn and Edwards, 2010; Griffiths and Males, 2017). High water storage allows plants to maintain relatively stable leaf water potential and water content despite fluctuations of transpiration rate and water supply (Sack and Tyree, 2005). Thus, succulence allows avoiding drought damage at the cellular level and maintaining, as long as possible, metabolic activity (Eggli and Nyffeler, 2009; Ogburn and Edwards, 2010; Griffiths and Males, 2017; Males 2017). However, no sharp distinction exists between succulent and non-succulent species and, for this reason, succulence is considered as a "continuous" trait (Ogburn and Edwards, 2010; Griffiths and Males, 2017). This was also the case for the two *Salvia* species, with *So* showing a moderate succulence syndrome as well. In fact, *So* showed lower cuticular transpiration and higher V_L and T_L than *Sc,* and similarly high values of leaf capacitance before the turgor loss were recorded in *Sc* and *So* (Pivovaroff et al., 2014). Moreover, large parenchymatic cells without chloroplasts were observed around veins of the two study species (data not shown). These cells, observed also in other *Salvia* species (i.e., Kaharam et al., 2010; Erbano et al., 2012; Bercu et al., 2012), can exhibit high water retention efficiency and might be involved in water storage (Muries et al., 2019).

Different hydraulic behaviour between the two species emerged also in terms of K_L responses to dehydration. In *Sc*, K_L decline only occurred after the turgor loss point and at RWC values as low as about 65%. Similarly, an increase in PLRC was recorded at $\Psi_L<\Psi_{tlp}$ and at RWC of about 55%.

By contrast, in *So* the K_L decline started before the turgor loss point (i.e., P_{10} occurred at Ψ_L<-1.3 MPa) and at RWC of about 90%. Moreover, loss of rehydration ability occurred at $\Psi_L \sim \Psi_{tlp}$ and at RWC values as high as about 70%, already. Hence, different RWC thresholds were indicative of leaf hydraulic decline in *Sc versus So*. Surprisingly, thresholds of leaf hydraulic vulnerability corresponded to very similar absolute leaf water content in *Sc* and *So*. In fact, due to different leaf SWC in the two species, 10%, 50% and 88% loss of K_L occurred at different leaf water potential and RWC, but at similar absolute water content. Water content values approaching 3 g g^{-1} (corresponding to RWC values of about 60% in *Sc* and 85% in *So*) triggered leaf membrane damage in both species, strongly affecting K_L (see also comments below). In summary, higher SWC and succulence allowed *Sc* to maintain sufficiently high water content to delay hydraulic impairment under water deprivation and down to turgor loss point. Moreover, the critical leaf water content of 3 g g^{-1} induced a rapid increase in membrane and hydraulic damage (as recorded in terms of PLRC, REL and K_L) also in this species, as observed for *So*.

It can be noted that not only absolute leaf water content but also Ψ_L resulted a useful proxy to monitor the risk of hydraulic impairment. Ψ_L values of about -2 MPa induced 50% loss of K_L as well as Ψ_L values of about -1.3 MPa caused initial increase in leaf cell membrane damages. Actually, leaf water content and Ψ_L changes during dehydration provide different indicators of leaf hydraulic impairment during dehydration. Water content changes likely better convey the loss in cell volume and then cell membranes damage. Thus, it can better explain damages at cell level. By contrast, because Ψ_L thresholds vary enormously among species (Bartlett et al., 2012; Trueba et al., 2019) it may be particularly useful for monitoring drought-induced mortality at intra-specific (Sapes and Sala, 2021) or, as in the present study, at interspecific level.

2.3.2. Role of the extra-xylem pathway, and of cell membrane integrity, in governing K_L decline during dehydration

Leaf hydraulic conductance depends on the features of both xylem (K_x) and extra-xylem (K_{ox}) water pathways. During dehydration, the xylem pathway can be compromised by xylem embolism events that, in turn, are triggered when species-specific water potential values are surpassed (i.e., Sack and Scoffoni 2013; Petruzzellis et al., 2020). K_{ox} decline is putatively caused by different mechanisms related to alterations in cell turgor and in cell membrane permeability and/or integrity, loss in cell-to-cell connectivity and changes in the leaf evaporation sites (Buckley, 2015). Indeed, our data confirm that turgor loss point is a critical threshold for leaf hydraulic impairment of the two *Salvia* species (Bartlett et al., 2012; Scoffoni et al., 2014; Trueba et al.,

2019). In fact, it represented the threshold of leaf hydraulic decline for *Sc* and the value at which 50% loss of hydraulic conductance was recorded in *So*.

Higher shrinkage was recorded in *Sc* compared to *So*, i.e., in the species with lower ε_{max} and higher Ψ_{tlp}. However, in *Sc* no K_L (and likely K_{ox}) decline occurred until Ψ_{tlp}, despite ongoing leaf shrinkage, suggesting that leaf shrinkage per se does not always affect K_{ox}. This result is in contrast with some previous studies reporting relationships between leaf shrinkage and drought tolerance traits (as Ψ_{tlp}, π_0, ε and LMA) and suggesting that leaf shrinkage may drive leaf hydraulic decline during mild dehydration (Scoffoni et al., 2014). Despite leaf shrinkage, membrane integrity was preserved down to water potential approaching Ψ_{tlp}, i.e., at Ψ_L causing already about 10% and 50% loss of K_L in *S*c and *So,* respectively. These results suggest that leaf shrinkage, at least during the first steps of dehydration, did not cause any loss in membrane integrity, although it might have affected membrane water permeability, especially where a parallel K_{ox} decline was recorded. Only above species-specific thresholds, severe cell shrinkage would cause membrane damage leading to hydraulic decline. Thus, even relevant leaf shrinkage, as long as membrane integrity is maintained, would not cause irreversible leaf hydraulic dysfunction (Scoffoni et al., 2014; Trifilò et al., 2021).

2.4. Conclusion

Our study shows that absolute leaf water content, but not RWC, is a reliable proxy of species-specific risk of irreversible hydraulic damage. In fact, despite the robust correlations between RWC and leaf membrane damage, K_L and PLRC as recorded in *Sc* as well as in *So,* no statistically similar RWC threshold inducing leaf hydraulic impairment was recorded in *Sc* and *So*. By contrast, similar leaf absolute water content values induced similar leaf hydraulic damages. Future investigations on a higher number of species and, mainly, on the effects of the leaf water content on whole plant fitness are needed to confirm our findings.

The loss in membrane integrity that occurred independently on the amount of leaf shrinkage had a key role in driving K_L decline, likely causing K_{ox} failure. Moreover, the recorded cell membrane drought resistance thresholds for hydraulic impairment suggest that changes in leaf cell vitality (easily measurable via electrolyte leakage tests) may be a very useful tool for monitoring the risk of irreversible leaf hydraulic failure. By contrast, leaf shrinkage may be a poor indicator of dehydration-induced damage, especially when species with significant succulence syndromes are considered.

2.5. Supplementary Material

Table S1: Relative water content (RWC), leaf water potential (P) and percentage loss of rehydration capability (PLRC) thresholds recorded in *S. ceratophylloides* and *S. officinalis*. Confidence intervals (CI) are also reported.

	S. ceratophylloides			*S. officinalis*		
Parameter	**value**	**2.5% CI**	**97.5% CI**	**value**	**2.5% CI**	**97.5% CI**
P_{RWC50}	-1,87	-1,78	-1,98	-2,66	-2,56	-2,75
P_{PLRC10}	-1,59	-1,48	-1,71	-2,03	-1,81	-2,21
P_{PLRC50}	-2,63	-2,48	-2,92	-3,42	-3,19	-3,78
RWC_{PLRC10}	54,79	48,70	63,20	68,13	63,36	72,18
RWC_{PLRC50}	16,65	12,55	19,42	26,62	21,79	30,49
P_{10}	-1,66	-0,81	-1,87	-1,27	-1,02	-1,40
P_{50}	-2,14	-2,01	-2,72	-1,89	-1,80	-2,04
P_{88}	-3,22	-2,68	-3,99	-3,12	-2,78	-3,37
RWC_{KL10}	63,49	54,43	73,36	88,03	82,96	93,90
RWC_{KL50}	32,83	27,38	37,45	67,63	64,12	70,67
RWC_{KL88}	13,88	12,79	20,41	38,13	30,82	46,45
$PLRC_{10KL}$	14,47	3,48	22,38	3,33	1,85	4,45
$PLRC_{KL50}$	27,70	17,73	49,17	6,71	3,86	11,86
W_{PLRC10}	3,10	2,83	3,54	2,25	2,10	2,41
W_{PLRC50}	1,75	1,66	1,84	1,33	1,24	1,43
W_{KL10}	2,80	2,30	3,61	3,06	2,60	3,48
W_{KL50}	1,66	1,43	1,89	1,99	1,81	2,14
W_{KL88}	1,31	1,00	1,55	1,44	1,18	1,72

Legend:

P_{RWC50}: leaf water potential corresponding to 50% of the relative water content

P_{PLRC10}: leaf water potential inducing 10% loss of rehydration capability

P_{PLRC50}: leaf water potential inducing 50% loss of rehydration capability

RWC_{PLRC10}: relative water content inducing 10% loss of rehydration capability

RWC_{PLRC50}: relative water content inducing 50% loss of rehydration capability

P_{10}: leaf water potential inducing 10% loss of leaf hydraulic conductance

P_{50}: leaf water potential inducing 50% loss of leaf hydraulic conductance

P_{88}: leaf water potential inducing 88% loss of leaf hydraulic conductance

RWC_{KL10}: relative water content inducing 10% loss of leaf hydraulic conductance

RWC_{KL50}:relative water content inducing 50% loss of leaf hydraulic conductance

RWC_{KL88}:relative water content inducing 88% loss of leaf hydraulic conductance

$PLRC_{KL10}$: percentage loss of rehydration capability corresponding to 10% loss of leaf hydraulic conductance

$PLRC_{KL50}$: percentage loss of rehydration capability corresponding to 50% loss of leaf hydraulic conductance

W_{PLRC10}: water content inducing 10% loss of rehydration capability

W_{PLRC50}: relative water content inducing 50% loss of rehydration capability

W_{KL10}: water content inducing 10% loss of leaf hydraulic conductance

W_{KL50}: water content inducing 50% loss of leaf hydraulic conductance

W_{KL88}: water content inducing 88% loss of leaf hydraulic conductance

.

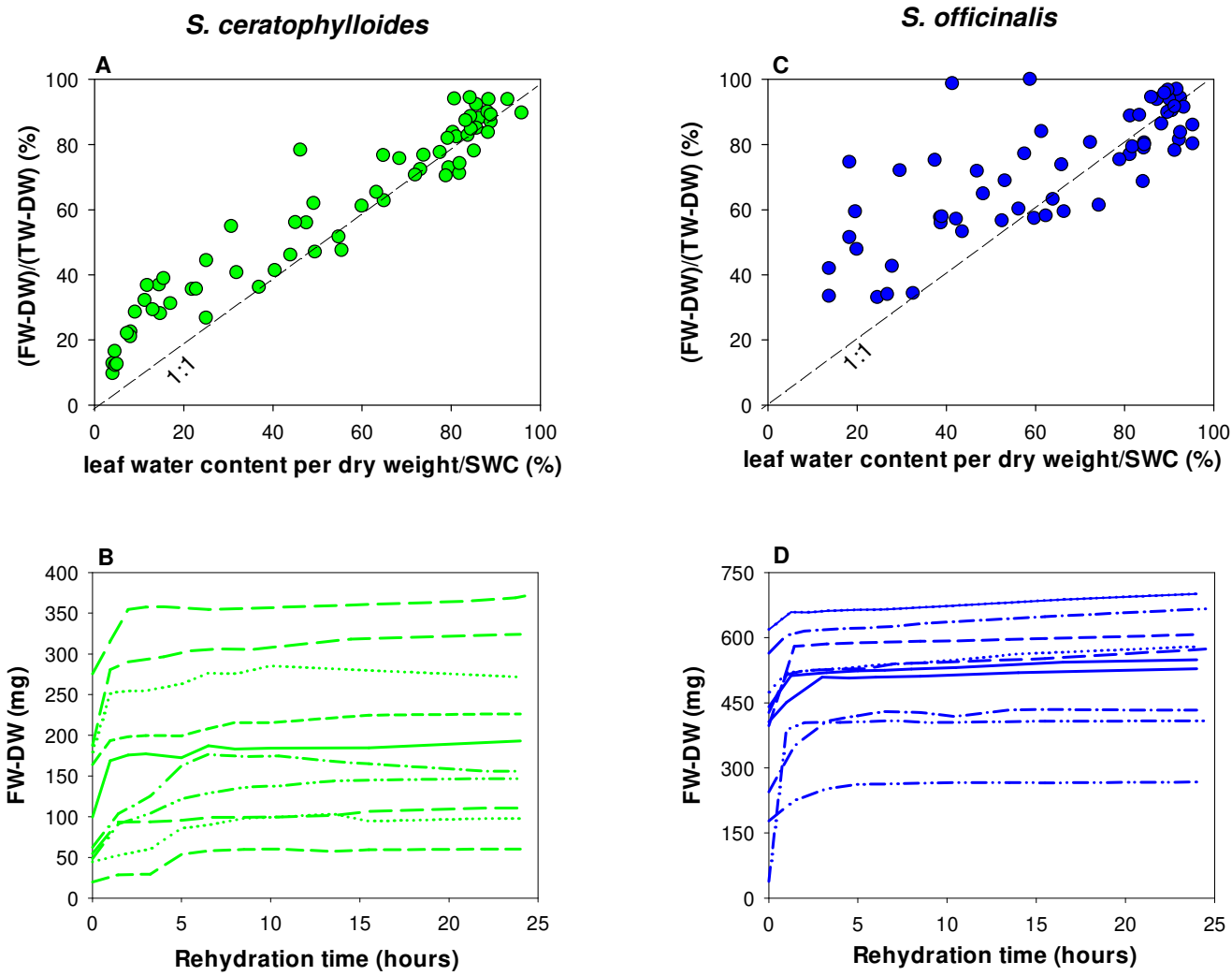

Figure S1: **A**) and **D**): Relationships between the relative water content estimated as: 100*(FW-DW)/ (TW-DW) and the relative water content measured as: 100* leaf water content per dry weight/SWC. Short dashed line indicates 1:1 relationship; **B**) and **D**) Monitoring of rehydration time of leaves at different initial water content measured as: FW-DW. Data have been recorded in *S. ceratophylloides* (Fig. 1A, B) and *S. officinalis* (Fig. 1C, D).
FW: fresh weight; TW: turgid weight, DW: dry weight; SWC: saturated water content

Chapter 3

Study 3

When water availability is low, two Mediterranean *Salvia* species rely on root hydraulics

Published as: **Abate E., Azzarà M., Trifilò P., 2021**. When water availability is low, two Mediterranean *Salvia* species rely on root hydraulics. ***Plants*** 10, 1888.

3. Introduction

In the last decades, the increase in severity and frequency of drought events is exposing vegetation to higher risk of drought-driven die-off (Allen et al., 2010; Carnicer et al., 2011; Menezes-Silva et al., 2019). According to climate projections, global warming is not expected to be homogeneous: higher increase in temperature and drought events have been forecasted for the Mediterranean region (e.g., Giorgi, 2006; Mariotti et al., 2015; Drobinski et al., 2020). This, in turn, may lead to more relevant negative feed-back on biodiversity richness of the Mediterranean biome, exacerbating the recorded ongoing vegetation pattern shifts (Cramer et al., 2018; Lionello and Scarascia, 2018; Penuelas et al., 2018; Juhlke et al., 2021) and increasing the extinction risk of endemic flora (Underwood et al., 2009; Ubran, 2015; Molina- Venegas 2020). Mediterranean region shows high levels of plant diversity and endemism, as a result of different co-occurring factors (Rundel et al., 2016; Molina-Venegas et al., 2017). The high numbers of endemic plant species are adapted to cope with warm and, frequently, long dry periods that typically occur in Mediterranean biome. Thus, the Mediterranean biodiversity hotspot is coupled to different specific adaptive strategies for delaying and/or tolerating tissue dehydration (*i.e.*, Vilagrosa et al., 2003; Villagrosa et al., 2014; Hernandez et al., 2010; West et al., 2012; Nardini et al., 2014; Gazol et al., 2017). However, increasing temperature and drought events might lead to exceed species-specific drought resistance threshold. In fact, vegetation response to ongoing climate change is a complex process involving the coordination of different, and not well-understood, physiological mechanisms. Plant hydraulics play a critical role in vegetation ability to cope with drought (Mc Dowell et al., 2017) and hydraulic failure is considered the major driver of vegetation die-off (Anderegg et al., 2016; Choat et al., 2018). Nevertheless, many questions on plant hydraulics remain unresolved (Mc Dowell et al., 2019; Klein et al., 2018) and looking for robust proxy for predicting plant die-back is urgent.

Changes in plant water content in response to drought have recently received a renewed attention (Martinez-Vilalta et al., 2019). Plant water status is linked to different key physiological mechanisms, including water transport and its regulation as well as carbon metabolism (Sapes et al., 2019; Sapes et al., 2021). On this view, the relative water content (RWC) has been suggested as a simple indicator of plant mortality risk. However, the species-specific cell desiccation tolerance is still largely unknown. In fact, at the best of our knowledge, only few studies investigated water content thresholds leading drought-induced mortality risk and it is unclear if a specific organ (leaf, stem, root) or whole plant water content can be an actual proxy of mortality risk. Rosner et al., (2019) have reported good correlations between stem RWC and the loss of

hydraulic conductivity in some tree species. However, in a most recent study, Mantova et al. (2021) pointed out that stem RWC is useful for predicting the loss of hydraulic conductivity in woody angiosperms but not in conifers.

In the present study we reported the hydraulic performance, including changes in relative water content, of two native Mediterranean species, *Salvia ceratophylloides* Ard. (*Sc*), a perennial herbaceous species (Crisafulli et al., 2010; Spampinato et al., 2011; Vescio et al., 2021), and *Salvia officinalis* L. (*So*), a perennial evergreen sub shrub (Pignatti, 2002), experiencing mild and severe drought events and then, re-watering. In detail, we compared the drought resistance strategy of *Sc versus So* (i.e., a drought-tolerant species, Raimondo et al., 2015; Savi et al., 2016) and the plant recover ability of the two *Salvia* species in order to investigate if and how mild or severe leaf hydraulic impairment and/or loss in cell rehydration ability can affect the whole plant hydraulics. In fact, similar whole plant drought vulnerability is expected on species with similar leaf hydraulic safety (Blackman et al., 2014; Nardini and Luglio, 2014; Fang et al., 2020). However, to the best of our knowledge, no study focused on species showing a moderate succulence syndrome. Recently, Abate et al. (2021a) reported higher leaf succulence in *Sc vs So*. This, in turn, led to different RWC thresholds but similar leaf water potential and leaf water content for leaf dehydration vulnerability in the two *Salvia* species (Abate et al., 2021a). On this basis, we tested the impact of leaf hydraulic impairment on the whole plant drought vulnerability in *Sc* and *So*. Moreover, we checked: *i*) possible relations between leaf, stem and root drought-driven water content and/or loss in cell rehydration ability and plant hydraulics of the two *Salvia* species in order to test possible tool(s) for monitoring the plant die-back and, then, for predicting the drought-driven risk of mortality; *ii*) if hydraulic traits and/or drought resistance mechanism of *Sc* may expose this species to potentially higher risk of extinction under predicted climate change scenario. *S. ceratophylloides* is a rare endemic perennial herbaceous species of southern Italy (Crisafulli et al., 2010). Until 2008 such a species had been considered “extinct in the wild” but most recent studies documented the presence of natural populations in its native area (i.e., Calabria, Italy) suggesting that the vulnerability of *S. cerathophylloides* has been likely induced by anthropogenic causes (as an improper use of the soil) more than an unsuited species-specific water use strategy (Spampinato et al., 2011; Vescio et al., 2021).

3.1. Materials and Methods

3.1.1. Plant material and growth conditions

Experiments have been performed on 48 samples per species of *S. ceratophylloides* (*Sc*) and *S. officinalis* (*So*) plants. Seeds were planted in greenhouse trays in October 2019, after maintaining them immersed in water for 24 h. By a month from sprouting, each seedling was transferred in a 3.4L-pot, filled with forest soil collected from Colli San Rizzo (Messina, Italy) and grown in a greenhouse until the beginning of May 2020. The greenhouse received natural light, with maximum daily values of photosynthetic photon flux density (PPFD) averaging 810 ± 260 μmol s^{-1} m^{-2}, air temperature ranging from 21 ± 2 °C to 17 ± 2 °C (day/ night), and air relative humidity of 55 ± 3%.

In May 2020, the samples were transferred in a garden of the Department CHIBIOFARAM, University of Messina, Italy, and regularly irrigated at field capacity for a month. Then, in June 2020 *Sc* and *So* plants were randomly divided in two groups (Fig. 1). One group (n=16) was regularly irrigated at field capacity during the whole experimental period (*i.e.*, watered samples, W). The second group (*i.e.*, water-stressed samples, S, n=32) was further divided in two groups (n=16) submitted to two different levels of water stress (Fig. 1). Specifically, water stress was induced by withdrawing irrigation until the two *Salvia* species reached the leaf water potential (Ψ_L) inducing about 50% (*i.e.*, Ψ_L~-2.0 MPa, S_{P50} samples) and 88% (*i.e.*, Ψ_L~-3.1 MPa, S_{P88} samples) loss of leaf hydraulic conductance, K_L, as recorded by some of us in a precedent study (Abate et al., 2021a). Then, a subset of S_{P50} (n=8) and S_{P88} samples (n=8) was measured (see below) and the other subset of S_{P50} (n=8) and S_{P88} samples (n=8), was re-irrigated and measured after 7 days (*i.e.*, Rec_{SP50} and Rec_{SP88} samples, respectively). During the experimental period no rainy events occurred. The temperature ranged from 18°C to 26 °C and the mean relative humidity was 65 ± 3.2% (weather station of Torre Faro, Messina, Italy).

3.1.2. Gas exchange and water status

Preliminary measurements on plants of similar age and growth conditions of those used in this study, showed that S_{P50} value was reached after 5-6 days and 3-4 days from withholding water in *Sc* and *So*, respectively, while S_{P88} value was recorded after10-11 days in *Sc* and after 7- 8 days in *So* from suspending irrigation. To avoid defoliation, we monitored the leaf water potential (*i.e.*, Ψ_L) declines on two leaves per day, as collected from different plants, starting from the 4th and 2nd day from withholding irrigation in S_{P50} *Sc* and *So* samples, respectively. Similarly, Ψ_L value of S_{P88}

samples were measured starting from the 8th and 5th day from suspending irrigation in *Sc* and *So*, respectively. This experimental procedure led us to remove no more than 2 leaves per sample.

Leaf water potential was measured by a portable pressure chamber (3005 Plant Water Status Console, Soilmoisture Equipment Corp., Goleta, CA, USA).

Ψ_L as well as leaf conductance to water vapour (g_L), transpiration rate (E_L) and photosynthetic rate (A_n) were measured at midday in W, S and re-irrigated samples using a portable LCi Analyzer System (ADC Bioscientific Ltd, Herts, UK). The water use efficiency (WUE) of each measured plant was estimated by the ratio: A_n/E_L. At least six plants per species and per treatment were measured.

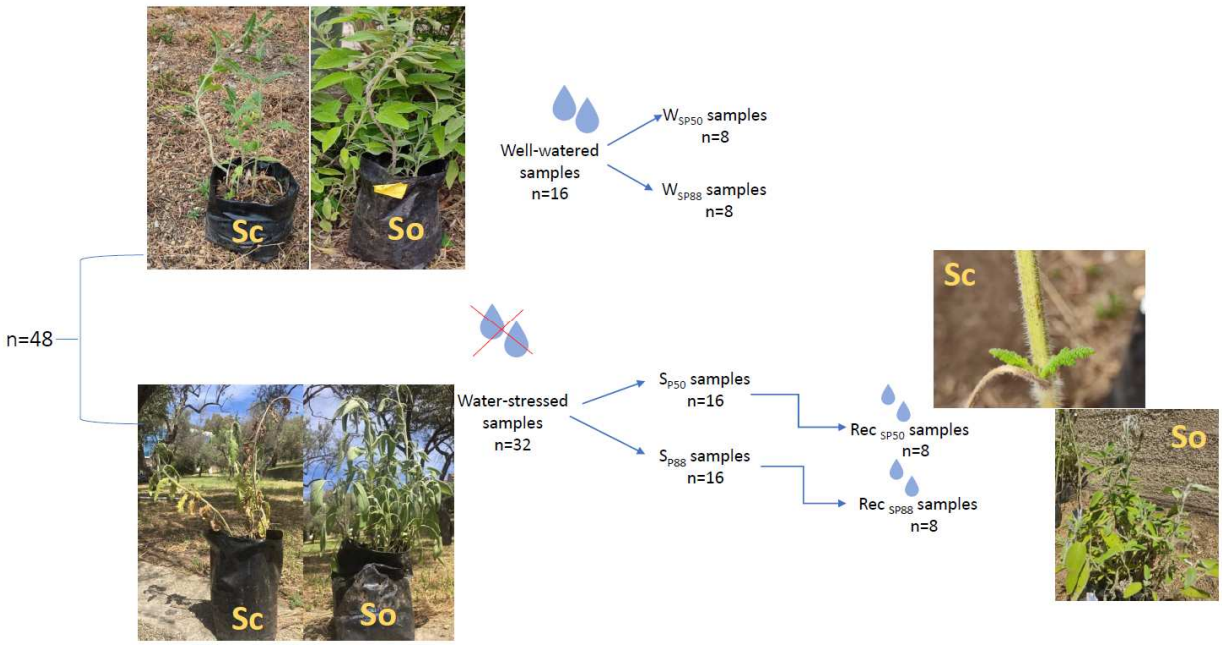

Figure 1: Experimental design: 48 potted samples of *S. ceratophylloides* (*Sc*) and *S. officinalis* (*So*) were divided in two groups: watered samples (n=16) and watered-stressed samples (n=32). Watered samples (W) were regularly irrigated at field capacity during the experimental period and measured, as control samples, at the same time of watered-stressed samples (*i.e*, 8 samples for each drought treatment). Watered-stressed samples were further divided in two groups subjected to a mild (*i.e*., S_{P50} samples, n=16) and a severe (S_{P88}, n=16) water-stress treatment, respectively. A subset of these samples (n=8) was measured when the imposed water stress level was reached while the other subset of drought-treated samples (n=8) was re-irrigated at field capacity (*i.e*., Rec_{SP50} and Rec_{SP88} samples) and, then, measured.

3.1.3. Estimating the relative water content, rehydration capacity and cell membrane integrity of leaf, stem and root samples experiencing drought-recovery treatment

Immediately after gas exchange and water status measurements and on the same W, S and Rec measured samples, the soil was kindly removed from root system and at least 2 samples of about 2 cm-long root and stem samples and 2 leaves per plant and treatment were collected for RWC, PLRC and REL measurements.

RWC was calculated as: 100*[(FW-DW)/DW]/SWC and PLRC as: 100*100-[(TW-DW)/ DW]/SWC where FW is the fresh weight (*i.e.*, the sample weight as measured immediately after sampling), TW is the turgid weight (*i.e.*, the sample weight as measured after maintaining the petiole or the whole stem and root sample immersed in deionized water for at least 8 hours), DW is the dry weight (*i.e.*, the oven-dried sample weight) and SWC is the saturated water content (*i.e.*, TW/DW, g g^{-1}) of sample at full turgor. Applied formula for estimating RWC allowed us to avoid mistakes as caused by cell loss rehydration ability, especially of low water status samples Abate et al., 2021a). Cell membrane integrity was indirectly estimated by electrolyte leakage test measurements (Trifilò et al., 2021). Leaf discs of about 0.5 cm^2 as well as 2 cm-long root and stem samples were cut with a razor blade and inserted in a test tube containing 8 mL of distilled water. Samples were stirred for 30 min at room temperature and, then, the initial electrical conductivity of the solution (EC_i) was recorded by a conductivity meter (Cond 5, XS instruments, Italy). Samples was then subjected to three freeze-thaw cycles (-20°C, +20°C) to induce complete membrane disruption and processed as above to measure the final electrical conductivity of the solution (EC_f). The relative electrolyte leakage (REL) was calculated as: (EC_i/EC_f) *100.

3.1.4. Structural traits and biomass allocation

Watered samples used for estimating RWC values were also measured for estimating: leaf dry matter content, (LDMC) as well as stem (SDMC) and the root (RDMC) dry matter content (as analogue of LDMC). LDMC, SDMC and RDM values were estimated by the ratio between leaf, stem or root dry weight and the corresponding turgid weight. Moreover, stem/ leaf dry weight ratio and root/ shoot dry weight ratio were also calculated. Root, stem and leaves dry biomass was estimated by oven drying samples for 3 d at 70°C.

3.1.5. Plant hydraulic conductance measurements by EFM

Plant hydraulic conductance (K_{plant}) values were measured in *planta* by the Evaporative Flux Method, EFM as:

K_{plant}: E_L / (Ψ_{soil} - Ψ_L)

where Ψ_{soil} was the soil water potential estimated by a psycrometer (WP4, Decagon Devices, Pullman, WA, USA). All hydraulic conductance values were corrected to a temperature of 20 ^oC to take into account changes in water viscosity.

Hydraulic measurements were estimated in at least 6 samples per species (*i.e.*, *S. ceratophylloides* and *S. officinalis*) and per treatment.

The EFM is expected for providing relative values of hydraulic conductance because its intrinsic limit in estimating the transpiration of the whole plant. Nevertheless, different studies have reported comparable data between EFM and other hydraulic measurements (Tsuda and Tyree, 2000; Trifilò et al., 2010; Aranda et al., 2005). Moreover, the method is considered suitable for comparing values when recorded in similar environmental conditions. Thus, in order to perform reliable hydraulic measurements, the water stress treatment was not imposed the same day in all samples. This experimental procedure allowed us to perform measurements on the same day (and, then, similar environmental condition) on at least 3 W, 3 S and 3 Rec samples per species and treatment so avoiding, as possible, differences in transpiration rate values induced by different boundary layer resistance. Nevertheless, temperature as well as RH values (and then VPD) were very similar during all the experimental period.

3.*1.6. Statistical analysis*

Data were analysed with the SigmaStat 12.0 (SPSS, Inc., Chicago, IL, USA) statistics package. To test leaf structural traits, plant biomass and water storage traits a t-test was performed. To test the differences among species (S, *i.e.*, *Sc* and *So*) and the effects irrigation treatment (T, *i.e.*, well-watered, W, water-stressed, S and re-irrigated, Rec, samples) on g_L, E_L, A_n, WUE, Ψ_L, K_{plant}, RWC, PLRC and REL a two-way ANOVA test was performed. When the difference was significant, a post hoc Holm-Sidak test was carried out. The significance of correlations was tested using the Pearson product-moment coefficient. Significance was evaluated in all cases at $P < 0.05$. Relationships between K_{plant} and leaf, stem, and root RWC, PLRC and REL values and associate 95% confidence intervals (C.I.s) were assessed in order to obtain species-specific and plant organ specific thresholds. Specifically, values of RWC (RWC_{50K} and RWC_{80K}), PLRC ($PLRC_{50K}$, $PLRC_{80K}$) and REL (REL_{50K} and REL_{80K}) corresponding to 50% and 80% loss of K_{plant} were estimated for each plant organ in *Sc* and *So*.

3.2. Results

S. ceratophylloides and *S. officinalis* differed strongly in biomass and structural traits (Table 1). *So* showed higher shoot biomass compared to *Sc*. Indeed, significant higher values of number of leaves per plant (about 165 *versus* 50), whole plant leaf area (2800 *versus* 800 cm^2), leaves dry weight (13 *versus* 2 g), and stem dry weight (1.1 *versus* 0.3 g) were recorded in *So versus Sc*. Moreover, a different shoot biomass allocation was recorded: *Sc* showed a statistically significant two-fold higher stem/leaf ratio than *So* (Table 1). The two study species showed similar root dry mass (*i.e*., about 1.3 g) but a 3-times higher root/shoot ratio value was recorded in *Sc* compared to *So* plants. *Sc* showed a higher leaf and stem satured water content (SWC) values than *So*. By contrast, not statistically significant different values of root SWC were recorded in the two species.

Table 1. Mean values ± SD of structural and biomass data and water storage traits as measured in well watered samples of *S. ceratophylloides* and *S. officinalis* plants (n=10). Differences between species were statistically analised and correspondig *P*-values are reported. N leaves/plant: number of leaves per plant; A_L: whole plant leaf area; LDMC: leaf dry mass content; DW leaves: leaves dry weight per plant; N shoots/plant: number of shoots per plant; DW stem: stems dry weight per plant; SDMC and RDMC: stem and root dry matter content, respectively; DW root: root dry weight; Stem/leaf ratio and Root/shoot ratio: stem/leaf dry weight ratio and root/ shoot dry weight ratio; SWC_{leaf}, SWC_{stem} and SWC_{root} leaf, stem and root saturated water content, respectively.

	S. ceratophylloides	*S. officinalis*	*P* value
Structural and biomass data			
N leaves/plant	47.7 ± 7.7	164.7 ± 59.3	**<0.001**
A_L (cm^2)	776 ± 80	2788 ± 976	**<0.001**
LDMC	0.16 ± 0.01	0.25 ± 0.03	**<0.001**
DW leaves, g	2.2 ± 0.9	12.7 ± 1.9	**<0.001**
N shoots/plant	2.4 ± 0.5	2.5 ± 1.3	0.411
DW stem, g	0.3 ± 0.1	1.1 ± 0.2	**<0.001**
SDMC	0.22 ± 0.03	0.31 ± 0.03	**<0.001**
Stem/leaf ratio	1.78 ± 0.95	0.95 ± 0.02	**0.007**
DW root, g	1.1 ± 0.4	1.4 ± 0.4	0.104
RDMC	0.14 ± 0.03	0.18 ± 0.01	**0.004**
Root/shoot ratio	2.2 ± 0.9	0.6 ± 0.3	**<0.001**
Water storage traits			
SWC_{leaf}, g g^{-1}	4.8 ± 0.4	2.7 ± 0.3	**<0.001**
SWC_{stem}, g g^{-1}	3.3 ± 0.6	2.4 ± 0.6	**<0.001**
SWC_{root}, g g^{-1}	5.2 ± 1.4	4.4 ± 0.5	0.061

The higher biomass values recorded in *So versus Sc* was likely the result of higher photosynthesis rate (A_n) and water use efficiency (WUE) values as recorded in well-watered samples of *So versus Sc* (Fig. 2). In response to mild (S_{P50}) and severe (S_{P88}) drought events, strong decreases in

stomatal conductance to water vapour (g_L), transpiration rate (E_L) and photosynthetic rate (A_n) were recorded in the two study species. However, it can be noted that in response to mild water stress, higher values of gas exchange and WUE occurred in *So versus Sc*. Moreover, a different drought sensitivity of the two *Salvia* species was recorded. In fact, in response to water shortage, a prompt stomatal closure occurred in *Sc* but not in *So* (Fig. S1). As a consequence, at S_{P50} (i.e., Ψ_L~ -2 MPa) *So* showed g_L loss of about 70% while in *Sc* samples cuticular conductance values were recorded already. S_{P50} treatment didn't induce permanent damages in the two *Salvia* species. Indeed, after a week of re-irrigation, S_{P50} samples showed all measured parameters statistically similar to values recorded before drought.

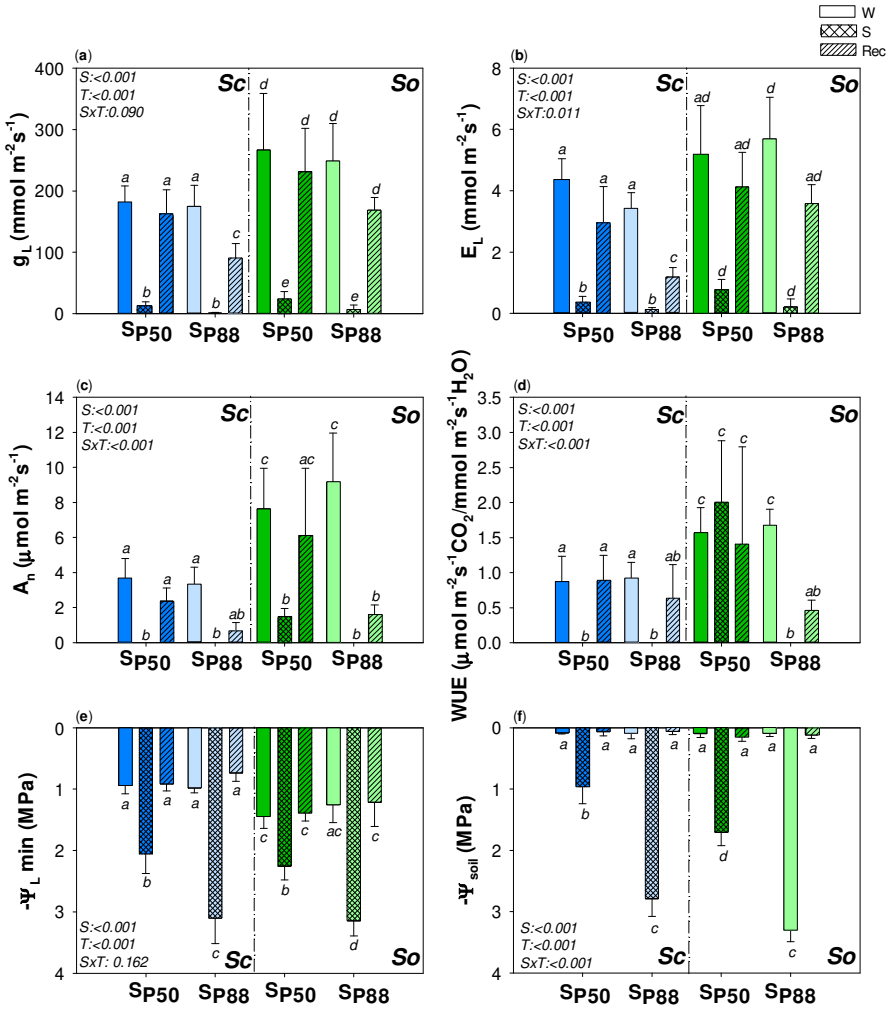

Figure 2. Mean ± SD (n=6) values of:**a**) midday leaf conductance to water vapour, g_L; **b**) transpiration rate, E_L, **c**) photosynthetic rate, A_n, **d**) water use efficiency, WUE, **e**) leaf water potential,Ψ_L and **f**) soil water potential,Ψ_{soil} as recorded in well-watered (W, none pattern), watered-stressed (S, slanting dash) and re-irrigated (Rec, mesh dash) plants of *S. ceratophylloides* (*Sc*, blue columns) and *S. officinalis* (*So*, green columns) submitted to two different water stress levels, *i.e.*, S_{P50} and S_{P80} (for details, see the text). *P* values as obtained by the two-way ANOVA analysis are reported. Different letters indicate statistically significant differences between groups.

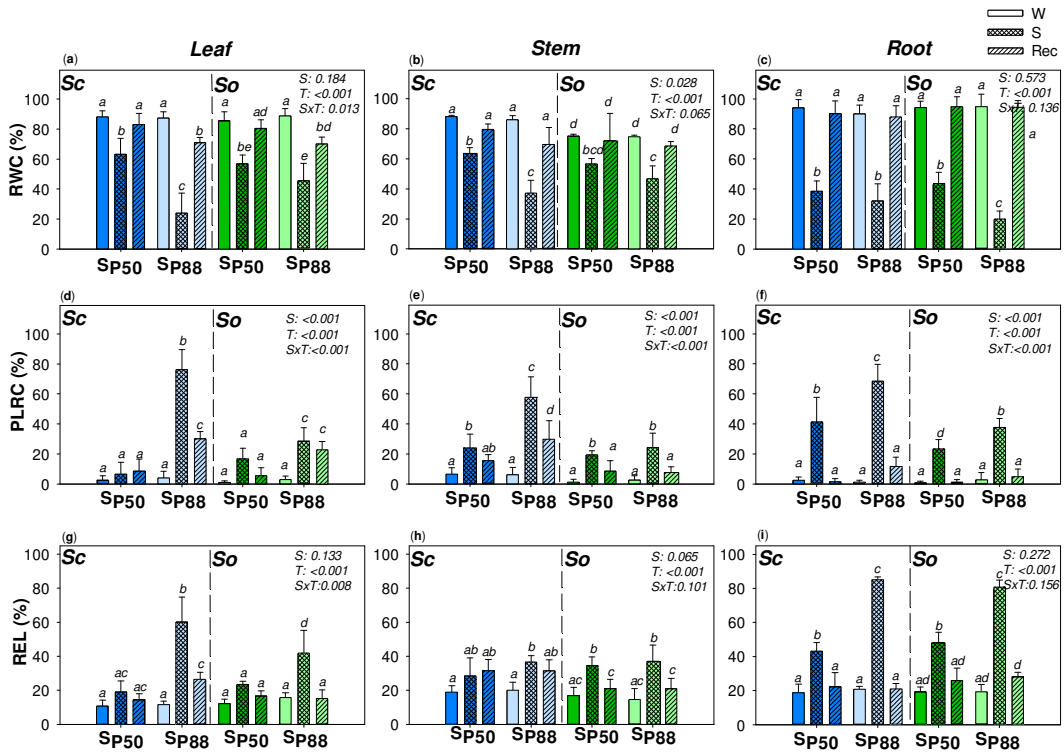

Figure 3. Mean ± SD (n=5) values of relative water content (RWC); percentage loss of rehydration capability (PLRC) and relative electrolyte leakage (REL) as recorded in leaf (**a, d, g**), stem (**b, e, h**) and root (**c, f, i**) samples of well watered (W, none pattern), watered stressed (S, slanting dash) and re-irrigated (Rec, mesh dash) plants of *S. ceratophylloides* (*Sc*, blue columns) and *S. officinalis* (*So,* green columns) submitted to two different water stress levels, *i.e.*, S_{P50} and S_{P80} (for details, see the text). *P* values as obtained by the two-way ANOVA analysis are reported. Different letters indicate statistically significant differences between groups.

By contrast, no full recovery of gas exchange and WUE was recorded after the applied severe water stress, despite the full recovery of the leaf water potential.Applied drought treatments strongly affected the relative water content of leaf, stem and root samples of the two *Salvia* species (Fig. 3). Surprisingly, however, after the re-watering a full recovery of root RWC values has been recorded, even when a severe water stress was experimented by *Sc* and *So* samples. This recovery was coupled to new roots growth, as observed in both species (data not shown). A different behavior was observed in the stem and leaf samples of the two *Salvia* species, especially in response to severe drought treatment. In fact, water stress inducing 50% loss of leaf hydraulic conductance (K_L, *i.e.*, S_{P50}) didn't affect the leaf and stem cell ability to recover water content in *Sc* and *So* samples and no permanent damage was recorded after re-watering in the two *Salvia* species. By contrast, experiencing about 88% loss of leaf hydraulic conductance (*i.e.*, S_{P88}), only a partial recovery of leaf RWC values in *Sc* as well as *So* samples has been recorded. The inability to recover the leaf water content was likely induced by a residual 20% loss in cell rehydration

capability, as recorded in the two species even after re-watering. However, it can be noted that leaf *Sc* samples were more severely affected by S_{P88} treatment. In accordance, S_{P88} leaf samples of *Sc* showed higher leaf cell membrane damages (*i.e.*, REL ~70% *versus* 40%, respectively) and higher percentage loss of cell rehydration capability (PLRC) values (*i.e.*, 80% *versus* 20%, respectively) compared to *So* S_{P88} leaf samples. Moreover, *So* stem samples were not permanently affected by experiencing severe water stress. By contrast, in Rec_{SP88} *Sc* stem samples a residual 20% PLRC and REL values high as about 35% were recorded. *So* and *Sc* well-watered samples showed similar plant hydraulic conductance (K_{plant}) values (Fig. 3). Moreover, similar K_{plant} values were recorded when the two *Salvia* species were submitted to the two drought treatments and, then, re-irrigated (Fig. 4).

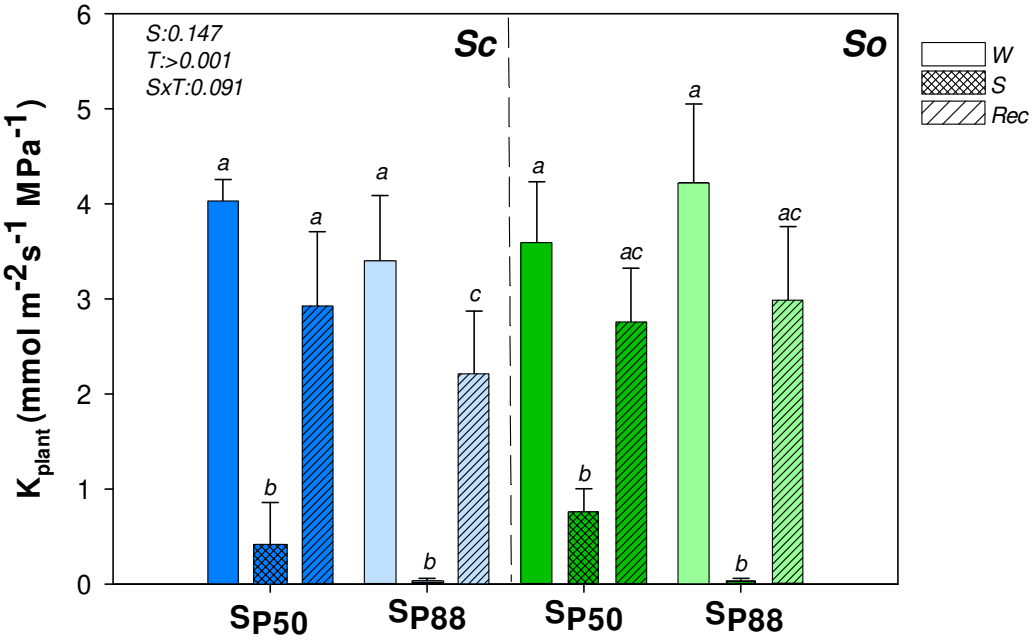

Figure 4. Mean ± SD (n=6) values of plant hydraulic conductance (K_{plant}) as recorded in well watered (W, none pattern), watered stressed (S, slinting dash) and re-irrigated (Rec, mesh dash) plants of *S. ceratophylloides* (*Sc*, blue columns) and *S. officinalis* (*So*, green columns) submitted to two different water stress levels, *i.e.*, S_{P50} and S_{P80} (for details, see the text). *P* values as obtained by the two-way ANOVA analysis are reported.Different letters indicate statistically significant differences between groups.

Very robust correlations were recorded between K_{plant} and leaf, stem and root relative water content in the two *Salvia* species (Figs. 5,6). Drought-driven K_{plant} decline was clearly strongly related to the cell loss rehydration capability as well as to drought-driven cell membrane damages. It can be noted that RWC, PLRC and REL thresholds of K_{plant} impairment were similar among the

three plants organs as well as between *Sc* and *So* (Figs. 5, 6, Table S1). Only leaf RWC value leading to 80% loss of K_{plant} was significantly lower in *Sc versus So*, as well as no confidence intervals overlapping has been recorded between *Sc* leaf *versus So* root REL value leading to 50% loss of K_{plant} (Figs. 4, 5, Table S1). Nevertheless, overall, in all three plant organs, RWC values low as about 65% as well as PLRC values of about 15% led to K_{plant} loss of 50% in the two *Salvia* species. It can be noted that large confidence intervals were recorded between leaf PLRC and REL values and the corresponding plant hydraulic conductance declines. By contrast, most robust correlations were recorded between K_{plant} and stem and root samples.

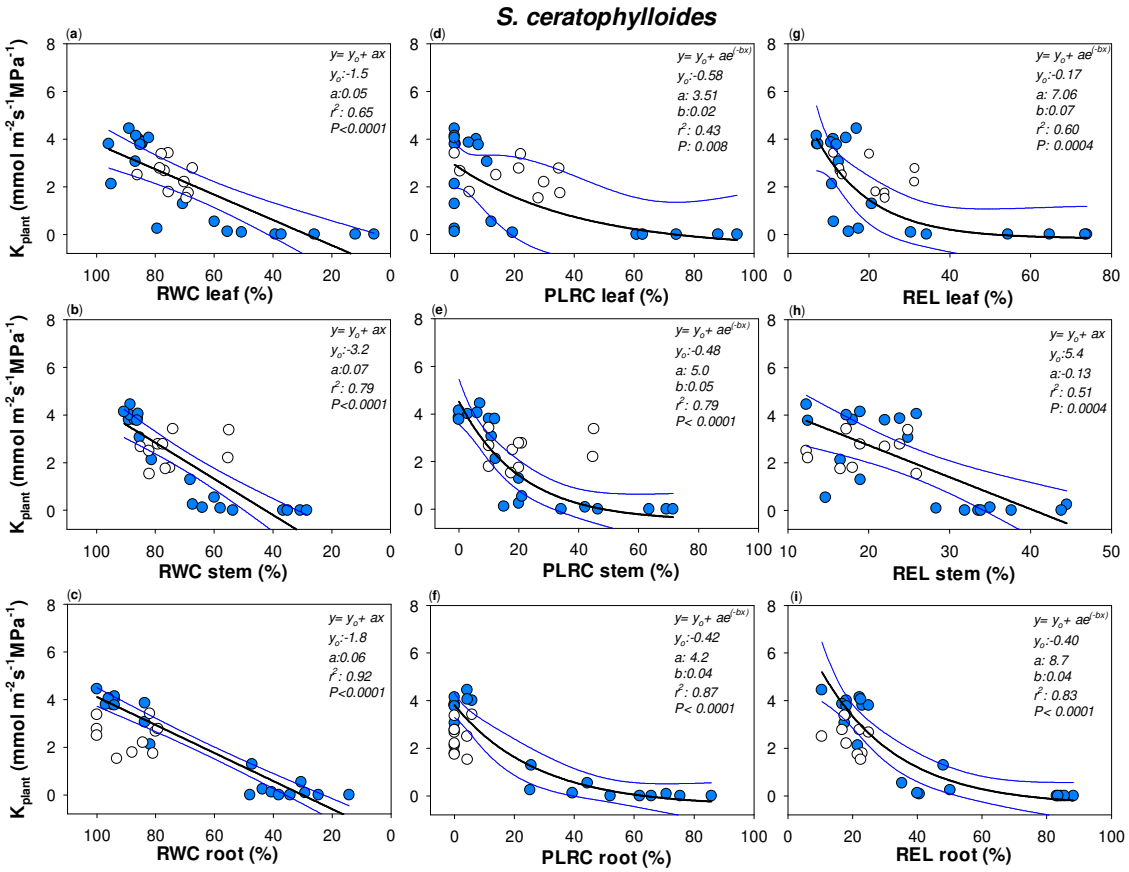

Figure 5: Relationships between plant hydraulic conductance (K_{plant}) and **a**) leaf, **b**) stem and **c**) root relative water content (RWCleaf, RWCstem and RWCroot, respectively),**d**) leaf, **e**) stem and **f**) root percentage loss of leaf rehydration capacity (PLRC leaf, PLRC stem, PLRC root) and **g**) leaf, **h**) stem and **i**) root relative electrolyte leakage (REL leaf, REL stem and REL root) as measured in *S. ceratophylloides*. Best fitted regression curves are designed by dark line. Confidence intervals are designed by blue lines. White symbols indicate data recorded in re-irrigated samples and not included in the regression. Regression equation, coefficient values, correlation coefficients (r^2) and *P*-values are also reported.

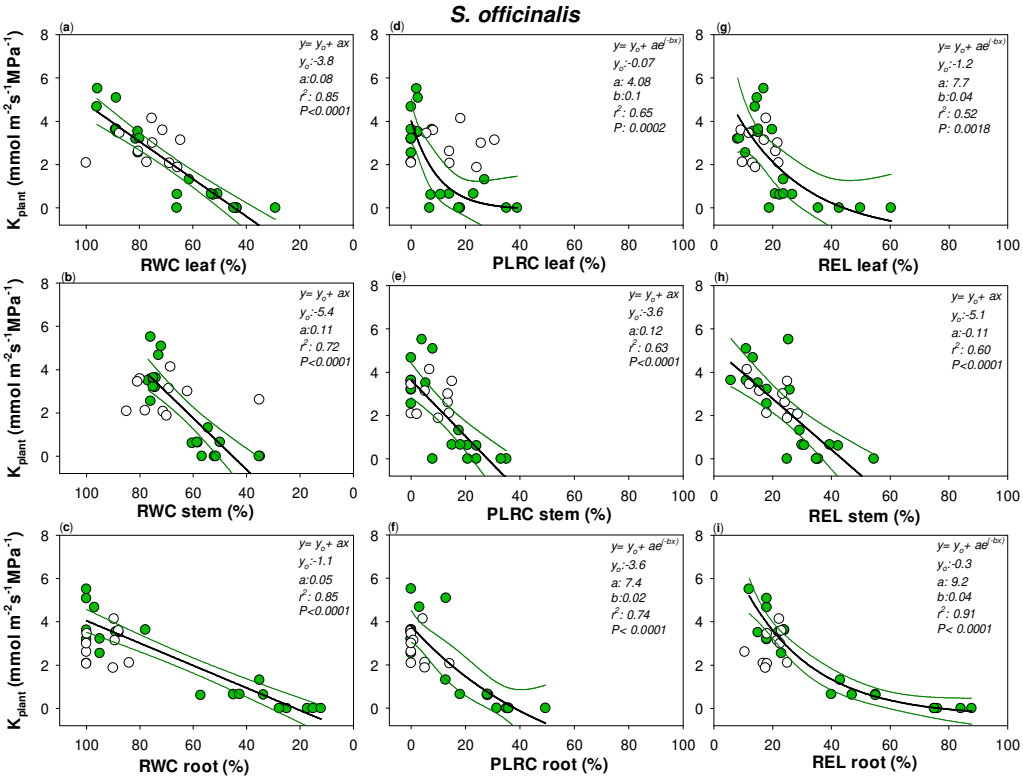

Figure 6: Relationships between plant hydraulic conductance (K_{plant}) and **a**) leaf, **b**) stem and **c**) root relative water content (RWC leaf, RWC stem and RWC root, respectively), **d**) leaf, **e**) stem and **f**) root percentage loss of leaf rehydration capacity (PLRC leaf, PLRC stem, PLRC root) and **g**) leaf, **h**) stem and **i**) root relative electrolyte leakage (REL leaf, REL stem and REL root) as measured in *S. officinalis*. Best fitted regression curves are designed by dark line. Confidence intervals are designed by green lines. White symbols indicate data recorded in re-irrigated samples and not included in the regression. Regression equation, coefficient values, correlation coefficients (r^2) and *P*-values are also reported.

3.3. Discussion

S. ceratophylloides and *S. officinalis* exhibited different resistance mechanisms for coping drought but a similar plant hydraulics recovery ability, especially in response to severe drought. In detail, recovery from mild water stress led to similar water content valuesin the three plant organsof the two *Salvia* species. However, different gas exchange and water use efficiency values occurred in *Sc versus So*. By contrast, experiencing about 80% of K_L loss caused different residual leaf and stem cell damages in *Sc versus So* samples but similar impact on gas exchange. Nevertheless, a similar K_{plant} recovery was recorded in *Sc* and *So* in response to the two drought-recovery treatments and no plant death was recorded neither after a month by the end of the experimental period (personal observation). Hydraulic recovery was obtained by new roots production and, then, renewed root functioning in *Sc* and *So* samples. This avoided permanent loss in root cell rehydration capability and cell membrane damages in fine roots (*i.e.*, site of water and nutrient uptake). Overall, these results strongly suggest that root hydraulics plays a key role

in whole plant recovery ability of the two Mediterranean native *Salvia* species. Moreover, our findings highlight that drought-driven changes in leaf RWC and PLRC values don't always provide an actual proxy of plant hydraulic failure, especially when succulent and/or water saving species are taken into account. In accordance, likely as a consequence of relevant cell damages, a consistent leaf shedding in *S. ceratophylloides* S_{P88} samples occurred (Fig. 1). Nevertheless, after a week of re-watering new sprouting leaves were observed in *Sc* Rec_{SP88} samples (Fig. 1). On this view, leaf hydraulic impairment weakly affected plant hydraulic conductance decline in *Sc* (*i.e.*, a water saver species showing a moderate succulence syndrome). Not at last, drought resistance strategy showed by *Sc* may affect its survival under frequent and extreme drought events.

3.3.1. Two different drought resistance strategies but a similar root hydraulics recovery ability

S. ceratophylloides invested less in biomass accumulation than *S. officinalis*, as lower LDMC, SDMC and RDMC values suggested. This was likely the result of lower stomatal conductance, photosynthesis rate and WUE as recorded in well-watered *Sc versus So* samples. These findings, along with the different leaf and stem SWC values recorded in the two *Salvia* species, confirmed a more pronounced succulent syndrome in *S. ceratophylloides* than in *S. officinalis* (Abate et al., 2021a). Overall, our results lead to consider *S. ceratophylloides* a resource conserving species. By contrast, *S. officinalis* exhibited a resource acquisitive strategy (Wright et al., 2004). In fact, well watered samples of *So* showed higher A_n, WUE as well as leaf, stem and root dry matter content values than *Sc* plants. Moreover, *So* showed a lower stomatal conductance reduction in response to mild drought: this led to higher gas exchange than *Sc*. Thus, our data confirmed a drought-tolerant mechanism in *So* samples (Raimondo et al., 2015; Savi et al., 2016). By contrast, a water-saving strategy was recorded in *Sc*. In fact, in response to mild stress, full stomatal closure was recorded in this species and, in response to severe stress, leaves shedding occurred. To avoid losses in carbon gain, species adapted to water shortage can increase their water-use efficiency (WUE) (*i.e.*, Brouillette et al., 2014). This strategy can be coupled to specific anatomical traits (as high vessel density and fibres and, then, high leaf mass per area) aimed to minimizing water loss (i.e., Poorter et al., 2009). In accordance, leaf mass area (LMA) increases along aridity gradients at a global scale (Wright et al., 2004). However, *Sc* showed a lower LMA value than *So* (Abate el al., 2021a) as well as a relevant reduction in WUE values in response to mild drought. Thus, the strategy adopted by *Sc* to cope with drought may explain the limited diffusion of this species in the Mediterranean region. In fact, the prompt stomatal closure, typically recorded in the water-saving species, as well as the inability to improve WUE under mild stress lead to an unavoidable severe

decrease in carbon uptake. In long term, especially after several severe drought events, this reduction in carbon assimilation may limit the sustainability of plant metabolism and its ability to recover from drought. This, in turn, may increase the chance of plant die-back. On this view, water-saving strategy is actually less efficient than drought-tolerant mechanism (Forner et al., 2014).

Nevertheless, similar plant hydraulic conductance decline and, mainly, similar hydraulic recovery ability in response to drought-re-irrigation treatment were recorded in the two *Salvia* species. Indeed, in response to a mild drought, no permanent damages of K_{plant} were recorded. Moreover, even drought-driven relevant leaf hydraulic dysfunction (*i.e.*, K_L loss ~88/%) led to similar residual K_{plant} loss of about 40% in *Sc* and *So*. The recovery of the two *Salvia* species was obtained mainly by root hydraulics recovery. In fact, *Sc* and *So* root hydraulics didn't remain negatively affected even by severe drought event. Root hydraulic conductance recovery can be obtained with the growth of new roots so by-passing the irreversible and permanent drought-driven damages occurring at root level (North and Nobel, 1991, 1996; Trifilò et al., 2004; Cuneo et al., 2020). However, root hydraulics can be restored even before growing new roots by renewing the permeability of damaged roots, as documented in succulent *Agave* and *Opuntia* species (Nobel and Sanderson, 1984; North and Nobel, 1991). Our results strongly confirmed that a high root biomass allocation, as recorded in both species, plays a key role in coping drought (Padilla et al., 2009; Markesteijn and Poorter, 2009; Lopez-Iglesias et al., 2014), and highlight the urgency to fill gaps in our knowledge on the relevance of root hydraulics in regulating whole plant hydraulics, especially under drought (Trifilò et al., 2004; Creek et al., 2018; Rodriguez-Domiguez and Brodribb, 2019; Bourbia et al., 2021; Weigelt et al., 2021). Additional experiments aimed to investigate coupled physiological and morphological root traits and, especially, their changes in response to drought are needed toimprove our lacking knowledge on this topic.

3.3.2. Water content and loss in rehydration capability actually drive plant hydraulics

Water content but also loss of rehydration capability and cell membrane damages were actually proxy of the drought-driven plant hydraulic conductance decline in the two *Salvia* species. However, it can be noted that, despite robust correlations occurred in all three organs, higher correlations values were recorded in root samples of the two *Salvia* species. Moreover, the recorded large confidence intervals in the relationships between the drought-driven leaf PLRC and REL increases and the corresponding K_{plant} declines suggested a low reliability of these leaf parameters as indicator of plant hydraulic failure. On the other hand, in water saving species, as *Sc* is, leaf shedding occurs promptly to reduce water loss and, at the same time, can limit xylem

embolism spread. This, in turn, avoids that hydraulic failure extends to the more carbon-expensive organs, according to the 'hydraulic segmentation hypothesis (Pivovaroff et al., 2014). As a consequence, in this case, the leaf hydraulic failure may not necessarily lead to unavoidable plant hydraulic failure but it may be the signal of the implementation of an adaptive strategy aimed to maintain adequate plant water content and/or tolerate substantial water losses and tissue dehydration. On this basis, this specie-specific drought resistance strategy may over shadow link(s) between drought-driven plant decline and some leaf hydraulics traits.

3.4. Conclusions

Results recorded in the present study highlight as root plays a key role in plant drought resilience in the two measured *Salvia* species. Large biomass allocation into the root system likely allows to higher accumulation of reserves for sustaining post-drought recovery. Further studies monitoring leaf, stem and root water content and loss in cell rehydration capability can actually provide important insights enabling to a comprehensive understanding of drought resistance strategies of Mediterranean species and more accurate prediction of their fate in response to global warming.

3.5. Supplementary Material

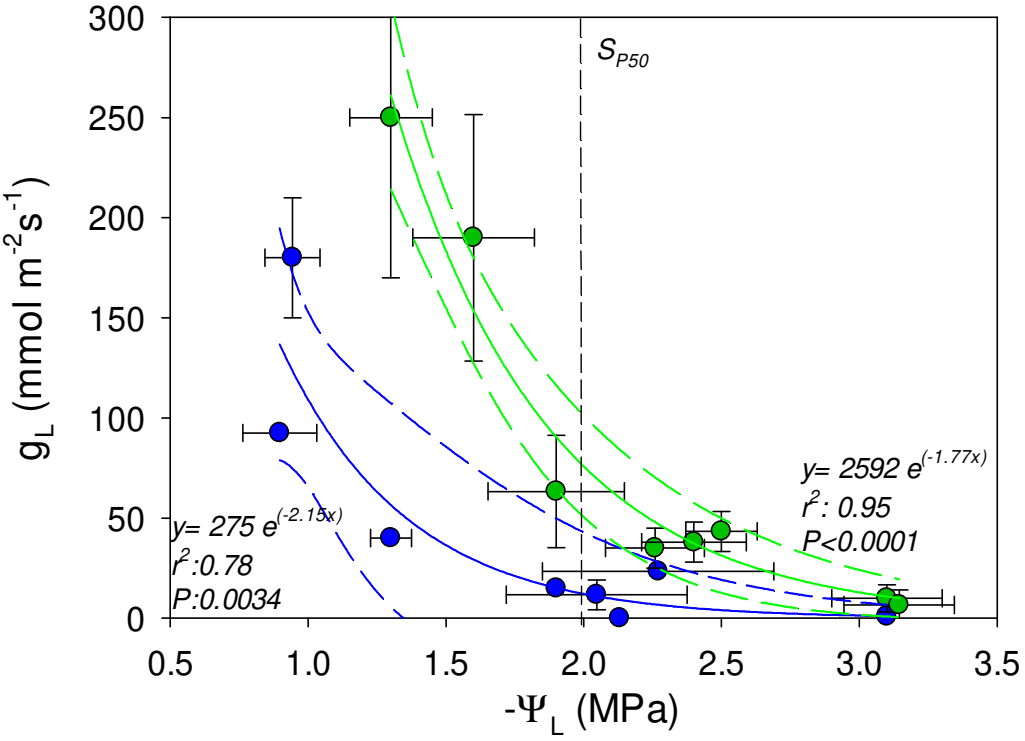

Figure S1: Relationships between mean ± SD values of midday leaf conductance to water vapour (g_L) and leaf water potential (Ψ_L) as recorded in *S. ceratophyllodes* (blue circle symbols) and *S. officinalis* (green circle symbols) samples during dehydration. Solid and long-dashed lines indicate the best-fit regression curve and corresponding 95% confidence intervals, respectively. Short-dashed line indicate the leaf water potential leading to 50% loss of leaf hydraulic conductance (S_{P50}). Regression equation, correlation coefficient (r^2) and P-values are reported.

Table S1: RWC, PLRC and REL values inducing 50% (i.e., RWC_{50K}, $PLRC_{50K}$, REL_{50K}, respectively) and 80% (i.e, RWC_{80K}, $PLRC_{80K}$ and REL_{80K}, respectively) loss of the plant hydraulic conductance as recorded in *S. ceratophylloides* (Sc) and *S. officinalis* (So) plants. Confidence intervals (CI) are also reported.

	Leaf				Stem				Root		
	RWC_{50K}	2.5% CI	97.5% CI		RWC_{50K}	2.5% CI	97.5% CI		RWC_{50K}	2.5% CI	97.5% CI
Sc	64	75	54		67,5	74	62		64	54	69
So	67,5	71	64		62	65,5	58		60	65	52,5
	RWC_{80K}	2.5% CI	97.5% CI		RWC_{80K}	2.5% CI	97.5% CI		RWC_{80K}	2.5% CI	97.5% CI
Sc	35	48	16		44	55	40		38	44	31,5
So	56	61	51		50	55	42,5		31	40	21
	$PLRC_{50K}$	2.5% CI	97.5% CI		$PLRC_{50K}$	2.5% CI	97.5% CI		$PLRC_{50K}$	2.5% CI	97.5% CI
Sc	14	0	50		15	10	21		15	9	25
So	6	4,5	14		14	9	17,5		15	9	24
	$PLRC_{80K}$	2.5% CI	97.5% CI		$PLRC_{80K}$	2.5% CI	97.5% CI		$PLRC_{80K}$	2.5% CI	97.5% CI
Sc	50	14	n.d.		34	21	n.d.		39	25	56
So	19	9	n.d.		24	18	34		30	20	n.d.
	REL_{50K}	2.5% CI	97.5% CI		REL_{50K}	2.5% CI	97.5% CI		REL_{50K}	2.5% CI	97.5% CI
Sc	16	13	25		25,5	20,5	31		30	26	37,5
So	21	15,5	30		26	21	32,5		32,5	29	39
	REL_{80K}	2.5% CI	97.5% CI		REL_{80K}	2.5% CI	97.5% CI		REL_{80K}	2.5% CI	97.5% CI
Sc	31	20	n.d.		38	32	n.d.		51	41	69
So	35	24	n.d.		39	32,5	50		55	45	70

Chapter 4

Study 4

Check-up of leaf, stem and root drought-driven water status as proxy of plant die-back

In preparation

4. Introduction

Increasing in frequency and intensity of drought events, as a consequence of climate changes (IPCC 2013; Pokherel et al., 2021), have causing severe effects on global ecosystems, including widespread tree mortality and crop failure (i.e., Allen et al., 2010; Hartmann et al., 2018; Klein and Hartmann, 2018; Lesk et al., 2016; Goulart et al., 2021). Stimulated by the ecological and social dramatic effects of vegetation mortality as well as by plant die-off feedbacks on climate changes, in the last twenty years a renewed and increasing interest into processes underlying drought-driven plant die-back and die-off has occurred (i.e., McDowell et al., 2008; 2019; Allen et al., 2015; Choat et al., 2018).

Past and recent literature have highlighted the key role of water transport functioning on plant resistance and resilience to water stress (Nardini et al., 2018). In accordance, there is general consensus that the blockage of the long-distance water transport system (i.e., hydraulic failure) is the major driver of vegetation mortality. As a consequence of plant dehydration, xylem water potential decreases leading to xylem embolism spread and the consequent water flow blockage. This finally provokes plant die-off (Choat et al., 2018). In fact, hydraulic impairment is coupled to stomatal conductance reduction up to stomatal closure and, then, to carbon assimilation blockage. Photosynthesis cessation leads to carbon starvation and to higher vulnerability to pests, i.e., co-occuring events causing climate change-driven vegetation die-off (Hartmann et al., 2018; Mc Dowell et al., 2019; Tomasella et al., 2021). Recently, Zweifel et al (2021) showed that the plant growth itself depends primarily on tree water relations and it is secondarily driven by current carbon allocation, at least in the short term.

Despite insight advances, however, many questions on plant hydraulics remain unresolved, including methodologically doubts for estimating species-specific xylem embolism vulnerability and/or plant ability to recover from drought (Klein et al., 2018; McDowell et al., 2019, Cardoso et al., 2020). Moreover, estimating loss of xylem hydraulic conductivity is very time-expensive and implicates high personnel and plant material costs. And, not least, commonly, the loss of hydraulic conductivity is estimated at stem level as proxy of whole hydraulic pathway (i.e., Choat et al., 2018). However, root as well as leaf extra-xylem water pathway play a key role into leading drought-driven hydraulic conductance (Vandeleur et al., 2014; Trifilò et al., 2016; 2021; Scoffoni et al., 2017; Tardieu et al., 2017; Abate et al., 2021b).

Overall, a reliable and easy-to-measure indicator of mortality risk is still lacking and the gaps in our knowledge leads to shortcoming of tree mortality predictive models (Powell et al., 2013; Fisher et al., 2018; Hood et al., 2018; Schwantes et al., 2018).

Recently, the measuring of the relative water content (RWC) has been proposed as tool for monitoring the risk of tree die-back (Martines-Vilalta et al., 2019), also considering canopy water content estimating at large scale by remotely sensed satellite data (i.e., Saatchi et al., 2013; Rao et al., 2019; Marusig et al., 2020). Water transport and its possible impairment is clearly related to soil water availability and plant water content. Moreover, gas exchange and plant productivity strongly depend by leaf water supply and, then, leaf water content (i.e., Brodribb et al. 2005; Trueba et al., 2019; Xiong and Nadal, 2020). On this view, RWC values tightly affect plant water transport integrity and carbon assimilation (Martines-Villata et al., 2019). In accordance, robust correlations have been recorded between relative water content and hydraulic conductance values (Trueba et al., 2019; Rosner et al., 2019; Mantova et al., 2021; Abate et al., 2021a), water content, hydraulic failure and carbon starvation (Sapes et al., 2019; Sapes and Sala, 2021) as well as between drought-driven percentage loss of rehydration capability (PLRC), RWC, relative electrolyte leakage (REL, as a proxy of cell membrane damages that, in turn, are associated with mortality) and leaf water transport efficiency (Guadagno et al., 2017; Trueba et al., 2019; Trifilò et al., 2021; Abate et al., 2021b). In a recent study, John et al. (2018) reported that the leaf RWC threshold leading to 10% PLRC decreases with increasing aridity experienced during the growing season. These results strongly encourage the use of water content and related parameters to cell water content as proxy of plant health. However, the workflow on water content measurements as tool for monitoring the plant health is not without challenges and needs to be implemented. As an example, it is unclear if whole plant or a specific plant organ water content threshold may be reliable indicator of mortality risk. Rosner et al. (2019) have reported good correlations between stem RWC and the loss of hydraulic conductivity in some tree species. However, RWC appeared useful for predicting the loss of hydraulic conductivity in woody angiosperms but not in conifers (Mantova et al., 2021). There is general consensus that leaf hydraulic vulnerability is the major driver of plant hydraulics (Brodribb and Holbrook, 2004; Brodribb et al., 2005; Hochberg et al., 2017; Skelton et al., 2017; Scoffoni et al., 2016; Wang et al., 2018; Xiong and Nadal, 2020). Therefore, it is plausible to hypothesize that leaf water content and/or related parameters might be a reliable proxy of plant water status. On this view, leaf cell dehydration tolerance threshold may be a promising tool for monitoring the drought-driven plant die-back across species, leaf habits and ecosystems (John et al., 2018). However, we don't know the impact of leaf water status and/or leaf cell PLRC on plant mortality risk. Recently, Abate et al. (2021a) reported that leaf water content, and not the leaf RWC, is a better proxy of hydraulic failure in two *Salvia* species. Moreover, Abate et al. (2021b), recorded weak correlations between leaf hydraulic failure of the

two *Salvia* species and whole plant decline. To the best of our knowledge, measurements of mortality risk as a function of leaf, stem, root and, then, plant water content were performed only in *Pinus pondersa* samples (Sapes et al., 2019; Sapes and Sala, 2021).

Therefore, we don't actually know if we can use measurements of leaf, stem and/or root water content as proxy of whole plant RWC decline, and, then, of mortality risk. Not least, no studies about possible artefacts on estimating dehydration thresholds as measured by fast and artificial dehydration method (i.e., bench dehydration method) have been performed.

In the present study we measured leaf, stem and root RWC, PLRC and REL values at different dehydration levels as obtained by bench dehydrated and pot dehydrated samples. Specifically, we tested: *i*) if a fast (and not actually natural) dehydration experimental procedure (as the commonly used bench dehydration method) may affect cell dehydration threshold values. Moreover, we checked: *ii*) possible differences in cell dehydration thresholds among leaf, stem and root samples and their impact on whole plant dehydration and mortality risk; *iii*) possible coordination between leaf, stem and root dehydration thresholds and stomatal closure, as proxy of drought-driven carbon starvation risk. Measurements have been performed on three species: *Helianthus annuus* L. (an herbaceous species), *Populus nigra* L. (a deciduous tree) and *Quercus ilex* L. (an evergreen).

4.1. Material and Method

4.1.1. Plant material and experimental planning

Experiments were performed in summer 2020 on one-year-old plants of *P. nigra* and *Q. ilex*) and the annual herbaceous *H. annuus* (n=80 per species). *P. nigra* and *Q. ilex* seedlings were kindly provided by Dip. Reg. Azienda Foreste Demaniali, Messina, Sicily, Italy. In February 2019 they were transferred in a garden of the campus of University of Messina and planted in 3.4 L pots filled with forest topsoil collected from Colli San Rizzo (Messina, Italy). Seeds of *H. annuus* were planted in greenhouse trays at the end of April 2020 (n= 40) and at the beginning of May (n=40) in order to measure samples of similar age (i.e., 9-15 weeks and, anyway, before flowering) during the experimental period. After the emergence of at least two developing leaves, seedlings were transferredin similar pots used for *Q. ilex* and *P. nigra* samples. All measured species were grown in the garden of the campus of University the Messina and regularly irrigated at field capacity every two days until the beginning of dehydration treatment. At the beginning of June, all samples were transferred in a greenhouse for submitting to dehydration treatments. The greenhouse received only natural light, with maximum daily values of photosynthetic photon flux density (PPFD) averaging 1370 ± 300 μmol s^{-1} m^{-2} (h: 11:00-12:30).

Sample dehydration was induced by two different experimental conditions: bench-dehydration and pot dehydration (Fig. 1). In bench dehydration treatment, well watered samples were maintained into a plastic bag for at least 8 hours after the irrigation and, then , gently pulled out of the plastic pot (Fig. 1B.). This experimental procedure allowed to obtain full hydrated samples (i.e., Time 0). gently pulled out of the plastic pot. The soil was cleaned up using low pressure water in order to avoid, as possible, damages to root. Then, the excess of water was quickly absorbed by paper towel and each sample was dehydrated inside a large plastic bag humidified with damp paper towel to prevent non-uniform transpiration. In pot dehydration treatment, dehydration was obtained by withholding irrigation.

During the dehydration treatments, samples were maintained in the greenhouse where the day/night temperature was 28 ± 3/22 ± 3 and the air relative humidity 61 ± 5. However, pot-dehydrated samples received natural light and were collected at different dehydration levels but at the same time slot (i.e.,11.30-12.30 am), bench-dehydrated samples were maintained in a large plastic bag in aired space of the greenhouse where no direct sunlight arrived and collected at different hours of the day and dehydration levels. Moreover, at least 2 well watered samples per each dehydration treatment and species were measured at pre-dawn, after maintaining pot samples inside a plastic bag during the whole night. The experimental procedure for cleaning up the soil from potted well watered samples was the same of bench dehydrated samples (Fig. 1B). In pot dehydrated samples (i.e., after 2-3 days by stopping irrigation), the soil was easily removed by root system without using low pressure water.

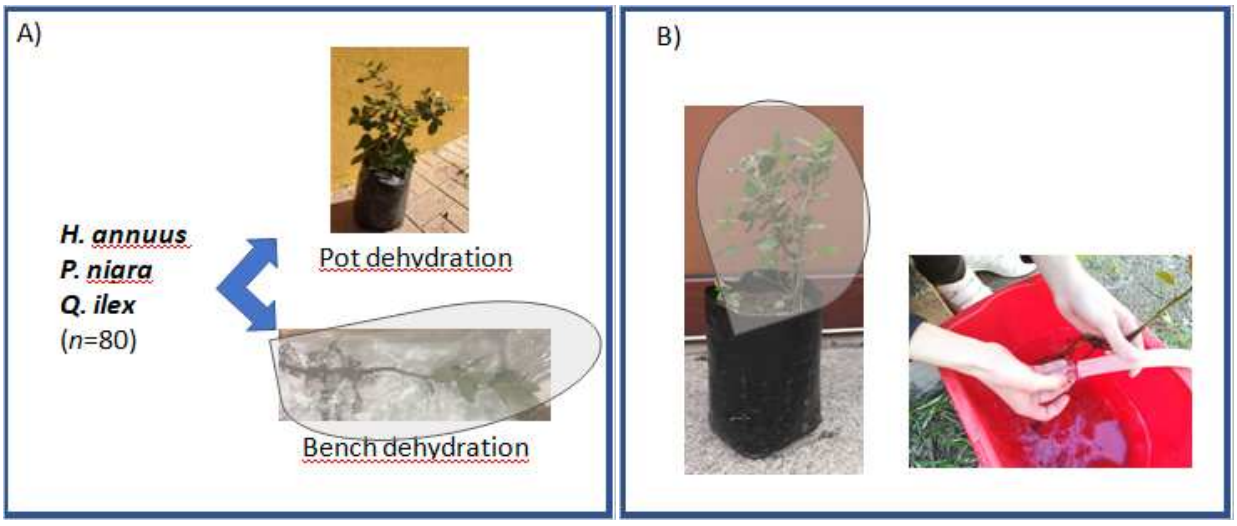

Figure 1: A) Experimental planning. Plants were dehydrated by whittholding water (i.e., Pot dehydration) or by gently cleaning up soil from the roots and, then, maintening the sample into a plastic bag (Bench dehydration). B) Details about removing soil by well-watered samples. Plants were fully irrigated and covered with a plastic bag for at least 8 hours (on the left). The soil was, then, removed by using water at low pressure.

4.1.2.Minimum cuticular conductance

The minimum cuticular conductance (g_{min}) value was estimated on six leaf samples per species by applying the experimental procedure described by John et al., (2018). Leaves were hydrated for >8 hours and, then, weighed for measuring their fresh weight (FW) and leaf area (A_L). A_L was measured with the software ImageJ (http://imagej.nih.gov/ij/) after acquiring leaf images with a scanner (HP Scanjet G4050, USA). Then, leaf samples were suspended by their petioles over a fan for inducing stomata closure and dehydrated for at least 2 hours. Finally, leaves were oven-dried for 72 hours at 70 ^{o}C to obtain their dry weight (DW). g_{min} was estimated by the ratio of minimum transpiration rate and the mole fraction vapour pressure deficit and two times the mean projected leaf area. During dehydration room temperature and relative humidity were recorded at 30s intervals using a thermohygrometer (Velleman, Gavere, Belgium).

4.1.3.Estimating leaf water potential at turgor loss point and drought-driven gas exchange and leaf water potential decline

In order to quantify the species-specific leaf water potential at the turgor loss point (Ψ_{tlp}), leaf water potential isotherms were measured on 5 leaves from different plants per species. Specifically, Ψ_{tlp} was estimated as the flex point of the relationship between the inverse value of leaf water potential ($1/\Psi_L$) as measured by a pressure bomb (PMS Instruments, Albany, OR, USA) and the water loss (Tyree and Hammel, 1972).

Leaf conductance to water vapour (g_L) was measured in pot dehydrated plants just before collecting samples for water content measurements by a portable LCi Analyzer System (ADC Bioscientific Ltd). Moreover, measurements of leaf water potential were also performed by using the pressure bomb. Monitoring of gas exchange and leaf water potential values was performed until cuticular conductance values (see below) were recorded.

4.1.4.Relative water content and rehydration capacity measurements

Measurements of relative water content (RWC) and percentage loss of leaf rehydration capacity (PLRC) were performed on leaf, stem and root samples collected from pot-dehydrated and bench dehydrated samples of all measured species. At different dehydration time, leaf, stem and root samples were cut by razor blade and immediately weighted for estimating their fresh weight (FW). Samples were, then, rehydrated by immersing them in distilled water for at least 8 h and, then, turgid weight (TW) was recorded. In detail, stem and root samples were fully immersed in the beaker containing the distilled water while leaves were rehydrated by immerging their petiole.

Finally, samples were oven dried for 3 days at 70 ^{o}C to obtain their dry weight (DW). RWC was then calculated as: 100*[(FW-DW)/DW]/SWC and PLRC as: 100*100-[(TW-DW)/ DW]/SWC where SWC is the saturated water content (g g^{-1}) of leaf, stem and root samples of well watered samples (i.e., plants at Ψ_L< -0.5 MPa) (Abate et al., 2021a).

Whole plant RWC was estimated by the proportion of each species-specific organ dry mass fraction multiplied by their respective RWC (Sapes and Sala, 2021).

4.1.5.Relative electrolyte leakage

To check the effects of dehydration on cell membrane damages, electrolyte leakage measurements were performed on leaf, stem and root samples collected at the same time and as near as possible to samples collected for water content estimating. In detail, leaf sample of about 1 cm^2, 3 cm-long stem and primary root samples were cut with a razor blade and immediately placed in test tube containing 8 mL of distilled water. Tubes were then stirred 30 minutes and the initial electrical conductivity of the solution (EC_i) was recorded by a conductivity meter (Cond 5, XS instruments, Italy). Samples were then subjected to three freeze/thaw cycles (i.e., T = -20 ^{o}C, +20 ^{o}C) to cause membrane disruption and processed as above described to estimate the final electrical conductivity of the solution (EC_f). The relative electrolyte leakage (REL) was calculated as (EC_i/EC_f) *100.

4.1.6. Mortality estimating

A set of 55 pot samples per species were used to assess the drought-driven plant die-back. In details, the set was divided in five groups of eleven plant per species. In each group, 3 samples for species were measured for estimating the native RWC and the remaining 8 samples were re-irrigated at field capacity and kept well-watered to estimate the percentage of plant die-off. More in detail, native RWC was estimated in well watered samples, in samples experimenting the leaf cell turgor (as estimated by leaf water potential measurements) and in samples not irrigated for other 2, 4 and 6 days (*H. annuus* samples) and 5, 10, 15 days (*P. nigra* and *Q. ilex* samples) after reaching the turgor loss. Samples were considered dead (Fig. 2) if, after 10 (sunflower plants) and 40 days (poplar and oak seedlings) from the day in which they were re-irrigated, their canopy were completely dry and no new buds appeared.

This experimental procedure was completed within the first week of August 2020.

Figure 2: Photos of *Q. ilex* (on the left) and *P. nigra* (on the right) samples considered die-off after re-irrigation. Please, note their canopy completely dry.

4.1.7 Statistical analysis

Statistical analysis was assessed using SigmaStat 12.0 (SPSS, Inc., Chicago, IL, USA) statistics package. Relationships between PLRC to RWC, PLRC to REL and REL to RWC were fitted separately in potted and bench dehydrated leaf, stem and root samples. Differences in relationships were considered statistically significant when the 95% confidence intervals (C.I.s) did not overlap. Because similar PLRC to RWC, PLRC to REL and REL to RWC relationships were recorded by the two dehydration methods, all data of each plant organ and measured species were, finally, fitted together. Relationships between RWC plant and leaf, stem and root PLRC and REL values were assessed too.

Relationships between *i*) g_L to Ψ_L, *ii*) g_L to leaf, stem and root RWC, PLRC and REL values, *iii*) g_L to whole plant RWC values, *iiii*) plant die-off to leaf, stem, root and whole plant RWC, *iiiii*) plant die off to leaf, stem and root PLRC and REL values and associate 95% (C.I.s) were assessed in order to obtain species-specific and plant-organ-specific threshold values. Specifically, values of Ψ_L (P_{gL20}, P_{gL50}, P_{gL80}), RWC (RWC_{gL20}, RWC_{gL50} and RWC_{gL80}), PLRC ($PLRC_{gL20}$, $PLRC_{gL50}$, $PLRC_{gL80}$) and REL (REL_{gL20}, REL_{gL50} and REL_{gL80}) and 95% C.I.s corresponding to 20%, 50% and 80% loss of g_L were estimated for each plant organ as well as for the whole plant and measured species. Moreover, RWC, PLRC and REL thresholds and associated 95% C.I.s

corresponding to 10%, and 50% of plant die-off for each plant organ and for each species were calculated too (RWC_{M10}, RWC_{M50}, $PLRC_{M10}$, $PLRC_{M50}$, REL_{M10} and REL_{M50}, respectively).
All regressions were considered significant t $P<0.05$.

4.2.Results

In all species, a fastest dehydration of samples occurred by bench compared to pot dehydration method (Fig. 3). Overall, whole dehydration of sunflower samples occurred within 11 days when dehydrated by pot method and within only 2-3 days (i.e., about 60 hours) when bench-dehydrated. Similarly, *P. nigra* and *Q. Ilex* samples lost their water content in about 25 days when pot dehydrated and in no more than 4 days (i.e., about 100 h) by bench dehydration method. It can be noted that, especially in *P. nigra* and *Q. ilex* samples, root dehydration occurred very quickly when bench dehydration was performed, i.e., within 10 hours. By contrast, root dehydration occurred at similar rate of leaf and stem dehydration by pot dehydration method, in all measured species.

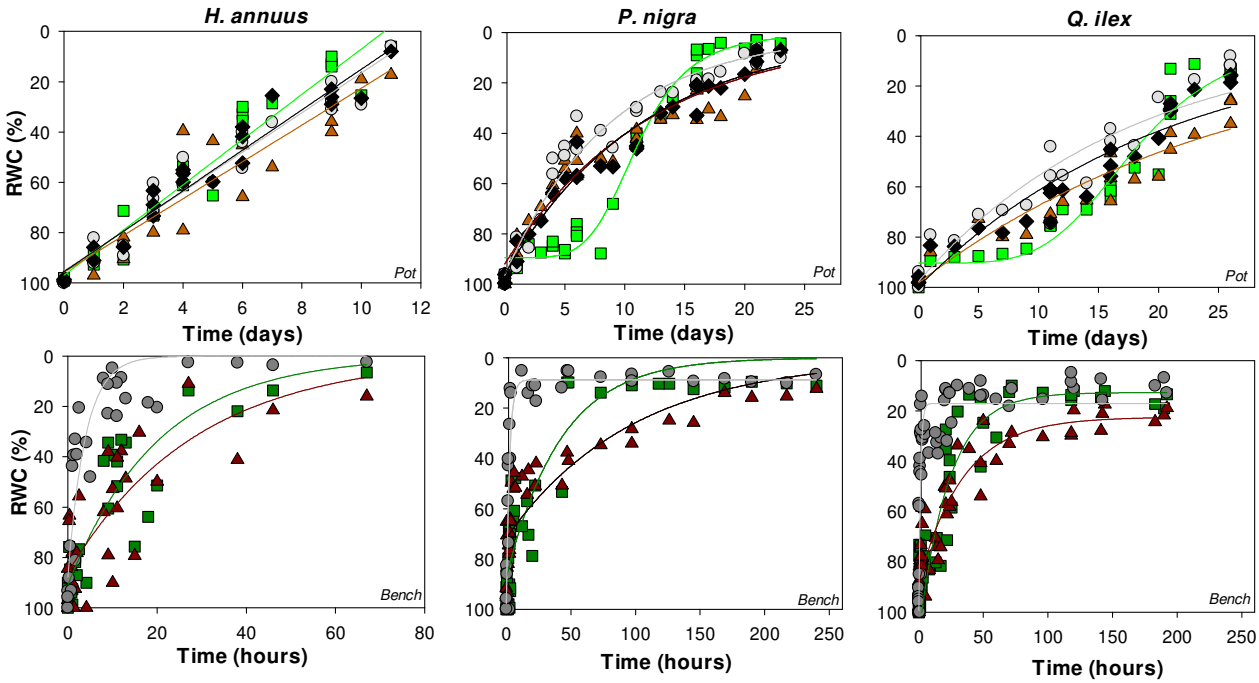

Figure 3: Decreasing of leaf (green squares), stem (brown triangles), root (gray circles) and whole plant (black diamonds) relative water content (RWC) over dehydration time (Time) as recorded by pot (Pot, light colors) and bench (Bench, dark colors) dehydration treatments in *H. annuus*, *P. nigra* and *Q. ilex*. Green, brown, gray and black solid lines show the regression curve of corresponding-color data set (see Table S1 for details on fitted curves).

Nevertheless, similar results have been recorded in pot versus bench dehydration method, tested by the overlapping of the species-specific leaf, stem and root bench *versus* pot dehydrated PLRC

to RWC (Figs. 4, 5 Table S2), PLRC to REL (Fig. 6, Table S3) and REL to RWC (Fig.7, Table S4) relationships.

Declining RWC reduced the loss of leaf, stem and root cell rehydration capacity (Fig. 4).

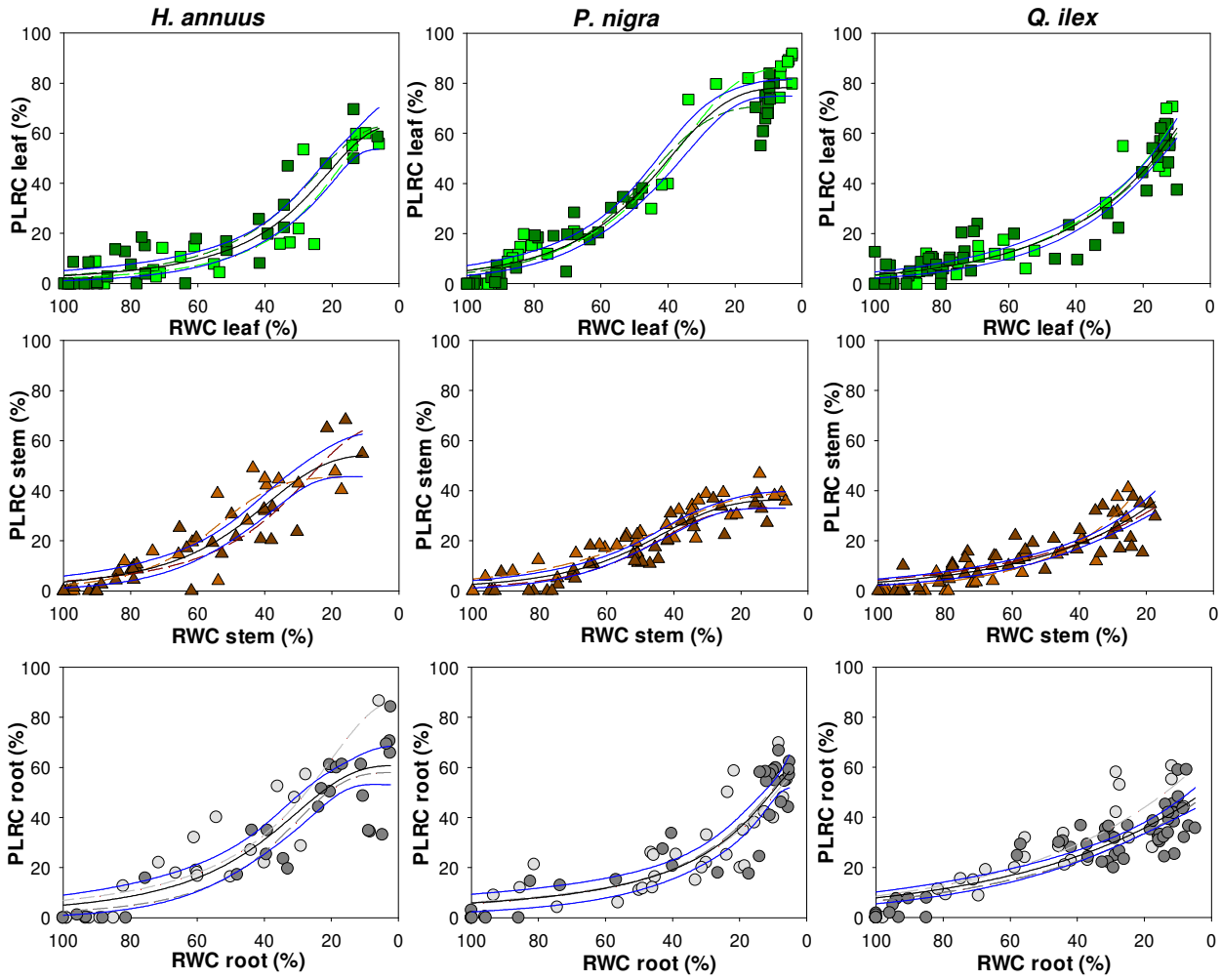

Figure 4: Relationships between the percentage loss of rehydration capacity (PLRC) and the relative water content (RWC) of dehydrating leaf (green squares), stem (brown triangles) and root (gray circles) samples as recorded by pot (light colors) and bench (dark colors)dehydration treatments in *H. annuus*, *P. nigra* and *Q. ilex*. Green, brown and gray long dash lines show the best fitted regression curve of pot (light colors) and bench (dark colors) leaf (green), stem (brown) and root (gray) samples. Dark and blue solid lines show the regression curve and associate 95% C.I.s as obtained by fitting data recorded by pot and bench dehydration treatment (for details on method and fitted curves, see the text and Table S2).

In detail, in *H. annuus*, similar RWC value inducing 10% PLRC was recorded in all three plant organs, (i.e., RWC_{PLRC10} ~ 65%, Figs. 4, 5, Table S2). By contrast, lower RWC values inducing 25% PLRC were recorded in leaf *versus* stem and root sunflower samples (i.e., RWC_{PLRC25} ~35% *versus* 48%, respectively).

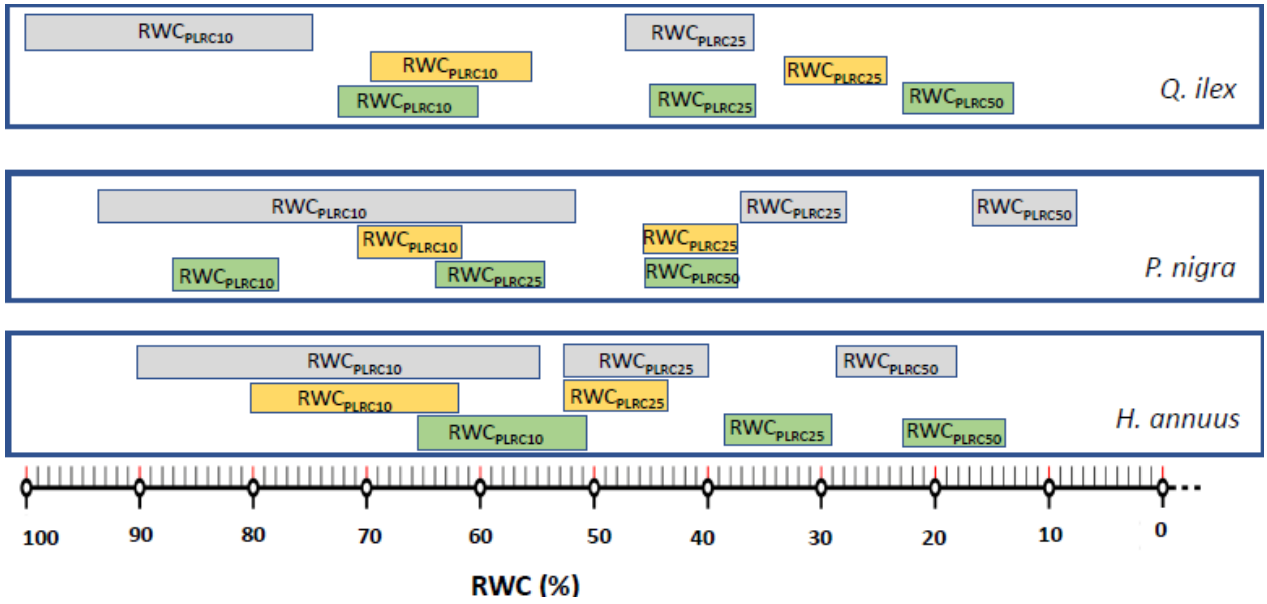

Figure 5: Relative water content, RWC, thresholds inducing 10%, 25% and 50% percentage loss of rehydration capability, PLRC (i.e., RWC_{PLRC10}, RWC_{PLRC25}, RWC_{PLRC50}, respectively) as recorded in leaf (green), stem (brown) and root (gray) samples *H. annuus*, *P. nigra* and *Q. ilex*.

In *P. nigra*, similar RWC_{PLRC10} value was recorded in leaf and root samples (i.e., about 80%) while stems showed a RWC_{PLRC10} of about 65% (i.e., lower than threshold measured in the leaves but statistically similar to threshold recorded in roots, Figs. 4, 5 Table S2). Moreover, statistically higher RWC_{PLRC25} value in leaf *versus* stem and root samples (i.e., 55% *versus* 40% respectively) were recorded in this species. Leaf and stem *Q. ilex* samples showed similar RWC_{PLRC10} value (i.e., about 65%), and significantly higher than the value recorded in the roots (i.e., 85%, Figs. 4, 5 Table S2). In this species, the RWC_{PLRC25} value was about 35% for leaf and root samples and about 25% for stem cells. Nevertheless, it can be noted that, overall, higher root RWC_{PLRC10} value occurred in all three species, although C.I.s overlapping occurred in leaf *versus* root of *H. annuus* and *P. nigra* samples.

Drought-driven increase in loss of rehydration capability strongly depended on cell membrane damages, as the robust correlations between PLRC and REL recorded in all three species and organs clearly indicated (Fig. 6, Table S3). It can be noted that in all plant organs and species the best-fitted regression curve was a linear model.

Cell membrane damages impacted the cell water content according to an exponential function (Fig. 7, Table S4). Thus, the initial declining in water content didn't lead to cell membrane damages. Increase of REL values occurred at RWC values low as about 75%.

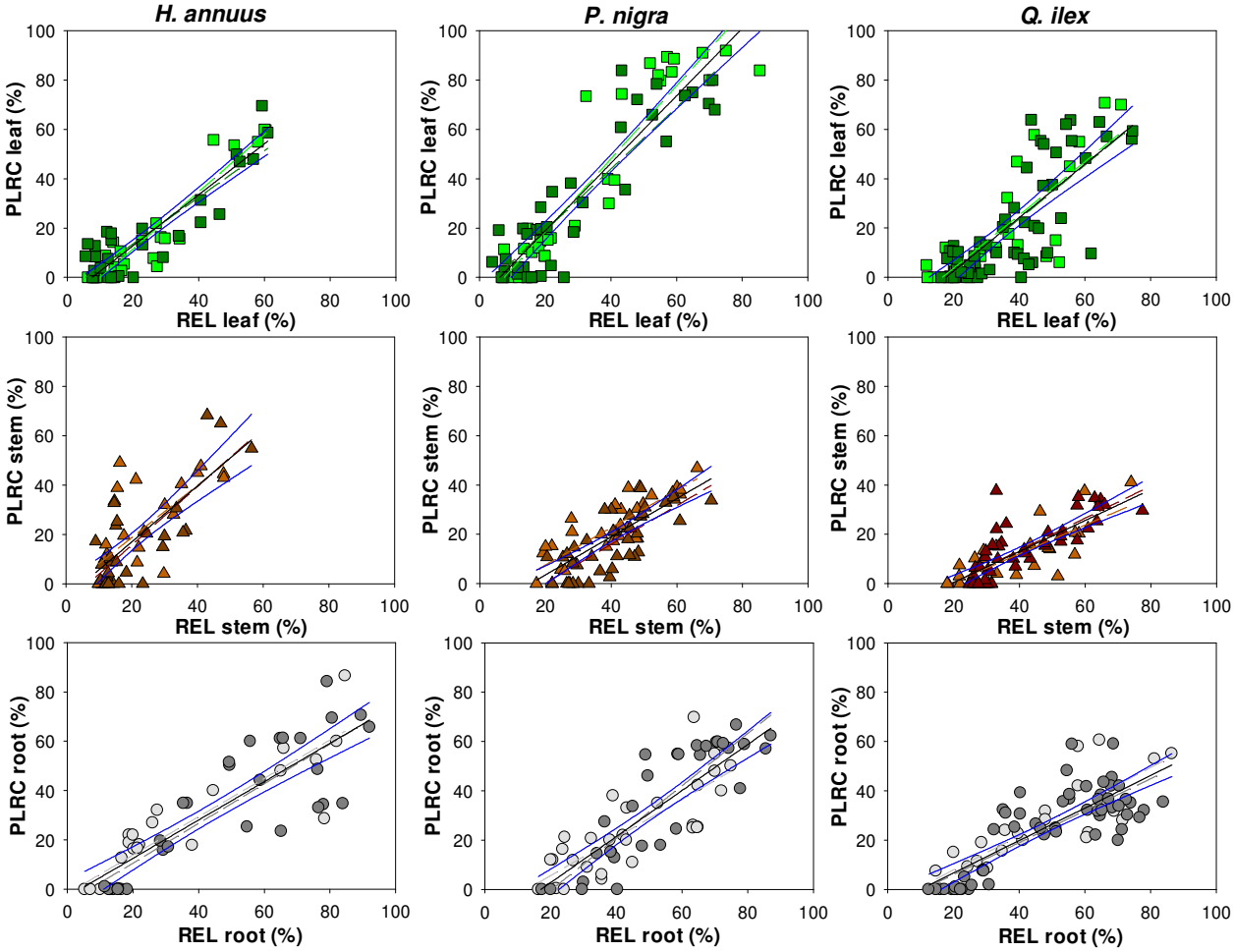

Figure 6: Relationships between the percentage loss of rehydration capacity (PLRC) and the relative electrolyte leakage (REL) of dehydrating leaf (green squares), stem (brown triangles) and root (gray circles) samples as recorded by pot (light colors) and bench (dark colors) dehydration treatments in *H. annuus*, *P. nigra* and *Q. ilex*. Green, brown and gray long dash lines show the best fitted regression curve of pot (light colors) and bench (dark colors) leaf (green), stem (brown) and root (gray) samples. Dark and blue solid lines show the regression curve and associate 95% C.I.s as obtained by fitting data recorded by pot and bench dehydration treatment (for details on method and results on fitted curves, see the text and Table S3).

Robust correlations were recorded between stomatal conductance to water vapour and water status too (Fig. 8). As expected, g_L decreased in response to dehydration: in accordance, a coordination between g_L and leaf water potential as well as between g_L and leaf RWC was recorded in all three study species. It can be noted that in *P. nigra*, where the higher vulnerability of leaf cell loss rehydration capability was recorded (Fig. 4, Table S2), the fastest stomatal closure occurred in response to dehydration (Fig. 8). In this species, a relevant stomatal closure occurred at leaf water potential higher than the turgor loss point (i.e., -1.1 *versus* -2.0 MPa), while in *H. annuus* and *Q. ilex* P_{gL80} values were similar to the species-specific leaf water potential at turgor loss point. Moreover, *H. annuus* and *Q. ilex* showed similar leaf, stem and root RWC thresholds leading to 80% loss of g_L (i.e., RWC_{gL80}~ 65%, Figs. 7, 8 A, Table S5). By contrast in poplar, leaf RWC_{80gL} value high as about 85%, was recorded (i.e., Figs. 8, 9 A).

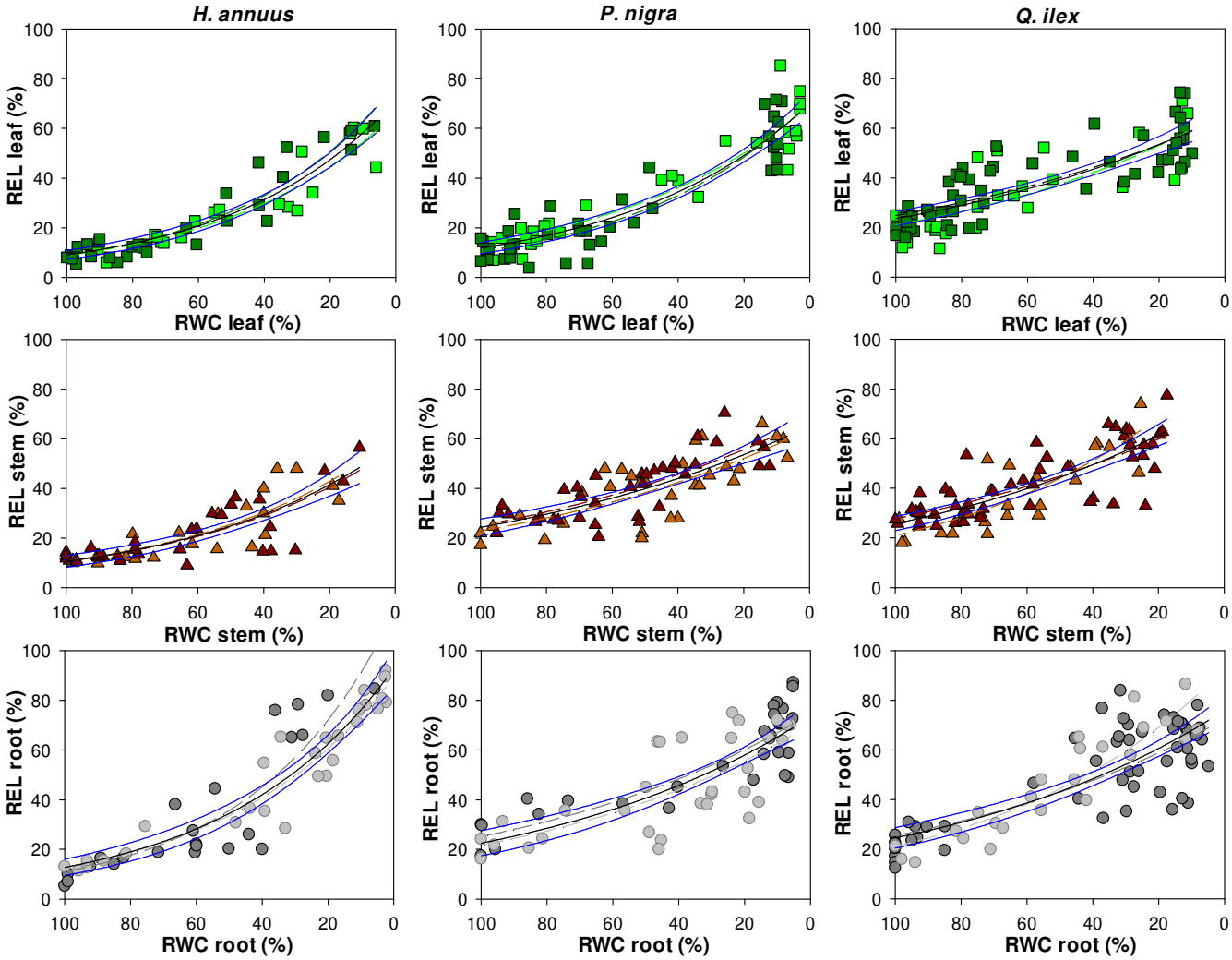

Figure 7: Relationships between the relative electrolyte leakage (REL) and the relative water content (RWC) of dehydrating leaf (green squares), stem (brown triangles) and root (gray circles) samples as recorded by pot (light colors) and bench (dark colors) dehydration treatments in *H. annuus*, *P. nigra* and *Q. ilex*. Green, brown and gray long dashed lines show the best fitted regression curve of pot (light colours) and bench (dark colours) leaf (green), stem (brown) and root (gray) samples. Dark and blue solid lines show the regression curve and associate 95% C.I.s as obtained by fitting data recorded by pot and bench dehydration treatment (for details on method and results on fitted curves, see the text and Table S4).

Drought-driven stomatal closure was coupled to changes in PLRC too. Thus, leaf PLRC values of about 15% as well as stem and root PLRC values of about 20% led to g_L loss of about 80% in *H. annuus* and *P. nigra*. In *Q. ilex* stem samples no relationship between g_L and PLRC was recorded (Figs. 8, 9 B).

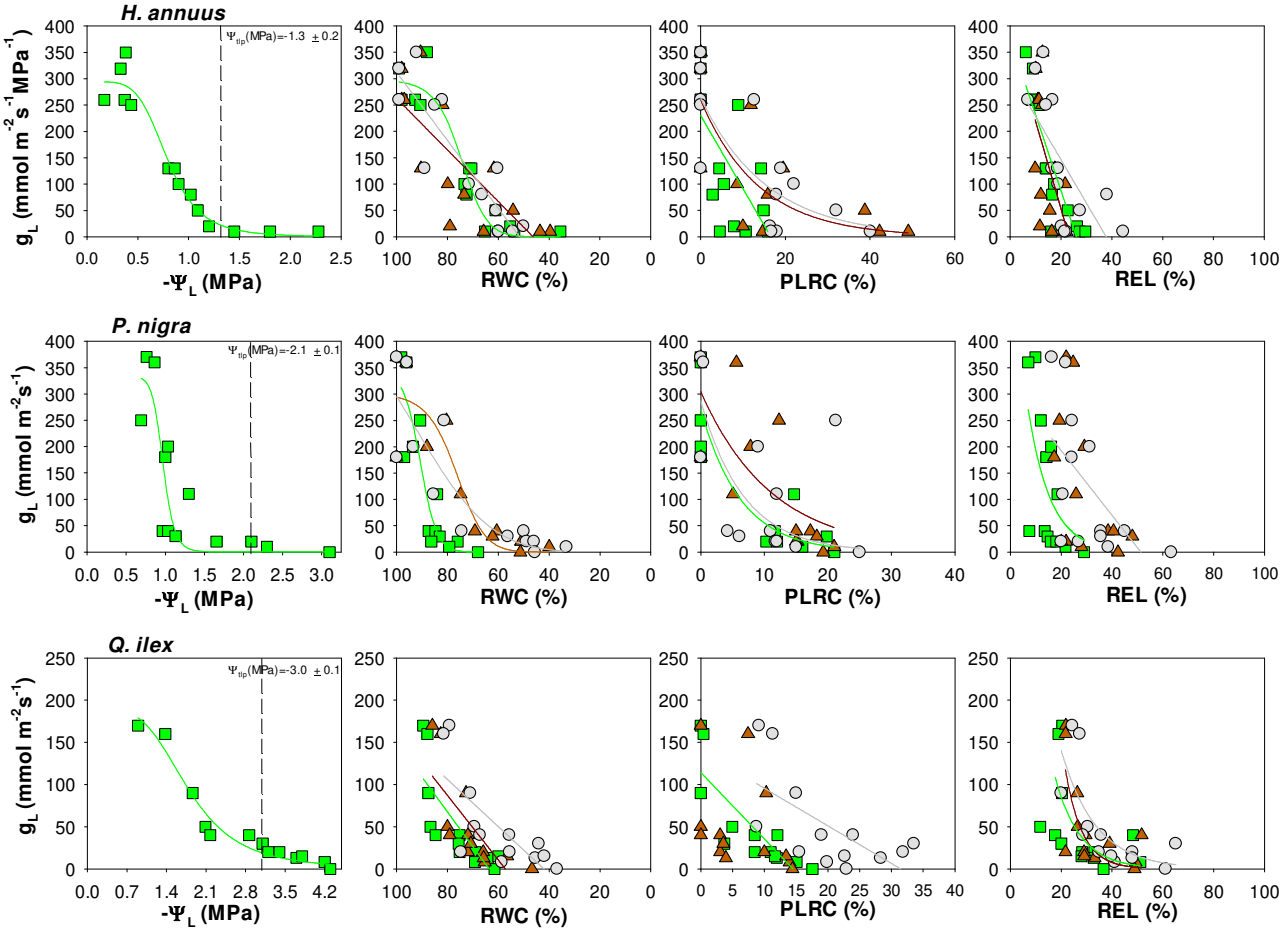

Figure 8: Relationships between stomatal conductance to water vapour (g_L) and leaf water potential (Ψ_L), relative water content (RWC), percentage loss of rehydration capability (PLRC) and relative electrolyte leakage (REL) of dehydrating leaf (green squares), stem (brown triangles) and root (gray circles) samples as recorded by pot dehydration treatment in *H. annuus*, *P. nigra* and *Q. ilex*. Green, brown and gray solid lines show the regression curve (for details on regression results, see Table S5). Mean values ± SD of the species-specific leaf water potential at turgor loss point (Ψ_{tlp}) are reported and indicated by long dashed lines.

Cell membrane damages, especially of leaf and root cells, impacted on stomatal conductance values of all three species. In fact, an increase in cell membrane damages corresponding to REL values of 25% (for all sunflower plant organs, leaf poplar and leaf and stem oak) and of about 30% (i.e., *P. nigra* and *Q. ilex* root samples) led to 80% loss of stomatal conductance (Figs. 8, 9 C).

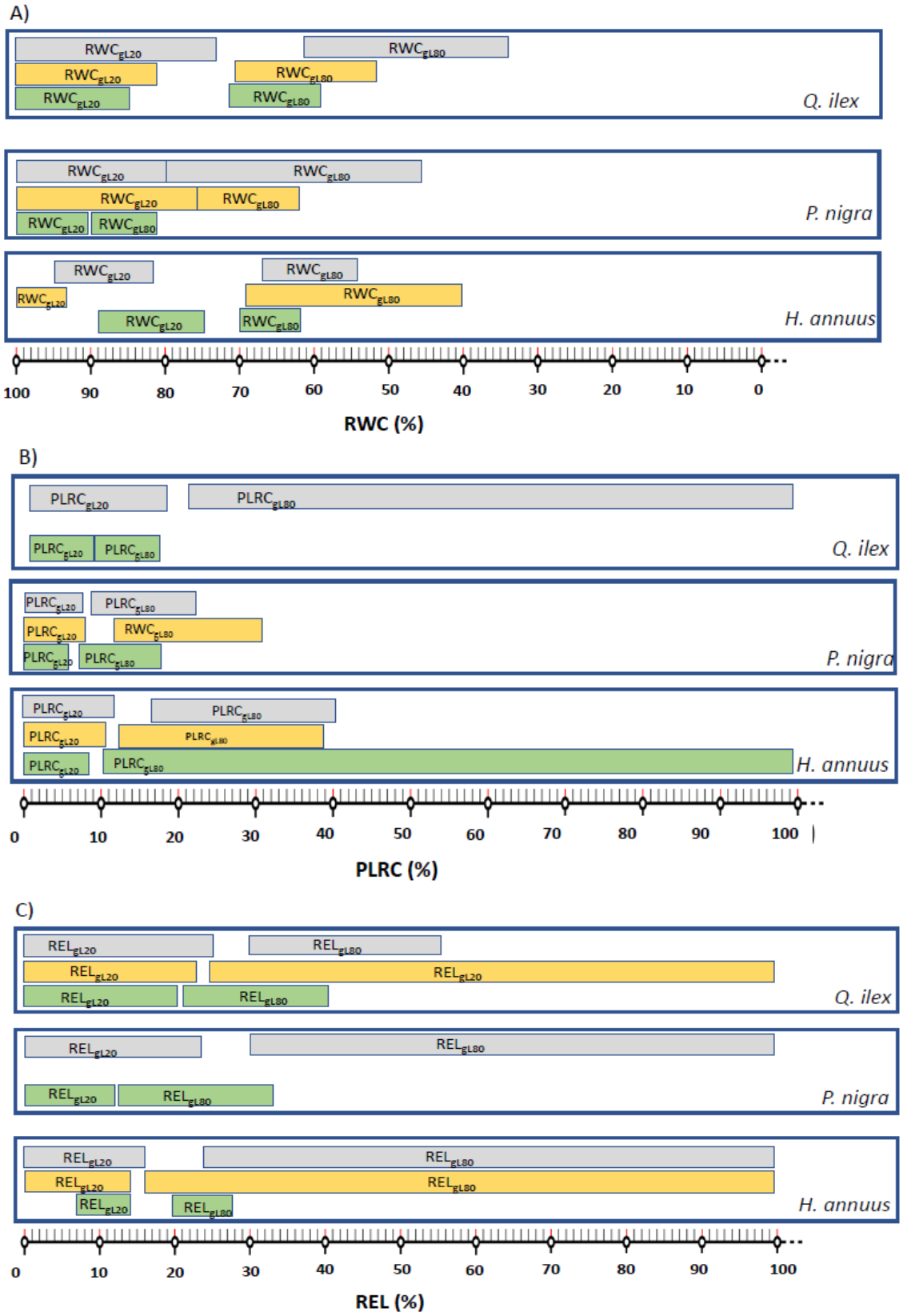

Figure 9: A) Relative water content, RWC, B) percentage loss of rehydration capability, PLRC, and C) relative electrolyte leakage, REL, thresholds inducing 20% and 80% percentage loss of stomatal conductance to water vapour, g_L (i.e., RWC_{gL20}, RWC_{gL80}, $PLRC_{gL20}$, $PLRC_{gL80}$,REL_{gL20}, REL_{gL80}, respectively) as recorded in leaf (green), stem (brown) and root (gray) samples *H. annuus*, *P. nigra* and *Q. ilex*

Overall, leaf, stem and root drought-driven cell damages impacted on the whole plant RWC decline (Fig. 10).

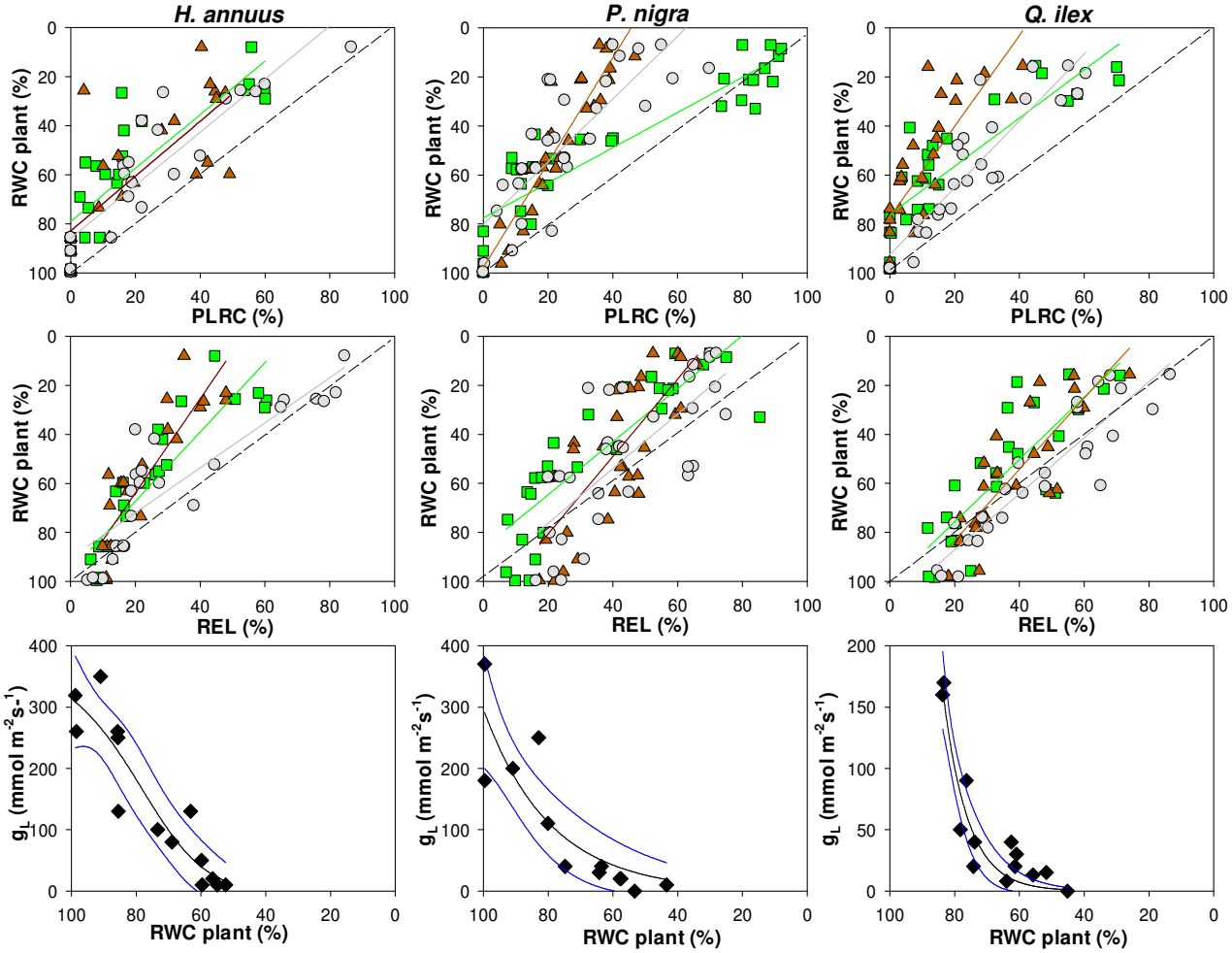

Figure 10: Relationships between whole plant relative water content (RWC plant) and leaf (green squares), stem (brown triangles) and root (gray circles) percentage loss of rehydration capability (PLCR) and relative electrolyte leakage (REL) and relationships between leaf stomatal conductance to water vapour (g_L) and RWC plant (black diamonds) as recorded by pot dehydration treatment in *H. annuus*, *P. nigra* and *Q. ilex*. Green, brown, gray and dark solid lines show the regression curve (for details on regression results, see Table S6). Moreover, C.I.s of g_L *versus* RWC plant relationships are shown by blue solid lines.

In accordance, robust linear correlations were recorded between the species-specific RWC plant values and leaf, stem and root PLRC and REL values. Not at last, similar plant RWC thresholds leading to stomatal closure were recorded in the three species. In accordance, plant RWC values of about 85% and 70% led to 20% and 80% loss of g_L, respectively in sunflower samples as well as in the two woody species (Fig. 10, Table S6).

Percentage of plant die-off occurred as function of water status (Fig. 11). Moreover, leaf, stem and root RWC drought-driven declines were similarly reliable proxies of plant mortality in all three

species. In fact, similar leaf, stem and root as well as whole plant RWC values of about 50% led to 10% of plant die-off in the two woody species (i.e., *P. nigra* and *Q. ilex*) as well as in sunflower plants where, however, tendentially higher RWC thresholds were recorded (Figs. 11, 12 Table S7).

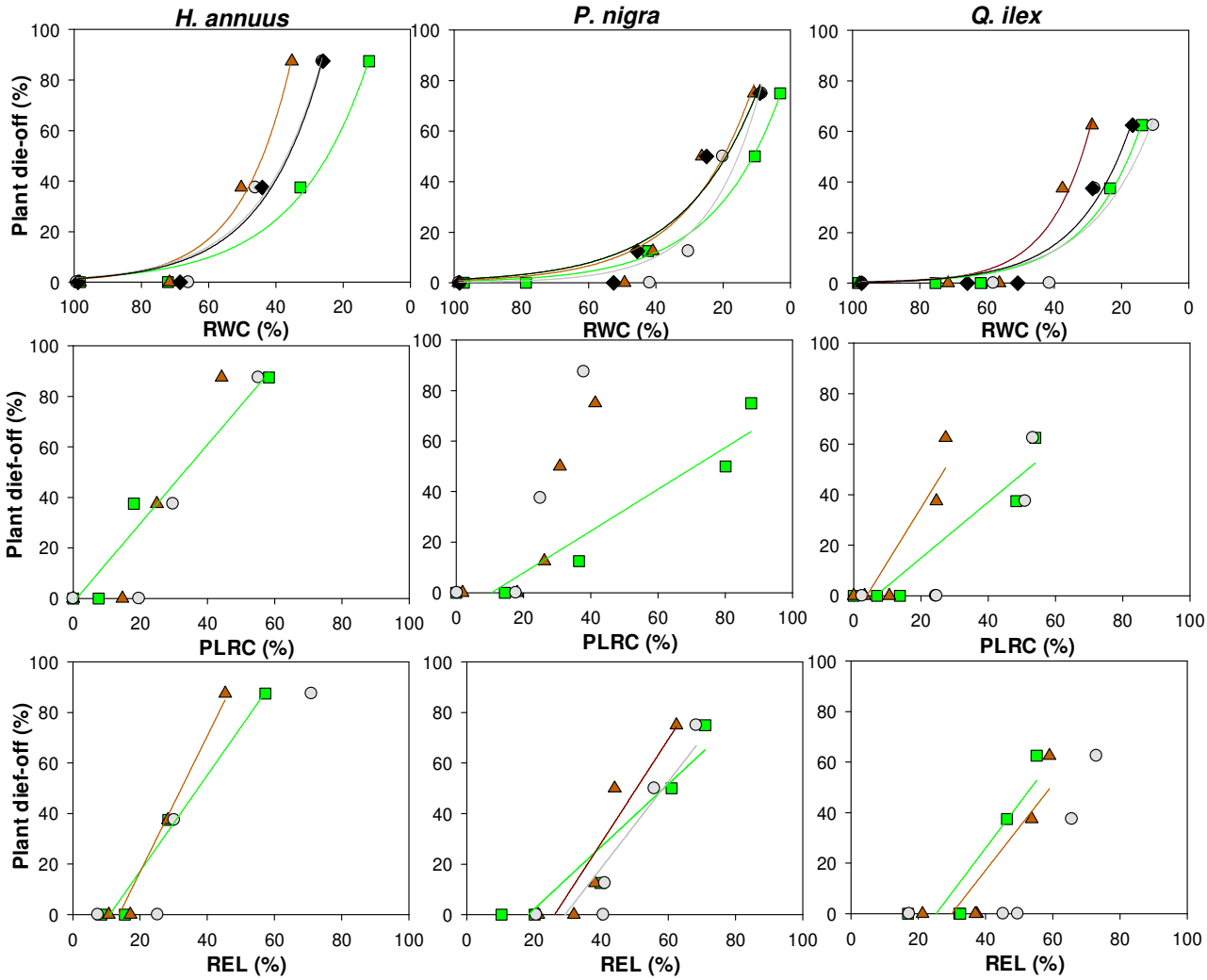

Figure 11: Relationships between percentage plant die-off and relative water content (RWC), percentage loss of rehydration capability (PLRC) and relative electrolyte leakage (REL) as recorded in leaf (green squares), stem (brown triangles) and root (gray circles) samples of *H. annuus*, *P. nigra* and *Q. ilex*. Relationships between plant die-off and plant RWC (black diamond) of all three species are also reported Green, brown, gray and dark solid lines show the regression curve (for details on regression results, see Table S6).

We checked the RWC threshold leading to 50% of plant mortality (RWC_{M50}) too. However, in all three species, root RWC_{M10} *versus* RWC_{M50} overlapped. Moreover, C.I.s overlapping occurred also in plant and stem species-specific RWC thresholds. Therefore, significantly different RWC_{10M} and RWC_{50M} values were recorded for leaf samples in all three species and for whole plant in only *P. nigra* (Figs. 11, 12 Table S7). More in detail, in sunflower plants, 50% of plant

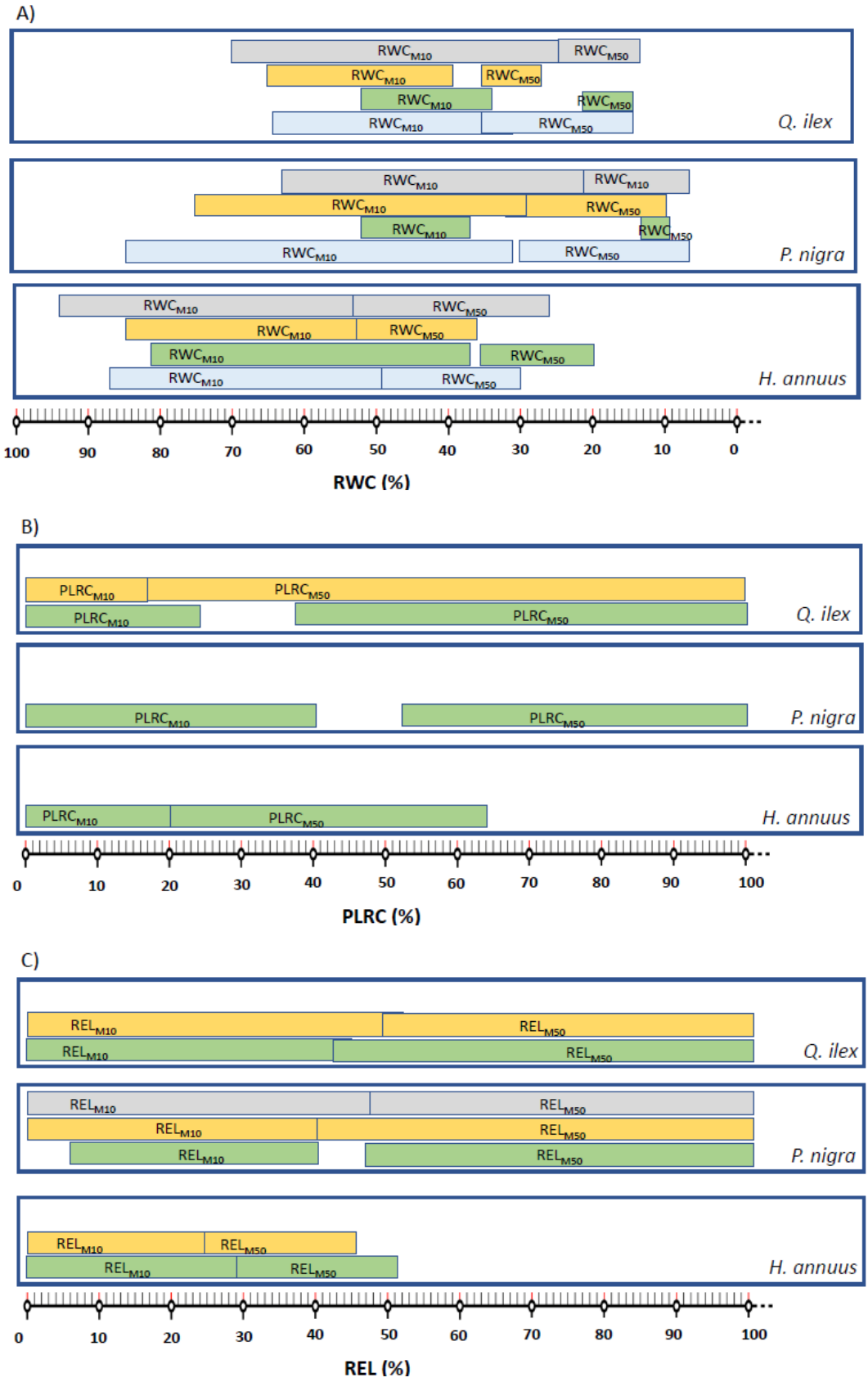

Figure 12: A) Relative water content B) percentage loss of rehydration capability and C) relative electrolyte leakage thresholds inducing 10% and 50% percentage of plant mortality (i.e., RWC_{M10}, RWC_{M50}, $PLRC_{M10}$, $PLRC_{M50}$,REL_{M10}, REL_{M50}, respectively) as recorded in whole plant (light blue), leaf (green), stem (brown) and root (gray) samples of *H. annuus*, *P. nigra* and *Q. ilex.*

mortality was recorded at leaf RWC values of about 30%, in *P. nigra* leaf RWC_{50M} was about 12% and in *Q. ilex* it was about 18%.

Robust correlations were recorded also between plant-die off and PLRC and REL values but not in all plant organs and species. Leaf PLRC values as well as leaf and stem REL values were strongly related to plant mortality in all measured plants. In particular, a leaf PLRC threshold of about 15% as well as leaf REL values of about 20% caused 10% plant-die-off in all three species. Moreover, leaf PLRC values of about 55% led to about 50% plant die-off in sunflower as well as in the two woody species.

4.3. Discussion

Our results strongly support the hypothesis that RWC can be used as reliable tool for evaluating the risk of drought-driven plant mortality. In fact, leaf, stem and root RWC declines in response to water shortage were indicators of increase of plant die-off in all three study species. However, the reliability as proxy of plant die-off of the three plant organs is, likely, not similar. Moreover, water-content-related parameters as PLRC and REL proved to be good indicators of plant mortality risk too. In detail, similar leaf PLRC and REL thresholds of drought-driven plant die-off were recorded in all three species. Furthermore, species-specific stem and/or root PLRC and REL thresholds leading to plant death were also recorded.

4.3.1. Estimating RWC thresholds by pot versus bench dehydration method

We firstly tested the experimental procedure for sample dehydration. Bench dehydration method is commonly used to estimate plant water status in response to drought as well as drought-driven hydraulic conductance decline (i.e., Cochard et al., 2013; John et al., 2018; Kiorapostolou et al., 2019). This experimental procedure has the relevant advantage to obtain samples with low water content quickly, thus shorting the time of measurements. Nevertheless, this artificial fast dehydration method may cause artefactual results, including the loss of possible biochemical and/or molecular time-depending responses and/or whole plant coordinated responses.

Overall, in the present study, good similarity of results recorded by the two experimental procedures were recorded. Indeed, independently by the method, similar decline in PLRC values as a function of drought-driven RWC was obtained as well as similar RWC *versus* REL relationships were occurred in all three organs and species. Therefore, the two methods are reliable tools for estimating RWC but also PLRC and REL thresholds.

4.3.2.Leaf, stem and root water status thresholds for drought-driven cell damagesand stomatal closure

In all three species, higher RWC values at which 10% PLRC were recorded in root and, then, in leaf samples, although in *H. annuus* and *P. nigra* the overlapping of leaf and root RWC_{PLRC10} thresholds occurred. This result supports the hypothesis that not only the leaves but also fine roots can operate as a hydraulic fuse aimed to disconnect plant from drying soil (Zimmermann, 1983; Jackson et al., 2000; Cuneo et al., 2016). This strategy protects the hydraulic integrity of more carbon expensive plant portions, including longer-living roots and stems (Tyree and Ewers, 1991). On this view, loss in cell rehydration capability coupled to xylem embolism and/or root shrinkage (Pratt et al., 2015; Creek et al., 2018; North and Nobel, 1997) and mechanical damages (Cuneo et al., 2016) can contribute to limit outward flow back into drying soils. Moreover, in all three species, root water status as well as root loss of cell rehydration capability and cell membrane damages were strongly related to stomatal closure. In accordance, a statistical similar RWC of about 60%, PLRC of about 20% as well as REL value of about 30% led to 80% of stomatal closure in all three species. By contrast, stem PLRC and REL values were not always related to gas exchange. In other words, in addition to the expected link between leaf water status and stomatal regulation, a tight coordination between root water status, cell membrane damages and stomatal closure have been observed. Past and recent findings showed a key role of root system into stomatal regulation through chemical compounds, hydraulic conductance changes and drought-driven damages (i.e., Tardieu and Davies, 1992; McCormack et al., 2015; Cuneo et al., 2016; Tardieu et al., 2017; Rodriguez-Dominguez and Brodribb, 2019). On the other hand, root is the primary sensing-drought organ. In accordance, increased accumulation of reactive oxygen species involved in root response to drought have been documented (i.e., Zhao et al., 2001; Alam et al., 2010; Mukarram et al., 2021). On this view, it is reasonable to hypothesize that drought-driven changes in root water status and cell membrane damages, including loss of rehydration capability, might trigger (chemical?) signals involved in gas exchange regulation. Further studies, however, need to confirm this hypothesis.

Nevertheless, it can be noted that, in all three species, the species-specific leaf RWC_{PLRC10} values corresponded to the species-specific leaf RWC thresholds leading to 80% decline of stomatal conductance. More in details, statistically similar RWC thresholds of about 70% in sunflower and *Q. ilex* and of about 85% in *P. nigra* led to 10% PLRC as well as to 80% loss of g_L. These results suggest that the initial loss in rehydration capability of leaf cells was promptly coupled to a relevant stomatal closure to limit further water loss and, then, more relevant damages. Our data are

in agreement with data reported by Trueba et al (2019) that recorded a similar significant stomatal closure in response to initial leaf loss rehydration capability, as occurring before photochemical decline.

Moreover, in all three species, increase in cell membrane damages corresponding to REL values of 25%-30% and leaf PLRC values of about 15% led to 80% loss of stomatal conductance to water vapour.

If confirmed in other species, these thresholds might be used as proxy of initial decline of carbon assimilation.

4.3.3. Not only RWC but also PLRC and REL can be used as reliable tools for predicting plant die-off

The use of RWC as indicator of plant die-off have received an increasing attention in the last years on the basis of different links between water content and mortality risk (Martines-Vilalta et al., 2019). In accordance, plant water content predicted the mortality risk of *Pinus ponderosa* seedlings (Sapes and Sala, 2021) and actually integrated drought-driven hydraulics and carbon starvation in this species (Sapes et al., 2019). In the present study, we recorded robust correlations between RWC and plant-die-off in other three different species: an herbaceous, a deciduous and an evergreen species. Overall, these results strongly support the hypothesis to use RWC as reliable indicator of mortality risk. In fact, robust correlations between RWC values of all three organs and the percentage of plant die-off were recorded. Moreover, an increase in plant mortality (i.e., >10% plant die-off) occurred at the same plant organs and RWC value in herbaceous and woody species (i.e., RWC ~50%), as well as at the same leaf PLRC threshold (i.e., PLRC~15%). Thus, common thresholds for triggering plant die-off were recorded in the three measured species. Our findings are in agreement with results recorded in other studies. Sapes and Sala (2021) reported that, in seedlings of *Pinus ponderosa*, a probability of 10% mortality occurred at a plant RWC value of about 65%. This threshold is apparently higher than value recorded in our species. However, the plant RWC C.I.s of all three species included this value. Moreover, John et al., (2018) reported that RWC leading to 10% of leaf PLRC changed as a function of leaf habit but also at increasing of aridity experienced during the growth season for 89 species. In summary, values of plant RWC lower than about 60%-50% as well as values of leaf PLRC higher than 15% comes to light as alarming thresholds of an abrupt increased risk of plant die-off.

The recorded initial high root vulnerability to drought, as recorded in all three measured species didn't limit plant ability to survive even after a severe stress. In fact, in the two woody species,

root RWC values low as about 25% didn't cause plant mortality higher than 30%. In the herbaceous species, a root RWC value of 40% led to about 40% plant die-off. This result is not surprising: new root growth as well as increase in permeability of damaged roots have been documented in species experimenting drought-re-watering treatment (i.e., North and Nobel, 1991; Cuneo et al., 2021, Abate et al., 2021b). Nevertheless, root and shoot re-sprouting need energy and carbon skeletons. On this view, we expect that repeated drought events, that leading to carbon starvation, may affect plant ability recovery. Further studies investigating the impact of more drought events on RWC thresholds are necessary.

Stem water status was recorded well correlated to plant mortality in all three study species. However, the stem PLRC values were related to plant mortality only in *Q. ilex*. Moreover, overlapping of C.I.s lowered d the reliability of this organ to predict plant die-off. In a recent study, Rosner et al. (2019) reported high reliability for estimating the loss of hydraulic conductivity using the relative the stem water content loss in 8 different species. However, reasonably, the presence of living cells in stems may impact the plant survival only until hydraulic connection continues to be. Moreover, high variability in percentage of stem parenchymatic cells exist among species (i.e., Morris et al., 2016; Kiorapostolou et al., 2019). This may explain because in some species no relation between plant mortality and stem RWC have been recorded (Mantova et al., 2021) as well as because, in the present study, stem cell loss in rehydration capability and REL values were not always related to plant mortality. In other words, stem living cells (beyond parenchimatic cells) and, mainly, their drought-driven damages may not necessarily relate to plant survival after re-watering because: *i*) cell stems survival can depend by shoot water storage and hydraulic capacitance (i.e., Epila et al., 2017; Bryant et al., 2021) and /or *ii*) they cannot be involved into maintaining the integrity of long-distance water transport, especially when are present at low percentage (i.e., Plavcova et al., 2016; Trifilò et al., 2019). Nevertheless, it can be noted that the measured samples for estimating plant mortality was relatively low in our study (i.e., 8 samples per species). Thus, we cannot exclude that measuring higher number of species might give more exact RWC thresholds, especially of stem samples.

4.4. Conclusions

Present study showed reliable findings on the predictive power of RWC for foreseeing plant mortality across the three measured species. Moreover, leaf PLRC and REL values showed a likewise reliability to monitor plant die-back and, then, the risk of mortality. In particular, RWC

values of about 50% as well as the PLRC threshold of about 15% and REL values higher than 25%-30% were indicator of increasing risk of plant-die-off.

We agree that our results on seedlings samples may be different from thresholds recorded in adult plant. In fact, further studies *in planta* on adult samples are requested. Nevertheless, our findings offer encouraging data to perform further studies investigating RWC, PLRC and REL thresholds for plant mortality risk.

4.5. Supplementary Material

Table S1: Fitted regressions recorded between leaf, stem, root and whole plant time of dehydration and relarive water content in pot *versus* bench dehydrated samples of *H. annuus*, *P. nigra* and *Q. ilex*. Model type, equation, coefficient values, correlation coefficients (r^2) and P-values are reported.

Species	**organ**	**dehydration method**	**model type**	**equation**	**y_0**	**a**		**r^2**	***P***	**dehydration method**	**model type**	**equation**	**a**	**b**		**r^2**	***P***
H. annuus	Leaf	pot dehydration	linear	$y=y_0+ax$	96,9	-8,9		0,94	**<0.0001**	bench deydration	exponential	$y=ae^{-bx}$	91	0,05		0,79	<0.0001
			model type	**equation**	**y_0**	**a**		**r^2**	***P***		**model type**	**equation**	**a**	**b**		**r^2**	***P***
	Stem	pot dehydration	linear	$y=y_0+ax$	95,7	-7,4		0,85	**<0.0001**	bench deydration	exponential	$y=ae^{-bx}$	86,1	0,03		0,63	<0.0001
			model type	**equation**	**y_0**	**a**		**r^2**	***P***		**model type**	**equation**	**a**	**b**		**r^2**	***P***
	Root	pot dehydration	linear	$y=y_0+ax$	95,2	-7,9		0,94	**<0.0001**	bench deydration	exponential	$y=ae^{-bx}$	87,3	0,25		0,8	<0.0001
			model type	**equation**	**y_0**	**a**		**r^2**	***P***								
	whole plant	pot dehydration	linear	$y=y_0+ax$	95,5	-8		0,95	**<0.0001**								
Species	**organ**	**dehydration method**	**model type**	**equation**	**a**	**b**	**x_0**	**r^2**	***P***	**dehydration method**	**model type**	**equation**	**a**	**b**		**r^2**	***P***
P. nigra	Leaf	pot dehydration	sigmoidal	$y= a/[1+ (x/x_0)^b]$	89,4	5	11,1	0,98	**<0.0001**	bench deydration	exponential	$y=ae^{-bx}$	87,2	0,02		0,85	<0.0001
			model type	**equation**	**a**	**b**		**r^2**	***P***		**model type**	**equation**	**a**	**b**		**r^2**	***P***
	Stem	pot dehydration	exponential	$y=ae^{-bx}$	91,9	0,08		0,93	**<0.0001**	bench deydration	exponential	$y=ae^{-bx}$	71,5	0,01		0,76	<0.0001
			model type	**equation**	**a**	**b**		**r^2**	***P***		**model type**	**equation**	**y_0**	**a**	**b**	**r^2**	***P***
	Root	pot dehydration	exponential	$y=ae^{-bx}$	96,4	0,11		0,96	**<0.0001**	bench deydration	exponential	$y=y_o+ae^{-bx}$	8,75	88,97	0,41	0,85	<0.0001
			model type	**equation**	**a**	**b**		**r^2**	***P***								
	whole plant	pot dehydration	exponential	$y=ae^{-bx}$	95,9	0,09		0,96	**<0.0001**								
Species	**organ**	**dehydration method**	**model type**	**equation**	**a**	**b**	**x_0**	**r^2**	***P***	**dehydration method**	**model type**	**equation**	**y_0**	**a**	**b**	**r^2**	***P***
Q. ilex	Leaf	pot dehydration	sigmoidal	$y= a/[1+ (x/x_0)^b]$	90,4	4,5	18	0,94	**<0.0001**	bench deydration	exponential	$y=y_o+ae^{-bx}$	12,7	96,3	0,04	0,26	0,0003
			model type	**equation**	**a**	**b**		**r^2**	***P***		**model type**	**equation**	**a**	**b**		**r^2**	***P***
	Stem	pot dehydration	exponential	$y=ae^{-bx}$	98,3	0,037		0,88	**<0.0001**	bench deydration	exponential	$y=y_o+ae^{-bx}$	22,5	65,8	0,029	0,9	<0.0001
			model type	**equation**	**a**	**b**		**r^2**	***P***								
	Root	pot dehydration	exponential	$y=ae^{-bx}$	97,7	0,056		0,9	**<0.0001**		**model type**	**equation**	**y_0**	**a**	**b**	**r^2**	***P***
			model type	**equation**	**a**	**b**		**r^2**	***P***	bench deydration	exponential	$y=y_o+ae^{-bx}$	17,1	82,4	0,74	0,85	<0.0001
	whole plant	pot dehydration	exponential	$y=ae^{-bx}$	99,8	0,048		0,9	**<0.0001**								

Table S2: Fitted regressions recorded between leaf, stem and root percentage loss of rehydration capacity (PLRC) and relarive water content (RWC) in pot versus bench dehydrated samples of *H. annuus*, *P. nigra* and *Q. ilex*. Model type, equation, coefficient values, correlation coefficients (r^2) and P-values are reported. Moreover RWC values leading to 10%, 25% and 50% of PLRC (i.e., RWC_{PLRC10}, RWC_{PLRC25}, RWC_{PLRC50}, respectively) and corresponding confidence intervals (CI) are also reported.

Species	organ		model type	equation	a	b	x_0	r^2	*P*	RWC_{PLRC10}	2,5% CI	97,5% CI	RWC_{PLRC25}	2,5% CI	97,5% CI	RWC_{PLRC50}	2,5% CI	97,5% CI
H. annuus	leaf		sigmoidal	$y= a/[1+ (x/x_0)^b]$	63,2	2,4	29,8	0,85	**<0.0001**	57,5	66	50	35	38	30,5	17	21	13,5
		dehydration method																
		pot method	sigmoidal	$y= a/[1+ (x/x_0)^b]$	63,3	2,6	33,3	0,87	**<0.0001**	46	62,5	40	31	37	25	14	21,5	5
		bench method	sigmoidal	$y= a/[1+ (x/x_0)^b]$	63,2	2,5	26,4	0,87	**<0.0001**	61	74	53	39	44	34	16	25	13,5
	Stem		sigmoidal	$y= a/[1+ (x/x_0)^b]$	54,4	3,4	46,4	0,81	**<0.0001**	73	80	63	49	53	45			
		dehydration method																
		pot method	sigmoidal	$y= a/[1+ (x/x_0)^b]$	45,5	5,2	57,2	0,85	**<0.0001**	72	89	64	55	61	48,5			
		bench method	sigmoidal	$y= a/[1+ (x/x_0)^b]$	65,5	2,7	33,6	0,85	**<0.0001**	66	80	58	43,5	48,5	37,5			
	Root		sigmoidal	$y= a/[1+ (x/x_0)^b]$	60,8	2,7	40,8	0,78	**<0.0001**	74,5	91	55,5	46	53	40	23	29	17
		dehydration method																
		pot method	sigmoidal	$y= a/[1+ (x/x_0)^b]$	86,3	2,1	32	0,84	**<0.0001**	80	100	65	49,5	56,5	42	28	34	22,5
		bench method	sigmoidal	$y= a/[1+ (x/x_0)^b]$	57,9	3,1	37,6	0,78	**<0.0001**	61	87	44	41	54	34	31	30	7,5

Species	organ		model type	equation	a	b	x_0	r^2	*P*	RWC_{PLRC10}	2,5% CI	97,5% CI	RWC_{PLRC25}	2,5% CI	97,5% CI	RWC_{PLRC50}	2,5% CI	97,5% CI
P. nigra	leaf		sigmoidal	$y= a/[1+ (x/x_0)^b]$	78,3	3,5	46,7	0,95	**<0.0001**	80	85	75	58	61	54,5	40	43	36
		dehydration method																
		pot method	sigmoidal	$y= a/[1+ (x/x_0)^b]$	86,2	3,2	43,2	0,97	**<0.0001**	81,5	85	73	57	62,5	53	39	42	35,5
		bench method	sigmoidal	$y= a/[1+ (x/x_0)^b]$	71,1	4	508	0,95	**<0.0001**	80,5	85	74	59,5	62	55	41	45,5	35,5
	Stem		sigmoidal	y= a/[1+ (x/x0)b]	36,3	3,7	49,8	0,84	**<0.0001**	65	70	60	40	43	36			
		dehydration method																
		pot method	sigmoidal	$y= a/[1+ (x/x_0)^b]$	38,9	3	52,1	0,86	**<0.0001**	74	87,5	65	42,5	47	38			
		bench method	sigmoidal	$y= a/[1+ (x/x_0)^b]$	33,3	4,17	49,2	0,85	**<0.0001**	59,5	65	55	37,5	41,5	33			
	Root		sigmoidal	$y= a/[1+ (x/x_0)^b]$	63,8	1,6	23,5	0,8	**<0.0001**	67	95	52	35	36	25,5	10	14	8
		dehydration method																
		pot method	sigmoidal	$y= a/[1+ (x/x_0)^b]$	61,5	1,5	23,9	0,72	**<0.0001**	69	0	46	32	42	24	6	10,5	8
		bench method	sigmoidal	$y= a/[1+ (x/x_0)^b]$	63,2	1,6	24,5	0,83	**<0.0001**	71	0	46	26	39	24,5	9	14	0

Species	organ		model type	equation	a	b		r^2	*P*	RWC_{PLRC10}	2,5% CI	97,5% CI	RWC_{PLRC25}	2,5% CI	97,5% CI	RWC_{PLRC50}	2,5% CI	97,5% CI
Q. ilex	leaf		exponential	$y=ae^{-bx}$	93,6	0,033		0,96	**<0.0001**	66,5	72	59	38	41	34,5	16	19	14
		dehydration method								69	76	59	37	41,5	34	15,5	17,6	13
		pot method	exponential	$y=ae^{-bx}$	85,4	0,032		0,89	**<0.0001**	65	73	59,5	37,5	40,5	35	16	18	14,5
		bench method	exponential	$y=ae^{-bx}$														
					a	**b**		r^2	*P*									
	Stem		exponential	$y=ae^{-bx}$	58,2	0,028		0,76	**<0.0001**	62	69	56	29	31,5	25			
		dehydration method																
		pot method	exponential	$y=ae^{-bx}$	102,9	0,041		0,85	**<0.0001**	55,5	62	49,5	34	36	30			
		bench method	exponential	$y=ae^{-bx}$	51,1	0,025		0,73	**<0.0001**	65	74	56,5	28	32,5	23			
					a	**b**		r^2	*P*									
	Root		exponential	$y=ae^{-bx}$	52,2	0,019		0,73	**<0.0001**	85,5	100	75	38	44	34,5			
		dehydration method																
		pot method	exponential	$y=ae^{-bx}$	66,1	0,02		0,75	**<0.0001**	91	100	74	45,5	55,5	44	14	19,5	0
		bench method	exponential	$y=ae^{-bx}$	50,44	0,02		0,79	**<0.0001**	77,5	97,5	65	38	44	34			

Table S3: Fitted regressions recorded between leaf, stem and root percentage loss of rehydration capacity (PLRC) and relative electrolyte leakage (REL) in pot *versus* bench dehydrated samples of *H. annuus*, *P. nigra* and *Q. ilex*. Model type, equation, coefficient values, correlation coefficients (r^2) and P-values are reported. Moreover, REL values leading to 10%, 25% and 50% of PLRC (i.e., REL_{PLRC10}, REL_{PLRC25}, REL_{PLRC50}, respectively) and corresponding confidence intervals (CI) are also reported.

Species	organ		model type	equation	y_0	a	r^2	*P*	REL_{PLRC10}	2,5% CI	97,5% CI	REL_{PLRC25}	2,5% CI	97,5% CI	REL_{PLRC50}	2,5% CI	97,5% CI
H. annuus	leaf		linear	$y=y_0+ax$	-7,8	1	0,83	**<0.0001**	18	15,5	20	31,5	30	35	56	51,5	60
		dehydration method															
		pot method	linear	$y=y_0+ax$	-11,6	1,1	0,89	**<0.0001**	19	16	22	31,5	29,5	35	53	49	59
		bench method	linear	$y=y_0+ax$	-5,3	0,94	0,79	**<0.0001**	17	13	20	31,5	29	36	59	52,5	69
	Stem		linear	$y=y_0+ax$	-5,7	1,1	0,55	**<0.0001**	15	10	17,5	27,5	24	31	48,5	42,5	57
		dehydration method															
		pot method	linear	$y=y_0+ax$	-8	1,1	0,59	**<0.0001**	12,5	0	17,5	26	20,5	34	48,5	40	
		bench method	linear	$y=y_0+ax$	-2,4	1	0,51	**<0.0001**	16	10	19,5	29	24	34	48,5	41	63
	Root		linear	$y=y_0+ax$	-3	0,77	0,74	**<0.0001**	16	10	24	35,5	30,5	40	68	62,5	75
		dehydration method															
		pot method	linear	$y=y_0+ax$	-1,7	0,77	0,79	**<0.0001**	16	5	23,5	34	27,5	40	66	59	79
		bench method	linear	$y=y_0+ax$	-5,5	0,8	0,69	**<0.0001**	20	5	30	37,5	28	45	69	62	79

Species	organ		model type	equation	y_0	a	r^2	*P*	REL_{PLRC10}	2,5% CI	97,5% CI	REL_{PLRC25}	2,5% CI	97,5% CI	REL_{PLRC50}	2,5% CI	97,5% CI
P. nigra	leaf		linear	$y=y_0+ax$	-11,1	1,5	0,86	**<0.0001**	15,5	11	19	25	23	27,5	42,5	40	45,5
		dehydration method															
		pot method	linear	$y=y_0+ax$	-5,9	1,2	0,81	**<0.0001**	15	10	20	25	20	28	40,5	37,5	45
		bench method	linear	$y=y_0+ax$	-8,4	1,4	0,84	**<0.0001**	14,5	9,5	19	25	21	28	45	40,5	49,5
	Stem		linear	$y=y_0+ax$	-11,9	0,77	0,6	**<0.0001**	30	24	32,5	47,5	45	51			
		dehydration method															
		pot method	linear	$y=y_0+ax$	-7,5	0,76	0,71	**<0.0001**	22,5	17,5	29	42,5	40	47			
		bench method	linear	$y=y_0+ax$	-15,4	0,78	0,59	**<0.0001**	32	29	36	51	47,5	57,5			
	Root		linear	$y=y_0+ax$	-15,8	0,9	0,72	**<0.0001**	29,5	22,5	33	44	41	47,5	71	66,5	76
		dehydration method															
		pot method	linear	$y=y_0+ax$	-9,8	0,77	0,64	**<0.0001**	28	19	33	45	40	51	76	69	100
		bench method	linear	$y=y_0+ax$	-21,5	1,1	0,76	**<0.0001**	30,5	24	36	44	38	48	68,5	63	74

Species	organ		model type	equation	y_0	a	r^2	*P*	REL_{PLRC10}	2,5% CI	97,5% CI	REL_{PLRC25}	2,5% CI	97,5% CI	REL_{PLRC50}	2,5% CI	97,5% CI
Q. ilex	leaf		linear	$y=y_0+ax$	-19,1	1,1	0,61	**<0.0001**	27,5	25	30	41	38	44	65,5	59,5	70,5
		dehydration method															
		pot method	linear	$y=y_0+ax$	-17,9	1,1	0,63	**<0.0001**	27,5	19	32	40	35	47	64	55	83
		bench method	linear	$y=y_0+ax$	-19,9	1,1	0,61	**<0.0001**	28	25	30	41	38	45,5	64,5	59	74
	Stem		linear	$y=y_0+ax$	-12	0,63	0,62	**<0.0001**	35	31	39	60	56	65			
		dehydration method															
		pot method	linear	$y=y_0+ax$	-11,03	0,58	0,6	**<0.0001**	36	31	42,5	64	55	75			
		bench method	linear	$y=y_0+ax$	-12,6	0,65	0,63	**<0.0001**	35	30	39	63,5	54	65			
	Root		linear	$y=y_0+ax$	-6,5	0,65	0,65	**<0.0001**	26	20	30	49	45	51	86	80	97
		dehydration method															
		pot method	linear	$y=y_0+ax$	-5,9	0,69	0,7	**<0.0001**	25	12	30,5	45	39	50,5	81	73	94
		bench method	linear	$y=y_0+ax$	-6,9	0,65	0,64	**<0.0001**	26	20	31,5	51	45	54	88	81	100

Table S4: Fitted regressions recorded between leaf, stem and root relative water content (RWC) and relative electrolyte leakage (REL) in pot *versus* bench dehydrated samples of *H. annuus, P. nigra* and *Q. ilex*. Model type, equation, coefficient values, correlation coefficients (r^2) and P-values are reported. Moreover, RWC values leading to 25% and 50% of REL (i.e., RWC_{REL25}, RWC_{REL50}, respectively) and corresponding confidence intervals (CI) are also reported.

Species	organ		model type	equation	a	b	r^2	P	RWC_{REL25}	2,5% CI	97,5% CI	RWC_{REL50}	2,5% CI	97,5% CI
H. annuus	leaf		exponential	$y=ae^{-bx}$					50	45	57,5	17	20	14
		dehydration method												
		pot method	exponential	$y=ae^{-bx}$	66,8	0,02	0,88	**<0,0001**	48	55	42,5	15	19,5	9,5
		bench method	exponential	$y=ae^{-bx}$					52,5	58	47	20,5	25	16
									RWC_{REL25}	2,5% CI	97,5% CI	RWC_{REL40}	2,5% CI	97,5% CI
	Stem		exponential	$y=ae^{-bx}$	58,3	0,017	0,67	**<0,0001**	50,5	54,5	44,5	22,5	27	15
		dehydration method												
		pot method	exponential	$y=ae^{-bx}$	60,5	0,017	0,71	**<0,0001**	52	60	44,5	26	31,5	10
		bench method	exponential	$y=ae^{-bx}$	56,7	0,017	0,65	**<0,0001**	48	55	40,5	20	28	10
									RWC_{REL25}	2,5% CI	97,5% CI	RWC_{REL50}	2,5% CI	97,5% CI
	Root		exponential	$y=ae^{-bx}$	92,9	0,019	0,85	**<0,0001**	64,5	75	59	31	35	27,5
		dehydration method												
		pot method	exponential	$y=ae^{-bx}$	89,5	0,019	0,92	**<0,0001**	62,5	100	40	30,5	49	15,5
		bench method	exponential	$y=ae^{-bx}$	115,5	0,02	0,79	**<0,0001**	62,5	75	55	35	40,5	29,5

Species	organ		model type	equation	a	b	r^2	P	RWC_{REL25}	2,5% CI	97,5% CI	RWC_{REL50}	2,5% CI	97,5% CI
P. nigra	leaf		exponential	$y=ae^{-bx}$	70,1	0,018	0,86	**<0,0001**	59	65	54	19	21,5	16
		dehydration method												
		pot method	exponential	$y=ae^{-bx}$	69,4	0,016	0,88	**<0,0001**	64	72,5	54	20	25	15,5
		bench method	exponential	$y=ae^{-bx}$	71,2	0,019	0,85	**<0,0001**	55	60	46	18	22,5	14
	Stem		exponential	$y=ae^{-bx}$	65,3	0,0099	0,59	**<0,0001**	95	100	84,5	27,5	32	20
		dehydration method												
		pot method	exponential	$y=ae^{-bx}$	64	0,01	0,76	**<0,0001**	89	100	72,5	25	32,5	12,5
		bench method	exponential	$y=ae^{-bx}$	68,02	0,01	0,79	**<0,0001**	95	100	84	29,5	37,5	22,5
	Root		exponential	$y=ae^{-bx}$	73,4	0,011	0,66	**<0,0001**	91	100	75	31	37	26
		dehydration method												
		pot method	exponential	$y=ae^{-bx}$	70,5	0,01	0,53	**<0,0001**	86	100	65,5	30	39	20
		bench method	exponential	$y=ae^{-bx}$	74,7	0,01	0,76	**<0,0001**	100	100	84	36,5	46	29,5

Species	organ		model type	equation	a	b	r^2	P	RWC_{REL25}	2,5% CI	97,5% CI	RWC_{REL50}	2,5% CI	97,5% CI
Q. ilex	leaf		exponential	$y=ae^{-bx}$	65,4	0,01	0,63	**<0,0001**	86	100	80	25	30,5	19
		dehydration method												
		pot method	exponential	$y=ae^{-bx}$	66,9	0,0116	0,64	**<0,0001**	85	100	69	24,5	34,5	10
		bench method	exponential	$y=ae^{-bx}$	64,8	0,009	0,64	**<0,0001**	99	100	86	25	32	14,5
	Stem		exponential	$y=ae^{-bx}$	76,4	0,01	0,64	**<0,0001**	99	100	98	38	44	34
		dehydration method												
		pot method	exponential	$y=ae^{-bx}$	92,5	0,015	0,72	**<0,0001**	90	99	77,5	40	45,5	32
		bench method	exponential	$y=ae^{-bx}$	72,6	0,0096	0,63	**<0,0001**	100	100	98	37	43	30
	Root		exponential	$y=ae^{-bx}$	75,9	0,01	0,67	**<0,0001**	100	100	87	35	40,5	30
		dehydration method												
		pot method	exponential	$y=ae^{-bx}$	92,8	0,015	0,83	**<0,0001**	94	100	81	40,5	45,5	35
		bench method	exponential	$y=ae^{-bx}$	72,5	0,01	0,64	**<0,0001**	100	100	98	35	42	28

Table S5: Fitted regressions recorded between leaf water potential and stomatal conductance to water vapour (g_L), between gL and leaf, stem and root relative water content (RWC), percentage loss of rehydration capacity (PLRC) and relative electrolyte leakage (REL) of *H. annuus*, *P. nigra* and *Q. ilex* plants Model type, equation, coefficient values, correlation coefficients (r^2) and P-values are reported. Moreover, leaf water potential (i.e., P_{gL20}, P_{gL50}, P_{gL80}) values, as well as RWC (i.e., RWC_{gL20}, RWC_{gL50}, RWC_{gL80}), PLRC (i.e., $PLRC_{gL20}$, $PLRC_{gL50}$, $PLRC_{gL80}$) and REL (REL_{gL20}, REL_{gL50}, REL_{gL80}) values leading to 20%, 50% and 80% loss of g_L and corresponding confidence intervals (CI) are also reported.

gL vs Ψ L																			
	model type	**equation**	**a**	**b**	**x_0**		**r^2**	***P***		**P_{gL20}**	**2,5% CI**	**97,5% CI**	**P_{gL50}**	**2,5% CI**	**97,5% CI**	**P_{gL80}**	**2,5% CI**	**97,5% CI**
H. annuus	sigmoidal	y= a/[1+ $(x/x_0)^b$]	294,1	4,9	1,8		0,95	**<0.0001**		0,6	0,5	0,75	0,8	0,65	0,85	1,1	0,95	1,2
P. nigra	sigmoidal	y= a/[1+ $(x/x_0)^b$]	332,9	13,4	0,97		0,72	**0,0018**		0,9	0	0,95	0,95	0,85	1,1	1,1	0,9	1,25
Q. ilex	sigmoidal	y= a/[1+ $(x/x_0)^b$]	190,7	3,91	1,78		0,95	**<0.0001**		1,3	1,05	1,5	1,85	1,65	2	2,55	2,35	2,85
gL vs RWC																			
		model type	**equation**	**a**	**b**	**x_0**	**r^2**	***P***		**RWC_{gL20}**	**2,5% CI**	**97,5% CI**	**RWC_{gL50}**	**2,5% CI**	**97,5% CI**	**RWC_{gL80}**	**2,5% CI**	**97,5% CI**
H. annuus	Leaf	sigmoidal	y= a/[1+ $(x/x_0)^b$]	298,4	-14,5	74,6	0,92	**<0.0001**		81	89	75	75	80	71	67,5	70	62
				yo	**a**		**r^2**	***P***										
	Stem	linear	y= y_0 + ax	-226,1	4,9		0,62	**0,0009**		94	100	96	75	85	64	55	69	40
	Root	linear	y= y_0 + ax	-332,9	6,4		0,8	**<0.0001**		87,5	96	82	74	69	78	61	67	54
		model type	**equation**	**a**	**b**	**x_0**	**r^2**	***P***										
P. nigra	Leaf	sigmoidal	y= a/[1+ $(x/x_0)^b$]	348,7	-27,3	90,8	0,81	**0,0003**		95	100	90,5	89,5	92,5	86	86	90	81
	Stem	sigmoidal	y= a/[1+ $(x/x_0)^b$]	302,5	-13,3	76,6	0,85	**<0.0001**		84	100	76	76	84	69	69	76	62
	Root	sigmoidal	y= a/[1+ $(x/x_0)^b$]	595,6	-5,2	100,3	0,76	**0,0007**		94	100	80	80,5	92,5	65,5	61	81	45
				yo	**a**													
Q. ilex	Leaf	linear	y= y_0 + ax	-262,4	4,12		0,61	**0,0015**		91	100	85	81	86	71	66	71	60
	Stem	linear	y= y_0 + ax	-219,4	3,8		0,55	**0,0039**		89	100	81	71	73	65	64	70	51,5
	Root	linear	y= y_0 + ax	-117,3	2,79		0,56	**0,0033**		85	100	72,5	69	84	59	47,5	60	33
gL vsPLRC																			
		model type	**equation**	**y_o**	**a**		**r^2**	***P***		**$PLRC_{gL20}$**	**2,5% CI**	**97,5% CI**	**$PLRC_{gL50}$**	**2,5% CI**	**97,5% CI**	**$PLRC_{gL80}$**	**2,5% CI**	**97,5% CI**
H. annuus	Leaf	linear	y= y_0 + ax	230,1	-13,9		0,43	**0,0112**		4	0	8	9	5	17,5	14	9	
	Stem	linear	y= y_0 + ax	259,4	0,07		0,63	**0,0007**		4,5	0	10	10,5	5,5	20,5	22,5	11	38
				a	**b**		**r^2**	***P***										
	Root	exponential	$y=ae^{-bx}$	264,05	0,06		0,64	**0,0006**		5	0	10	12,5	6	22	25,5	14	40
				a	**b**		**r^2**	***P***										
P. nigra	Leaf	exponenatial	$y=ae^{-bx}$	271,5	0,16		0,81	**<0.0001**		2	0	4	4	2	8	10	5	17
	Stem	exponenatial	$y=ae^{-bx}$	304,6	0,09		0,55	**0,0037**		3	0	5	7,5	2,5	19	20	10,5	30
	Root	exponenatial	$y=ae^{-bx}$	287,4	0,15		0,42	**0,0173**		2	0	4	4	0	11	11	5	20
Q. ilex	Leaf	linear	y= y_0 + ax	114,4	-7,9		0,68	**0,0005**		5	4,5	7	7,5	4,5	10	11	8	16
	Stem	linear	y= y_0 + ax	72,2	-3,4		0,11	0,26										
	Root	linear	y= y_0 + ax	140,2	-4,4		0,42	**0,0166**		11	0	17	17,5	7,5	24	26	20	
gL vs REL																			
		model type	**equation**	**y_o**	**a**		**r^2**	***P***		**REL_{gL20}**	**2,5% CI**	**97,5% CI**	**REL_{gL50}**	**2,5% CI**	**97,5% CI**	**REL_{gL80}**	**2,5% CI**	**97,5% CI**
H. annuus	Leaf	linear	y= y_0 + ax	375,5	-14,4		0,79	<0.001		10	7	14	16	14	18	23	20	26
	Stem	linear	y= y_0 + ax	384,7	-16,6		0,35	0,02		10	0	14	20	9	21	25	16	
	Root	linear	y= y_0 + ax	310,6	-8,2		0,47	0,0068		10	0	17,5	20	11	29	31	24	
		model type	**equation**	**a**	**b**		**r^2**	***P***										
P. nigra	Leaf	exponential	$y=ae^{-bx}$	598,3	0,11		0,36	0,029		8	0	12	12,5	0	20	20	13	33
		model type	**equation**	**y_o**	**a**		**r^2**	***P***										
	Stem	linear	y= y_0 + ax	318,1	-6,6		0,25	0,083										
	Root	linear	y= y_0 + ax	315,6	-6,1		0,35	0,033		14	0	24	27	0	41	41	30	
				a	**b**													
Q. ilex	Leaf	linear	$y=ae^{-bx}$	645	0,1		0,4	0,02		18	0	20	25	0	28	27	21	41
				a	**b**													
	Stem		$y=ae^{-bx}$	2938	0,14		0,5	0,0068		21	0	23	24	0	27	31	25	
	Root		$y=ae^{-bx}$	**616,5**	**0,074**		0,55	0,0038		21	0	25	27,5	0	31,5	42	32,5	55,5

Table S6: Fitted regressions recorded between whole plant relative water content (RWC plant) and leaf, stem and root percentage loss of rehydration capacity (PLRC), between RWC plant and leaf, stem and root relative electrolyte leakage (REL) and between RWC plant and leaf stomatal conductance to water vapour (g_L) of *H. annuus*, *P. nigra* and *Q. ilex* plants Model type, equation, coefficient values, correlation coefficients (r^2) and P-values are reported. Moreover, plant RWC values leading to 20%, 50% and 80% loss of gL (i.e., $RWC_{gL2}0$, RWC_{gL50}, RWC_{gL80})and corresponding confidence intervals (CI) are also reported.

H. annuus								
PLRC vs RWC plant								
	organ	**model type**	**equation**	**y_0**	**a**	**r^2**	***P***	
	Leaf	linear	$y=y_0+ax$	79,01	-1,1	0,71	**<0.0001**	
	Stem	linear	$y=y_0+ax$	82,8	-1,1	0,56	**<0.0001**	
	Root	linear	$y=y_0+ax$	85,9	-1,1	0,81	**<0.0001**	
REL vs RWC plant								
	organ	**model type**	**equation**	**y_0**	**a**	**r^2**	***P***	
	Leaf	linear	$y=y_0+ax$	95,6	-1,4	0,79	**<0.0001**	
	Stem	linear	$y=y_0+ax$	102,3	-1,9	0,77	**<0.0001**	
	Root	linear	$y=y_0+ax$	90,3	-0,9	0,76	**<0.0001**	
gL vs RWC plant								
	model type	**equation**	**a**	**b**	**x_0**	**r^2**	***P***	**RWC_{gL20}**
H. annuus	sigmoidal	$y=a/[1+(x/x_0)^b]$	384,9	-7,1	81,3	0,86	**<0.0001**	89
P. nigra	exponential	$y=ae^{bx}$	0,0026	0,131		0,88	**<0.0001**	94,5
Q. ilex	exponential	$y=ae^{bx}$	0,0026	0,1321		0,88	**<0.0001**	83

P. nigra								
PLRC vs RWC plant								
	organ	**model type**	**equation**	**y_0**	**a**	**r^2**	***P***	
	Leaf	linear	$y=y_0+ax$	77,6	-0,7	0,84	**<0.0001**	
	Stem	linear	$y=y_0+ax$	97,7	-2,1	0,86	**<0.0001**	
	Root	linear	$y=y_0+ax$	80,2	-1,3	0,67	**<0.0001**	
REL vs RWC plant								
	organ	**model type**	**equation**	**y_0**	**a**	**r^2**	***P***	
	Leaf	linear	$y=y_0+ax$	86,2	-1,1	0,75	**<0.0001**	
	Stem	linear	$y=y_0+ax$	112,3	-1,6	0,59	**<0.0001**	
	Root	linear	$y=y_0+ax$	98,4	-1,1	0,55	**<0.0001**	
	RWC_{gL50}	**2,5% CI**	**97,5% CI**	**$RWC80_{gL}$**	**2,5% CI**	**97,5% CI**		
	72,5	79	65,5	65	71	56		
	85,6	91	76	66	80	50		
	79	81	77,5	73	75	69		

Q. ilex							
PLRC vs RWC plant							
	organ	**model type**	**equation**	**y_0**	**a**	**r^2**	***P***
	Leaf	linear	$y=y_0+ax$	76,1	-0,98	0,74	**<0.0001**
	Stem	linear	$y=y_0+ax$	77,2	-1,8	0,64	**<0.0001**
	Root	linear	$y=y_0+ax$	92,5	-1,4	0,81	**<0.0001**
REL vs RWC plant							
	organ	**model type**	**equation**	**y_0**	**a**	**r^2**	***P***
	Leaf	linear	$y=y_0+ax$	101,2	-1,2	0,67	**<0.0001**
	Stem	linear	$y=y_0+ax$	112,5	-1,4	0,71	**<0.0001**
	Root	linear	$y=y_0+ax$	110	-1,1	0,83	**<0.0001**

Table S7: Fitted regressions recorded between plant die-off and leaf, stem, root and whole plant relative water content (RWC), percentage loss of rehydration capability (PLRC) and relative electrolyte leakage (REL) of *H. annuus*, *P. nigra* and *Q. ilex* plants Model type, equation, coefficient values, correlation coefficients (r^2) and P-values are reported. Moreover, RWC (RWC_{M10}, RWC_{M50}), PLRC ($PLRC_{M10}$, $PLRC_{M50}$) and REL (REL_{M10}, REL_{M50}) leading to 10% and 50% of plant mortality and corresponding confidence intervals (CI) are also reported.

RWC vs plant die-off													
Species	**organ**	**model type**	**equation**	**a**	**b**	**r^2**	***P***	**RWC_{M10}**	**2,5% CI**	**97,5% CI**	**RWC_{M50}**	**2,5% CI**	**97,5% CI**
H. annuus	leaf	exponenatial	$y = ae^{bx}$	155,5	0,05	0,99	**0,0043**	59	81	37,5	25	35	20
	stem	exponenatial	$y = ae^{bx}$	924,1	0,07	0,98	**0,0087**	65	86	50	44	54	39
	root	exponenatial	$y = ae^{bx}$	367	0,05	98	**0,015**	65	94	40	35,5	52,5	26
	whole plant	exponenatial	$y = ae^{bx}$	378,9	0,05	0,98	**0,0096**	64,5	87	42,5	36	49	30
P. nigra	leaf	exponenatial	$y = ae^{bx}$	86,3	0,05	0,99	**<0.0001**	45	52	37	11	13	10
	stem	exponenatial	$y = ae^{bx}$	134,9	0,05	0,92	**0,0099**	55	75	29	20	32	10
	root	exponenatial	$y = ae^{bx}$	135,9	0,06	0,93	**0,0077**	41	60	22,5	15,5	24	6
	whole plant	exponenatial	$y = ae^{bx}$	117,9	0,04	0,93	**0,0066**	55	85	31	19	30	7,5
Q.ilex	leaf	exponenatial	$y = ae^{bx}$	148,3	0,06	0,99	**0,0002**	44	54	34	17,5	20	15,5
	stem	exponenatial	$y = ae^{bx}$	648,5	0,08	0,97	**0,0019**	50,5	65	40,5	31,5	35	28
	root	exponenatial	$y = ae^{bx}$	115,7	0,055	0,9	**0,0138**	43	72,5	22,5	15	26,5	0
	whole plant	exponenatial	$y = ae^{bx}$	183,1	0,062	0,96	**0,0029**	46	64	31	20,5	25,5	14,5

PLRC vs plant die-off													
Species	**Organ**	**model type**	**equation**	**y_0**	**a**	**r^2**	***P***	**$PLRC_{M1}$**	**2,5% CI**	**97,5% C**	**$PLRC_{M50}$**	**2,5% CI**	**97,5% CI**
H. annuus	leaf	linear	$y=y_0 + ax$	-1,5	1,6	0,96	**0,022**	7,5	0	22	34	20	63
	stem	linear	$y=y_0 + ax$	-12,9	2,1	0,89	0,054						
	root	linear	$y=y_0 + ax$	-12,9	1,7	0,88	0,06						
P. nigra	leaf	linear	$y=y_0 + ax$	-8,6	0,83	0,92	**0,0094**	23,5	0	41	71	52,5	100
	stem	linear	$y=y_0 + ax$	-18,8	1,96	0,74	0,059						
	root	linear	$y=y_0 + ax$	-15,6	2,3	0,78	0,11						
Q. ilex	leaf	linear	$y=y_0 + ax$	-7,26	1,1	0,91	**0,0115**	15	0	24	52,5	37	100
	stem	linear	$y=y_0 + ax$	-8,3	2,15	0,85	**0,0241**	9	0	18	27,5	18	100
	root	linear	$y=y_0 + ax$	-16,9	0,38	0,76	0,053						

REL vs plant die-off													
Species	**Organ**	**model t**	**equation**	**y_0**	**a**	**r^2**	***P***	**REL_{M10}**	**2,5% CI**	**97,5% CI**	**REL_{M50}**	**2,5% CI**	**97,5% CI**
H. annuus	leaf	linear	$y=y_0 + ax$	-208	1,9	0,98	**0,011**	19,5	0	30	37	29,5	51,5
	stem	linear	$y=y_0 + ax$	-36,9	0,7	0,97	**0,015**	17,5	0	25	37,5	25	45,5
	root	linear	$y=y_0 + ax$	-17,6	1,5	0,89	0,053						
P. nigra	leaf	linear	$y=y_0 + ax$	-22,6	1,2	0,9	**0,011**	26	6	40	59	46	100
	stem	linear	$y=y_0 + ax$	-53,6	2	0,87	**0,019**	31,5	0	40,5	50,5	40	100
	root	linear	$y=y_0 + ax$	-49,9	1,7	0,83	**0,029**	35	0	49	59	45	100
Q. ilex	leaf	linear	$y=y_0 + ax$	-44,6	1,76	0,81	**0,0367**	31	0	45	54	42	100
	stem	linear	$y=y_0 + ax$	-50,85	1,699	0,78	**0,0447**	36	0	53	60	50	100
	root	linear	$y=y_0 + ax$	-33,97	1,07	0,65	0,0978						

Conclusions and future perspectives

Vegetation mortality is one of the most dramatic consequences of ongoing climate changes. Therefore, it is very urgent to identify reliable indicators that permit, easily and at large scale, to monitor plant die-off and, then, predict the risk of vegetation mortality. This gap in our knowledge strongly impacts the reliability of predictive models too.

Data recorded in the present Thesis offer an encouraging starting point to further investigate RWC, but also PLRC and REL values as proxy of plant mortality risk.

Results recorded in the **Study 1** highlighted the key role of leaf water status and cell membrane damages on leaf hydraulics and, as a direct consequence, on whole plant hydraulics. Moreover, leaf shrinkage well described leaf hydraulic decline, even in response to irradiance, in *P. nigra*. However, similar results were not recorded in *S. ceratophylloides* (**Study 2**). In particular, the lack of any leaf hydraulic conductance (K_L) decline until the turgor loss point coupled to leaf shrinkage, suggests to reject the hypothesis to use leaf shrinkage as a proxy to predict K_L vulnerability, at least in species with high leaf capacitance. Moreover, in *S. ceratophylloides* and *S. officinalis*, that showed a moderate succulence syndrome, common absolute water content and the leaf water potential (but not RWC) thresholds were related to leaf hydraulic failure (**Study 2**). Results of **Study 3** showed that, in species showing a moderate succulence syndrome, and, mainly, in water-saving species, leaf hydraulic failure poorly affects the plant hydraulic failure. Nevertheless, robust correlations between leaf, stem and, especially, root water content and drought-driven cell damages were recorded. Findings recorded in the **Study 4** better clarified the link between the specific-organ water content and plant-die-off. Root is the primary sensing-drought organ and novel insights on drought-driven changes in root water status and cell membrane damages, including loss of rehydration capability, and stomatal closure emerged. However, an increase in plant mortality (i.e., >10% plant die-off) occurred at the same plant and leaf RWC threshold in herbaceous and woody species, i.e., RWC ~50%, as well as at the same leaf PLRC threshold, i.e., PLRC~15%. In summary, common thresholds triggering plant die-off were recorded in the three study species.

Overall, our findings strongly suggest to use plant RWC but also leaf RWC thresholds (as well as leaf PLRC thresholds) to monitoring plant risk of mortality. Caution must be taken when succulent and/or water saving species are monitored.

It can be noted that, in the present Thesis, all studies were performed on seedlings growing in greenhouse. Moreover, measured samples were subjected to only one water stress cycle. Thus, it is reasonable to suspect that adult plants and/or samples experiencing more drought events may

show different thresholds compared to values recorded in my studies. Further studies are needed to clarify these key questions.

I hope that my small research contribute may motivate such future studies.

References

Abate E., Nardini A., Petruzzellis F., Trifilò P, 2021a. Too dry to survive: leaf hydraulic failure in two Salvia speciescan be predicted on the basis of water content. *Plant Physiol. Biochem.* 166, 215-224.

Abate E., **Azzarà M., Trifilò P., 2021b**. When water availability is low, two Mediterranean *Salvia* species rely on root hydraulics. *Plants* 10, 1888.

Adams H.D., Zeppel M.J., Anderegg W.R.,et al., 2017.A multispecies synthesis of physiological mechanisms indrought-induced tree mortality. *Nat.Ecol.Evol.*1, 1285–1291.

AlamI., Sharmin S. A., Kim K.H., Yang J. K., Choi M.S., Lee B.H, 2010. Proteome analysis of soybean roots subjected to short-term drought stress. *Plant Soil* 333, 491-505.

Allen C.D., Macalady A.K., Chenchouni H., et al., 2010. A global overview of drought and heat-induced tree mortality reveals emerging climate change risks for forests. *For.Ec.Man*. 259,660–684.

Allen C.D., Breshears D.D., Mcdowell N.G., 2015. On underestimation of global vulnerability to tree mortality and forest die-off from hotter drought in the Anthropocene. *Ecosph.* 6, art 129.

Anderegg W.R.L., Kane J.M., Anderegg L.D.L., 2013. Consequences of widespread tree mortality triggered by drought and temperature stress. *Nat. Clim. Change* 3, 30–36.

Anderegg W.R.L., Klein T., Bartlett M., Sack L., Pellegrini A.F.A., Choat B., Jansen S, 2016. Meta-analysis reveals that hydraulic traits explain cross-species patterns of drought-induced tree mortality across the globe. *Proc Natl. Acad. Sci.* 113, 5024-5029.

Anderegg W.R.L., Anderegg L.D.L., Kerr K.L., Trugman A.T., 2019.Widespread drought-induced tree mortality at dry range edges indicates that climate stress exceeds species' compensating mechanisms. *Global Change Biol*. 25, 3793–3802.

Aranda I., Gil L., Pardos J.A, 2005. Seasonal changes in apparent hydraulic conductance and their implications for water use of European beech (Fagus sylvatica L.) and sessile oak [Quercus petraea (Matt.) Liebl] in South Europe. *Plant. Ecol.* 179, 155-167

Baaziz K.B., Lopez D., Rabot A., Combes D., Gousset A., Bouzid S., Cochard H., Sakr S., Venisse J.S., 2012. Light-mediated K(leaf) induction and contribution of both the PIP1s and PIP2s aquaporins in five tree species: Walnut (*Juglansregia*) case study. *Tree Physiol.* 32, 423-434.

Bartlett M.K., Scoffoni C., Sack L., 2012. The determinants of leaf turgor loss point and prediction of drought tolerance of species and biomes: a global meta-analysis. *Ecol. Lett.* 15, 393–405.

Bartlett M.K., Klein T., Jansen S., Choat B., Sack L., 2016. The correlations and sequence of plant stomatal, hydraulic, and wilting responses to drought. *Proc. Natl. Acad. Sci.* 113, 13098-13103.

Bercu R., Negrean G., Broasca L., 2012. Leaf anatomical study of taxons Salvia nemorosasubsp. tesquicola, Salvia nutans, and Salvia × Sobrogensis from Dobrudja. *Bot. serb*. 36, 103–109.

Blackman C.J., Brodribb T.J., Jordan G.J., 2009. Leaf hydraulics and drought stress: response, recovery and survivorship in four woody temperate plant species. *Plant Cell. Environ.* 32,1584-1595

Blackman C.J., Brodribb T.J., 2011. Two measures of leaf capacitance: insights into the water transport pathway and hydraulic conductance in leaves. *Funct. Plant Biol*. 38, 118–126.

Blackman C.J., Gleason S.M., Chang Y., Cook A.M., Laws C., Westob M., 2014. Leaf hydraulic vulnerability to drought is linked to site water availability across a broad range of species and climates. *An. Bot.* 114, 435–440.

Boer H.J., Drake P.L., Wendt E., Price C.A., Schulze E.D., Turner N.C., Nicolle D., Veneklaas E.J., 2016. Apparent over investment in leaf venation relaxes leaf morphological constraints on photosynthesis in arid habitats. *Plant Physiol.* 172, 2286-2299.

Bouche P.S., Delzon S., Choat B., et al., 2016. Are needles of *Pinus pinaster* more vulnerable to xylem embolism than branches? New insights from X-ray computed tomography. *Plant Cell. Environ.* 39,860-870.

Bourbia I., Pritzkow C., Brodribb T.J., 2021. Herb and conifer roots show similar high sensitivity to water deficit. *Plant Physiol.*186, 1908-1918.

Brodribb T.J., Holbrook N.M., 2003. Stomatal closure during leaf dehydration, correlation with other leaf physiological traits. *Plant Physiol.* 132, 2166–2173.

Brodribb T.J., Holbrook N.M., 2004. Stomatal protection against hydraulic failure: a comparison of coexisting ferns and angiosperms. *New Phytol*. 162, 663–670.

Brodribb T.J., Holbrook N.M., Zwieniecki M.A., Palma B., 2005. Leaf hydraulic capacity in ferns, conifers and angiosperms: impacts on photosynthetic maxima. *New Phytol.* 165, 839–846.

Brodribb T.J., Feild T., Jordan G., 2007. Leaf maximum photosynthetic rate and venation are linked by hydraulics. *Plant Physiol.* 144, 1890-1898.

Brodribb T.J., Bienaimé D., Marmottant P., 2016. Revealing catastrophic failure of leaf networks under stress. *Proc. Natl. Acad. Sci*.113, 4865-4869

Brodribb T.J., Cochard H., Rodriguez Dominguez C., 2019. Measuring the pulse of trees; using the vascular system to predict tree mortality in the 21st century. *Conserv. Physiol.* 7,coz046.

Brouillette L.C., Mason C.M., Shirk R.Y., Donovan L.A., 2014. Adaptive differentiation of traits related to resource use in a desert annual along a resource gradient. *New Phytol*. 201,1316-1327.

Bryant C., Fueznzalida T., Brothers N., Mencuccini M., Sack L., Binks O., Ball M. C., 2021. Shifting access to pools of shoot water sustains gas exchange and increases sta hydraulic safety during seasonal atmospheric drought. *Plant Cell Environ.*, doi: 10.1111/pce.14080.

Buckley T.N., 2015. The contributions of apoplastic, symplastic and gas phase pathways for water transport outside the bundle sheath in leaves. *Plant Cell. Environ*. 38, 7–22.

Buira A., Fernandez-Mazuecos M., Aedo C., Molina-Venegas R., 2021. The contribution of the edaphic factor as a driver of recent plant diversification in a Mediterranean biodiversity hotspot. *J. Ecol.* 109, 987–999.

Cardoso A.A., Brodribb T.J., Lucani C.J., DaMatta F.M., McAdam S.A.M., 2018 Coordinated plasticity maintains hydraulic safety in sunflower leaves. *Plant Cell. Environ.* 41, 2567-2576

Cardoso A.A., Billon L.M., Borges A.F., Fernandez-de-Una L., Gersony J.T., Guney A., Johnson K.M., LemaireC., Mrad A., Wagner Y., Petit G., 2020. New developments in understanding plant water transport under droughtstress. *New Phytol.* 227, 1025–1027.

Carnicer J., Coll M., Ninyerola M., Pons X., Sánchez G., Peñuelas J., 2011. Widespread crown condition decline, food web disrup-tion, and amplified tree mortality with increased climate change-type drought. *Proc. Natl. Acad. Sci*. 108, 1474-1478.

Charra-Vaskou K., Badel E., Burlett R., Cochard H., Delzon S., Mayr S., 2012. Hydraulic efficiency and safety of vascular and non-vascular components in *Pinus pinaster* leaves. *Tree Physiol.* 32, 1161-1170

Chaumont F., Tyerman S.D., 2014. Aquaporins: highly regulated channels controlling plant water relations. *Plant Physiol*. 164,1600-1618.

Choat B., Brodribb T.J., Brodersen C.R., Duursma R.A., Lopez R., Medlyn B.E., 2018. Triggers of tree mortality under drought. *Nature* 558, 531–539.

Cochard H., Venisse J.S., Barigah T.S., Brunel N., Herbette S., Guilliot A., Tyree M.T., Sakr S., 2007. Putative role of aquaporins in variable hydraulic conductance of leaves in response to light. *Plant Physiol.* 143, 122-133.

Cochard H., Badel E., Herbette S., Delzon S., Choat B., Jansen S., 2013. Methods for measuring plant vulnerability to cavitation: a critical review. *.J Experim. Bot*. 64, 4779–4791.

Cowling R.M., Potts A.J., Bradshaw P., et al., 2015. Variation in plant diversity in Mediterranean climate ecosystems: the role of climatic and topographical stability. *J. Biogeogr.* 42, 552–564.

Cramer W., Guiot J., Fader M., et al., 2018. Climate change and interconnected risks to sustainable development in the Mediterranean. *Nat. Clim. Change* 8, 972–980.

Creek D., Blackmann C.J., Brodribb T.J., Choat B., 2018. Coordination between leaf, stem, and root hydraulics and gas exchange in three arid-zone angiosperms during severe drought and recovery. *Plant Cell. Envirn.* 12, 2869-2881

Creek D., Lamarque L.J., Torres-Ruiz J.M., Parise C., Burlett R., Tissue D.T., Delzon S., 2020. Xylem embolism in leaves does not occur with open stomata: evidence from direct observations using the optical visualization technique. *J. Exp. Bot.* 71, 1151-1159.

Crisafulli A., Cannavò S., Maiorca G., Musarella C.M., Signorino G., Spampinato G., 2010. Aggiornamenti floristici per la Calabria. *Inf. Bot. Ital*. 42, 437–448.

Cruz de Carvalho M.H., 2008. Drought stress and reactive oxygen species. *Plant Sign. Behav.* 3, 156-165

Cuneo I. F., Knipfer T., Brodersen C. R., Mc Elrone A. J., 2016. Mechanical failure of fine root cortical cells initiates plant Hydraulic cecline during drought. *Plant Physiol.* 172, 1669-1678.

Cuneo I.F., Barrios-Masias F., Knipfer T., Uretsky J., Reyes C., Lenain P., Brodersen C.R., Walker M.A., McElrone A.J., 2021. Differences in grapevine rootstock sensitivity and recovery from drought are linked to fine root cortical lacunae and root tip function. *New Phytol.* 229, 272-283

Delzon S., Cochard H., 2014. Recent advances in tree hydraulics high light the ecological significance of the hydraulic safety margin. *New Phytol.* 203, 355–358

Drobinski P., Da Silva N., Bastin S., Mailler S., Muller C., Ahrens B., Christensen O.B., Lionello P., 2020. How warmer and drier will the Mediterranean region be at the end of the twenty-first century? *Reg. Environ. Change* 20- 78.

Duursma R. A., Choat B (2017). Fitplc: an R package to fit hydraulic vulnerability curves. *J. Plant Hydraul.* 4, e002.

Eamus D., Boulain N., Cleverly J., Breshears D.D., 2013. Global change-type drought- induced tree mortality: vapor pressure deficit is more important than temperature per se in causing decline in tree health. *Ecol. Evol*. 3, 2711–2729.

Eggli U., Nyffeler R., 2009. Living under temporarily arid conditions-succulence as an adaptive strategy. *Bradleya* 27, 13–36.

Epila J., De Baerdemaeker N.J.F., Vergeynst L.L., Maes W. H., Beeckman H., Steppe K., 2017. Capacitive water release and internal leaf water relocation delay drought-induced cavitation in African *Maesopsis eminii. Tree Physiol.* 37, 481–490

ErbanoM., Ehrenfried A.S.L., Pereira Dos Santos L., 2012. Morphoanatomical and phytochemical studies of Salvia lachnostachys (Lamiaceae). *Microsc. Res. Tech*. 75, 1737–1744.

Fang J., Lutz J.A., Wang L., Shugart H.H., Yan X., 2020. Using climate-driven leaf phenology and growth to improve predictions of gross primary productivity in North American forests. *Global Change Biol*. 26, 6974–6988.

Fisher R. N., Brehme C. S., Hathaway S. A., Hovey T. E., Warburton M. L., Stokes D. C., 2018. Longevity and population age structure af the arroyo southwestern toad (*Anaxyrus californicus)* with drought implications. *Ecol. evolut.* 8, 6124-6132.

Flexas J., Scoffoni C., Gago J., Sack L., 2013. Leaf mesophyll conductance and leaf hydraulic conductance: an introduction to their measurement and coordination. *J. Exp. Bot.* 64, 3965-3981

Forner A., Valladeres F., Aranda I., 2014. Mediterranean trees coping with severe drought: Avoidance might not be safe. *Env. Exp. Bot*. 155, 529-540.

Gazol A., Sanguesa-Barreda G., Granda E., Camarero J.J., 2017. Tracking the impact of drought on functionally different woody plants in a Mediterranean scrubland ecosystem*. Plant Ecol.* 218, 1009–1020.

Giorgi F., 2006. Climate change hot-spots. *Geophys. Res. Lett*. 33, L08707.

Goulart H., Van der Wiel K., Folberth C., Balkovic J., Van den Hurk B., 2021. Weather-induced crop failure events under climate change: a storyline approach. *Earth Syst. Dyn. Discuss.* 1-38

Griffiths H., Males J., 2017. Succulent plants. *Curr. Biol*. 27, R890–R896.

Guadagno C. R., Ewewrs B.E., Speckman H. N., Aston T. L., Huhn B.J., DeVore S. B., Ladwing J. T., Strawn R. N., Weining C., 2017. Dead ora Alive? Using Membrane Failure and Chloroplyll a Fluorescence to Predict Plant Mortality from Drought. *Plant Physiol.* 175,223-234.

Guyot G., Scoffoni C., Sack L., 2012. Combined impacts of irradiance and dehydration on leaf hydraulic conductance:insights into vulnerability and stomatal control. *Plant Cell. Environ.* 35, 857–871.

Hammond W.M., Yu K., Wilson L.A., Will R E., Anderegg W.R.L., Adams H.D., 2019. Dead or dying? Quantifying the point of no return from hydraulic failure in drought- induced tree mortality. *New Phytol*. 223, 1834–1843.

Harayama H., Kitao M., Agathokleous E., Ishida A., 2019. Effects of major vein blockage and aquaporin inhibition on leaf hydraulics and stomatal conductance. *Proc. R. Soc. B* 286: 20190799.

Hartmann H., Ziegler W., Kolle O., Trumbore S., 2013. Thirst beats hunger – declining hydration during drought prevents carbon starvation in Norway spruce saplings. *New Phytol.* 200, 340–349.

Hartmann H., Moura C.F., Anderegg W.R.L., et al., 2018. Research frontiers for improving our understanding of drought- induced tree and forest mortality. *New Phytol.* 218, 15-28.

Hernandéz E.I., Vilagrosa A., Pausas J.G., Bellot J., 2010. Morphological traits and water use strategies in seedlings of Mediterranean coexisting species. *Plant Ecol*. 207, 233–244.

Hochberg U., Windt C.W., Ponomarenko A., Zhang Y.J., Gersony J., Rockwell F.E., Hoolbrook N.M., 2017. Stomatal closure, basal leaf embolism, and shedding protect the hydraulic integrity of grape stems. *Plant Physiol*. 174, 764-775.

Holbrook N.M., 2017. Stomatal closure, basal leaf embolism and shedding protect the hydraulic integrity of grape stems. *Plant Physiol.* 174, 764–775.

Hood M.S., Varner J. M., Van Mantgem P., Cansler C.A., 2018. Fire and tree death; understanding and improving modeling of fire-induced tree mortality. *Env. Res. Lett.* 13, 113004.

IPCC, 2013.Stocker T., Qin D., Plattner G-K et al. 2013. Summary for Policymakers. In: *Climate Change.*

IPCC, 2019.Shukla P.R., Skea J., Calvo Buendia et al., 2019. Climate Change and Land: an IPCC Special Reporton Climate Change, Desertification, Land Degradation, Sustainable Land Management, Food Security, and Greenhouse Gas Fluxes in Terrestrial Ecosystems.

Jackson R.B., Sperry J. S., Dawson T. D., 2000. Root water uptake and transport: using physiological processes in global predictions. *Trends Plant Sci.* 5, 482-488.

Johnson D. M., Meinzer F.C., Woodruff D.R., McCulloh K.A., 2009. Leaf xylem embolism, detected acoustically and by cryo-SEM, corresponds to decreases in leaf hydraulic conductance in four evergreen species. *Plant Cell. Environ.* 32, 828-836.

John G.P., Henry C., Sack L., 2018. Leaf rehydration capacity: associations with other indices of drought tolerance and environment. *Plant Cell. Environ.* 41, 2638–2653.

Johnson D.M., McCulloh K.A., Meinzer F.C., Woodruff D.R., 2012. Evidence for leaf xylem embolism as a primary factor in dehydration induced declines in leaf hydraulic conductance. *Plant Cell. Env.* 35, 760-769

Johnson D.M., Berry Z.C., Baker K.V., Smith D.D., McCulloh K.A., Domec J.C., 2018. Leaf hydraulic parameters are more plastic in species that experience a wider range of leaf water potentials. *Funct. Ecol.* 32,894-903

Juhlke T.R., Van Geldern, R., Barth J.A.C., Bendix J., Bräuning A., Garel E., Häusser M., Huneau F., Knerr I., Santoni S., Szymczak S., Trachte, K., 2021. Temporal off set between precipitation and water uptake of Mediterranean pine trees varies with elevation and season. *Science. Tot. Envirn*. 755, 142539.

Kahraman A., Celep F., Dogan M., 2010. Anatomy, trichome morphology and palynology of Salvia chrysophylla Stapf (Lamiaceae). *South Afr. J. Bot*. 76, 187–195.

Kaur G., Asthir B., 2017. Molecular responses to drought stress in plants. *Biol. Plant* 61, 201-209

Kim Y.X., Steudle E., 2007. Light and turgor affect the water permeability (aquaporins) of parenchyma cells in the midrib of leaves of *Zea mays*. *J. Exp. Bot.* 58, 4119-4129.

Kim Y.X., Steudle E., 2009. Gating of aquaporins by light and reactive oxygen species in leaf parenchyma cells of the midrib of *Zea mays*. *J. Exp. Bot.* 60, 547-556

Kiorapostolou N., Da Sois L., Petruzzellis F., Savi T., Trifilò P., Nardini A, Petit G., 2019. Vulnerability to xylem embolism correlates to wood parenchyma fraction in angiosperms but not in gymnosperms. *Tree Physiol.* 39,1675–1684.

Klein T., Hartmann H., 2018. Climate change drives tree mortality. *Science* 362, 758.

Klein T., Zeppel M.J.B., Anderegg W.R.L., Bloemen J., De Kauwe M.G., Hudson P., Ruehr N.K., Powell T.L., von Arx G., Nardini A., 2018. Xylem embolism refilling and resilience against drought-induced mortality in woody plants: processes and trade-offs. *Ecol. Res*. 33, 839–855.

Lesk C., Rowhani P.,Ramankutty N., 2016. Influence of extreme weather disasters on global crop production. *Nature* 529, 84-87.

Laur J., Hacke U.G., 2014. The role of water channel proteins in facilitating recovery of leaf hydraulic conductance from water stress in *Populus trichocarpa*. *PLoSONE* 9: e111751.

Li Y., Xu S., Gao J., Pan S., Wang G., 2016. Glucose- and mannose-induced stomatal closure is mediated by ROS production, $Ca^{2+}$and water channel in *Viciafaba*. *Physiol. Plant* 156, 252-261.

Lionello P., Scarascia L., 2018. The relation between climate change in the Mediterranean region and global warming. *Reg. Environ. Change* 18, 1481–1493.

Lo Gullo M.A., Nardini A., Trifilò P., Salleo S., 2003. Changes in leaf hydraulics and stomatal conductance following drought stress and irrigation in *Ceratonia siliqua* (Carob tree). *Physiol. Plant* 117, 186-194.

Lopez D., Venisse J.S., Fumanal B., Chaumont F., Guillot E., Daniels M.J., Cochard H., Julien J.L., Gousset-Dupont A., 2013. Aquaporins and leaf hydraulics: poplar sheds new light. *Plant Cell Physiol* 54,1963-1975.

Lopez-Iglesis B., Villar R., Poorter L., 2014. Functional traits predict drought performance and distribution of Mediterranean woody species. *Acta Oecol*. 56, 10-18.

Males J., 2017. Secrets of succulence. *J. Exp. Bot*. 9, 2121–2134.

Mantova M., Menezes-Silva P.E., Badel E., Cochard, H., Torres-Ruiz J.M., 2021. The interplay of hydraulic failure and cell vitality explains tree capacity to recover from drought. *Physiol. Plant.* 172, 247-257.

Mariotti A., Pan Y., Zeng N., Alessandri A., 2015. Long-term climate change in the Mediterranean region in the midst of decadal variability. *Clim. Dynam*. 44, 1437–1456.

Markesteijn L., Poorter L., 2009. Seedling root morphology and biomass allocation of 62 tropical tree species in relation to drought- and shade-tolerance. *J. Ecol*. 97, 311-325.

Martínez-Vilalta J., Anderegg W.R., Sapes G., Sala A., 2019. Greater focus on water pools may improve our ability to understand and anticipate drought-induced mortality in plants. *New Phytol*. 223, 22–32.

Marusig D., Petruzzellis F., Tomasella M., Napolitano R., Altobelli A., Nardini A., 2020. Correlation of field-measured and remotely sensed plant water status as atool to monitor the risk of drought-induced forest decline. *Forests* 11: 77.

Maurel C., Verdoucq L., Luu D.T., Santoni V., 2008. Plant aquaporins: membrane channels with multiple integrated functions. *Ann. Rev. Plant Biol.* 59, 595-624.

Maurel C., Prado K., 2017. Aquaporins and leaf water relations. In: Chaumont F., Tyrmen S., (eds) Plant aquaporins. Signaling and communication in plants. Springer, Cham

McCormack M.L., Dickie I.A., Eissenstat D.M., et al., 2015. Redefining fine roots improves understanding of below-ground contributions to terrestrial biosphere processes. *New Phytol*. 207, 505-518.

Mc Dowell N., Pockman W.T., Allen C.D., et al., 2008. Mechanisms of plant survival and mortality during drought: Why do some plants survive while others succumb to drought? *New Phytol.* 178, 719-739

McDowell N.G., Brodribb T.J., Nardini A., 2019. Hydraulics in the 21st Century. *New Phytol.* 224, 537–542.

Menezes-Silva P.E., Loram-Lourenço L., Alves R.D.F.B., Sousa L.F., Almeida S.E.D.S., Farnese F.S., 2019. Different ways to die in a changing world: Consequences of climate change for tree species performance and survival through an ecophysiological per-spective. *Ecol. Evol.* 9, 11979-11999.

Miniussi M., Del Terra L., Savi T., Pallavicini A., NardiniA., 2015. Aquaporins in *Coffea arabica*L.: identification, expression, and impacts on plant water relations and hydraulics. *Plant Physiol. Biochem.* 95, 92-102

Molina-Venegas R., Aparicio A., Lavergne S., Arroyo J., 2017. Climatic and topographical correlates of plant palaeo- and neo endemism in a Mediterranean biodiversity hotspot. *Ann. Bot*. 119, 229-238.

Molina-Venegas R., Ramos-Gutiérrez I., Moreno-Saiz J.C., 2020. Phylogenetic patterns of extinction risk in the endemic flora of a mediterranean hotspot as a guiding tool for preemptive conservation actions. *Front. Ecol. Evol*. 8, 571587.

Morris H., Plavcova L., Cvecko P., et al., 2016. A global analysis of parenchyma tissue fraction in secondary xylem of seed plants. *New Phytol.* 209, 1553-1565.
Mukarram M., Choudhary S., Kuriak D., Petek A., et al., 2021. Drought: Sensing, signaling, effects and tolerance in higher plant. *Phys. Plant.* 172, 1291-1300.
Muries B., Mom R., Benoit P., et al., 2019. Aquaporins and water control in drought-stressed poplar leaves: a glimpse into the extra-xylem vascular territories. *Environ. Exp. Bot.* 162, 25-3.
Nardini A., Tyree M.T., Salleo S., 2001. Xylem cavitation in the leaf of *Prunus lauro cerasus* and its impact on leaf hydraulics. *Plant Physiol.* 125, 1700-1709.
Nardini A., Salleo S., Raimondo F., 2003. Changes in leaf hydraulic conductance correlate with leaf vein embolism in *Cercis siliquastrum* L. *Trees* 17, 529-534.
Nardini A., Salleo S., 2003. Effects of the experimental blockage of the major veins on hydraulics and gas exchange of *Prunus lauro cerasus* L. leaves. *J. Exp. Bot.* 54, 1213-1219.
Nardini A., Salleo S., Andri S., 2005. Circadian regulation of leaf hydraulic conductance in sunflower (*Helianthus annuus* L. cv Margot). Plant Cell *Environ.* 28, 750-759.
Nardini A., Gascò A., Trifilò P., Lo Gullo M.A., Salleo S., 2007. Ion-mediated enhancement of xylem hydraulic conductivity is not always suppressed by the presence of Ca^{2+} in the sap. *J. Exp. Bot.* 58, 2609-2615.
Nardini A., Raimondo F., Lo Gullo M.A., Salleo S., 2010. Leaf miners help us understanding leaf hydraulic design. *Plant Cell. Environ.* 33, 1091-1100.
Nardini A., Pedà G., Salleo S., 2012. Alternative methods for scaling leaf hydraulic conductance offer new insights into the structure-function relationships of sun and shade leaves. *Funct. Plant Biol.* 39, 394-401.
Nardini A., Pedà G., Salleo S., 2012. Alternative methods for scaling leaf hydraulic conductance offer new insights into the structure-function relationships of sun and shade leaves. *Funct. Plant Biol*. 39, 394–401.
Nardini A., Luglio J., 2014. Leaf hydraulic capacity and drought vulnerability: possible trade-offs and correlations with climate across three major biomes. *Funct. Ecol*. 28, 810–818.
Nardini A., Lo Gullo M.A., Trifilò P., Salleo, S., 2014. The challenge of the Mediterranean climate to plant hydraulics: Responses and adaptations. *Envir. Exp. Bot.* 103, 68-79.
NardiniA., Savi T., Trifilò P., Lo Gullo M.A., 2018. Drought stress and the recovery from xylem embolism in woody plants. *Progress Bot.* 79, 197-231
Nobel P.S., Sanderson J., 1984. Rectifier-like activities of roots of two desert succulents. *J. Exp. Bot*. 35, 727-737.
North G.B., Nobel P.S., 1991. Changes in hydraulic conductivity and anatomy caused by drying and rewetting roots of Agave deserti. *Am. J. Bot*. 78, 906-915.
North G.B., Nobel P.S.,1996. Radial hydraulic conductivity of individual root y issues of *Opuntia ficus-indica* (L.) Miller as soil moisture varies. *Ann. Bot.* 1996, 77, 133-142.
Ogaya R., Peñuelas J., 2006. Contrasting foliar responses to drought in *Quercus ilex* and *Phillyrea latifolia*. *Biol. Plant* 50, 373-382.
Ogburn R.M., Edwards E.J., 2010. The ecological water use strategies of succulent plants. In: Kader, J.C., Delseny, M. (Eds.), *Adv. Botan. Res.* 55, 179–225.
Ohtsuka A., Sack L., Taneda H., 2018. Bundle sheath lignification mediates the linkage of leaf hydraulics and venation. *Plant Cell Environ* 41, 342-353
Padilla F.M., Miranda J.D., Jorquera M.AJ., Pugnaire, F.I., 2009. Variability in amount and frequency of water supply affects roots but not growth of arid shrubs. *Plant Ecol*. 204, 261-270.
Peñuelas J., Sardans J., Filella I., Estiarte M., et al., 2018. Assessment of the impacts of climate change on Mediterranean terrestrial ecosystems based on data from field experiments and long-term monitored field gradients in Catalonia. *Environ. Exp. Bot.* 152, 49-59.
Petruzzellis F., Tomasella M., Miotto A., Natale S., Trifilò, P., Nardini, A., 2020. A leaf selfie: using a smartphone to quantify leaf vulnerability to hydraulic dysfunction. *Plants* 9, 234.
Pignatti S., 2002. Flora d'Italia. *Edagricole.*
Pivovaroff A.L., Sack L., Santiago L.S., 2014. Coordination of stem and leaf hydraulic conductance in southern California shrubs: a test of the hydraulic segmentation hypothesis. *New Phytol*. 203, 842–850.
Plavcova L., Hoch G., Morris H., Ghiasi H., Jansen S., 2016. The amount of parenchyma and living fibers affects storage of nonstructural carbohydrates in young stems and roots of temperate trees. *Amer. J. Bot.* 103, 603-612.
Pokherel Y. et al., 2021. Global terrestrial water storage and drought severity under climate change. *Nat. Clim Change* 11, 226–233.
Poorter H., Niinemets U., Poorter L., Wright J.J., Villar R., 2009. Causes and consequences of variation in leaf mass area (LMA): a meta-analysis. *New Phytol*. 182, 565-588.
Powell K.I., Chase J. M., Tiffany M.K., 2013. Invasive plants have scale dependent effects on diversity by altering species- area relationships. *Science* 339, 316-318.
Prado K., Cotelle V., Li G., Bellati J., Tang N., Tournaire-Roux C., Martinière A., Santoni V., Maurel C., 2019. Oscillating aquaporin phosphorylation and proteins mediate the circadian regulation of leaf hydraulics. *Plant Cell.* 31, 417-429.

Pratt R.B., MacKinnon E.D., Venturas M.D., Crous C.J., Jacobsen A.L., 2015. Root resistance to cavitation isaccurately measured using a centrifuge technique. *Tree Phys. 35, 185-196.*

Raimondo F., Trifilò, P., Lo Gullo M.A., Andri S., Savi T., Nardini A., 2015. Plant performance on Mediterranean green roofs: interaction of species-specific hydraulic strategies and substrate water relations. *AoB Plants* 7, plv007.

Rao K., Anderegg W.R.L., Sala A., Martínez-Vilalta J., Konings A.G., 2019. Satellite-based vegetation optical depth as an indicator of drought-driven tree mortality. Remote *Sens. Environ.* 227, 125–136.

Raymond F., Ullmann A., Tramblay Y., Drobinski P., Camberlin P., 2019. Evolution of Mediterranean extreme dry spells during the wet season under climate change. *Reg. Environ. Change* 19, 2339–2351.

Rodriguez-Domiguez C.M., Brodribb T.J., 209. Declining root water transport drives stomatal closure in olive under moderate water stress. *New Phytol*. 225, 126-134.

Rosner S., Heinze B., Savi, T., Dalla-Salda G., 2019. Prediction of hydraulic conductivity loss from relative water loss: new insights into water storage of tree stems and branches. *Physiol. Plant.* 165, 843–854.

Rowland L., Da Costa A.C.L., Galbraith D.R., et al., 2015. Death from drought in tropical forests is triggered by hydraulics not carbon starvation. *Nature* 528, 119.

Rundel P.W., Arroyo M.T.K., Cowling R.M., Keeley J.E., Lamont B.B., Vargas P., 2016. Mediterranean biomes: evolution of their vegetation, floras, and climate. *Annu. Rev. Ecol. Evol. Syst*. 47, 383–407.

Saatchi S., Asefi Najafabady S., Malhi Y., et al., 2013. Persistent effects of a severe drought on Amazonian forest canopy. *Process Nat. Accad. Sci.* 110, 565-570.

Sack L., Tyree M.T., 2005. Leaf hydraulics and its implications in plant structure and function. *Vasc. Transp. Plants* 93-114

Sack L., Frole K., 2006. Leaf structural diversity is related to hydraulic capacity in tropical rain forest trees. *Ecol.* 87, 483-491

Sack L., Holbrook N.M., 2006. Leaf hydraulics. *Ann. Rev. Plant. Biol.* 57, 361-381

Sack L., Scoffoni C., 2013. Leaf venation: structure, function, development, evolution, ecology and applications in the past, present and future. *New Phytol*. 198, 983–1000.

Sack L., Melcher P.J., Zwieniecki M.A., Holbrook N.M., 2002. The hydraulic conductance of the angiosperm leaf lamina: a comparison of three measurement methods. *J. Exp. Bot.* 53, 2177–2184.

Sack L., Streeter C.M., Holbrook N.M., 2004. Hydraulic analysis of water flow through leaves of sugar maple and red oak. *Plant Physiol.* 134,1824-1833

Sala O.S., Stuart Chapin III, F., Armesto J.J., et al., 2000. Global biodiversity scenarios for the year 2100. *Science* 287, 1770–1774.

Salleo S., 1983. Water relations parameters of two Sicilian species of Senecio (groundsel) measured by the pressure bomb technique. *New Phytol*. 95, 179–188.

Salleo S., Raimondo F., Trifilò P., Nardini A., 2003. Axial-to-radial water permeability of leaf major veins: a possible determinant of the impact of vein embolism on leaf hydraulics? *Plant Cell. Environ.* 26,1749-1758

Sapes G., Roskilly B., Dobrowski S., Maneta M., Anderegg W.R.L., Martinez-Vilalta J., Sala A., 2019. Plant water content integrates hydraulics and carbon depletion to predict drought-induced seedling mortality. *Tree Physiol*. 39, 1300–1312.

Sapes, G., Sala, A., 2021. Relative water content consistently predicts drought mortality risk in seedling populations with different morphology, physiology, and times to death. *Plant Cel.l Environ*. doi:10.1111/pce.14149.

Savi T., Marin M., Luglio J., Petruzzellis F., Mayr S., Nardini A., 2016. Leaf hydraulic vulnerability protects stem functionality under drought stress in *Salvia officinalis*. *Funct. Plant. Biol*. 43, 370–379.

Schwantes A.M., Parolari A.J., Swenson J.J., Johnson D.M., Domec J.C., Jackson R.B., Pelak N., Porporato A. 2018. Accounting for landscape heterogeneity improves spatial predictions of tree vulnerability to drought. *New Phyt.* 220,132–146

Scoffoni C., Sack L., 2015. Are leaves 'freewheelin'? Testing for a Wheeler-type effect in leaf xylem hydraulic decline. *Plant Cel.l Environ.* 38, 534-543

Scoffoni C., Pou A., Aasamaa K., Sack L., 2008. The rapid light response of leaf hydraulic conductance: new evidence from two experimental methods. *Plant Cell. Environ.* 31, 1803–1812.

Scoffoni C., Rawls M., McKown A., Cochard H., Sack L., 2011. Decline of leaf hydraulic conductance with dehydration: relationship to leaf size and venation architecture. *Plant Physiol*. 156, 832–843.

Scoffoni C., McKown A.D., Rawls M., Sack L., 2012. Dynamics of leaf hydraulic conductance with water status: quantification and analysis of species differences under steady state. *J. Exp. Bot.* 63, 643-658.

Scoffoni C., Vuong C., Diep S., Cochard H., Sack L., 2014. Leaf shrinkage with dehydration: coordination with hydraulic vulnerability and drought tolerance. *Plant Physiol*. 164, 1772–1788.

Scoffoni C., Chatelet D.S., Pasquet-Kok J., et al., 2016. Hydraulic basis for the evolution of photosynthetic productivity. *Nature Plants* 2, 16072.

Scoffoni C., Albuquerque C., Brodersen C.R., et al., 2017a. Outside-xylem vulnerability, not xylem embolism, controls leaf hydraulic decline during dehydration. *Plant Physiol*. 173, 1197–1210.

Scoffoni C., Sack L., Ort D., 2017b. The causes and consequences of leaf hydraulic decline with dehydration. *J. Exp. Bot.* 68, 4479–4496.
Scoffoni C., Albuquerque C., Cochard H., et al., 2018. The causes of leaf hydraulic vulnerability and its influence on gas exchange in Arabidopsis thaliana. *Plant Physiol.* 178, 1584–1601.
Skelton R.P., Brodribb T.J., Choat B., 2017. Casting light on xylem vulnerability in an herbaceous species reveals a lack of segmentation. *New Phytol.* 214, 561–569.
Spampinato G., Crisafulli A., Marino A., Signorino G., 2011. Salvia ceratophylloides Ard.. *Infor. Bot. Ital.* 43, 381-458.
Scoffoni C., Albuquerque C., Cochard H., Buckley T.N., et al., 2018. The causes of leaf hydraulic vulnerability and its influence on gas exchange in *Arabidopsis thaliana*. *Plant Physiol.* 178, 1584-1601.
Seelig H.D., Wolter A., SchröderF.G., 2015. Leaf thickness and turgor pressure in bean during plant desiccation. *Scie Hort*184, 55-62
Sellin A., Sack L., Õunapuu E., Karusion A., 2011. Impact of light quality on leaf and shoot hydraulic properties: a case study in silver birch (*Betula pendula*). *Plant Cell. Environ.* 34,1079-1087
Skelton R.P., Brodribb T.J., Choat B., 2017. Casting light on xylem vulnerability in an herbaceous species reveals a lack of segmentation. *New Phytol.* 214, 561-569.
Skelton R.P., Dawson T.E., Thompson S.E., Shen Y., Weitz A.P., Ackerly D., 2018. Low vulnerability to xylem embolism in leaves and stems of North American oaks. *Plant Physiol* 177: 1066-1077.
Stocker B.D., Zscheischler J., Keenan T.F., Prentice I.C., Seneviratne S.I., Penuelas, J., 2019. Drought impacts on terrestrial primary production underestimated by satellite monitoring. *Nat. Geosci*. 12, 264–270.
Tardieu F., Davies W.J., 1992. Stomatal response to abscisic acid is a function of current lant water status. *Plant Phys.* 98, 540-545.
Tardieu F., Cabrera-Bosquet L., Pridmore T., Bennett M., 2017. Plant phenomics, from sensors to Knowledge. *Curr. Biol.* 27, 770-783.
Tomasella M., Petrussa E., Petruzzellis F., Nardini A., Casolo V., 2020. The possible role of non-structural carbohydrates in the regulation of tree hydraulics. *Internat. Journ. Molec. Sci*. 21: 144.
Tombesi S., Nardini A., Farinelli D., Palliotti A., 2014. Relationships between stomatal behavior, xylem vulnerability to cavitation and leaf water relations in two cultivars of Vitis vinifera. *Physiol. Plant.* 152, 453–464.
Tramblay Y., Koutroulisb A., Samaniegoc L., et al., 2020. Challenges for drought assessment in the Mediterranean region under future climate scenarios. *Earth Sci. Rev.* 210, 103348.
Trifilò P., Gascò A., Raimondo F., Nardini A., Salleo S., 2003. Kinetics of recovery of leaf hydraulic conductance and vein functionality from cavitation-induced embolism in sunflower. *J. Exp. Bot.* 54, 2323-2330
Trifilò P., Raimondo F., Nardini A., Lo Gullo M.A., Salleo S., 2004. Drought resistance of Ailanthus altissima: root hydraulics and water relations. *Tree Physiol.* 24, 107-114.
Trifilò P., Nardini A., Raimondo F., Lo Gullo M.A., Salleo S., 2010. Ion-mediated compensation for drought-induced loss of xylem hydraulic conductivity in field-growing plants of Laurus nobilis. *Funct. Plant Biol*. 38, 606-613.
Trifilò, P., Nardini A., Lo Gullo M.A., Barbera P.M., Raimondo F., 2015. Diurnal changes in embolism rate in nine dry forest trees: relationship with specie-specific xylem vulnerability, hydraulic strategy and wood traits. *Tree Physiol*. 35, 694–705.
Trifilò P., Raimondo F., Savi T., Lo Gullo M.A., Nardini A., 2016. The contribution of vascular and extra-vascular water pathways to drought-induced decline of leaf hydraulic conductance. *J. Exp. Bot*. 67, 5029–5039.
Trifilò P., Kiarapostolou N., Petruzzellis F., et al., 2019. Hydraulic recovery from xylem embolism in excised branches of twelve woody species: relationships with parenchyma cells and non-structural carbohydrates. *Plant Phys. Biochem.* 139, 513-520.
Trifilò P., Petruzzellis F., Abate E., Nardini A., 2021. The extra-vascular water pathway regulates dynamic leaf hydraulic decline and recovery in Populus nigra. *Physiol. Plant*. 2021, 172, 29-40.
Trueba S., Pan R., Scoffoni C., John G.P., Davis S.D., Sack L., 2019. Thresholds for leaf damage due to dehydration: declines of hydraulic function, stomatal conductance and cellular integrity precede those for photochemistry. *New Phytol*. 223, 134–149.
Tsuda M., Tyree M.T., 2000. Plant hydraulic conductance measured by the high pressure flow meter in crop plants. *J. Exp. Bot.* 51, 823-828.
Tyree M.T., Hammel H.T., 1972. The measurement of the turgor pressure and the water relations of plants by the pressure-bomb technique. *J. Exp. Bot*. 3, 267–282.
Tyree M.T., Ewers F.W., 1991. The hydraulic architecture of trees and other woody plants. *New Phytol.* 119, 345-360
Tyree M.T., Zimmermann M.H., 2002. Conducting units: tracheids and vessels. *Xylem Struct. Ascent. Sap.* 1-25.
Tyree M.T., Nardini A., Salleo S., Sack L., El Omari B., 2005. The dependence of leaf hydraulic conductance on irradiance during HPFM measurements: any role for stomatal response? *J. Exp. Bot.* 56, 737-744
Ubran M.C., 2015. Accelerating extinction risk from climate change. *Science* 348, 571-573.

Underwood E.C., Viers J.H., Klausmeyer K.R., Cox R.L., Shaw M.R., 2009. Threats and biodiversity in the mediterranean biome. *Divers. Distrib*. 15, 188–197.

Urli M., Porte A.J., Cochard H., Guengant Y., Burlett R., Delzon S., 2013. Xylem embolism threshold for catastrophic hydraulic failure in angiosperm trees. *Tree Physiol.* 33, 672–683.

Vandeleur R.K., Sullivan W., Athman a., Jordans C., Gilliham M., Kaiser B.N., Tyerman S.D. 2014. Rapid shoot-to-root signalling regulates root hydraulic conductance via aquaporins. *Plant Cell. Envirn*. 37, 520-538.

Vescio R., Abenavoli M.R., Araniti F., Musarella C.M., Sofo A., Laface V.L.A., Spampinato G., Sorgonà A., 2021. The assessment and the within-plant variation of the morpho-physiological traits and VOCs profile in endemic and rare Salvia ceratophylloides Ard. (Lamiaceae*). Plants*, 10, 474.

Vilagrosa A., Bellot J., Gil-Pelegrin E., 2003. Cavitation, stomatal conductance, and leaf die-back in seedlings of two co-occuring Mediterranean shrubs during an intense drought. *J. Exp. Bot*. 390, 2015-2024.

Vilagrosa A., Hernández E.I., Luis V.C., Cochard H., Pausas J.G., 2014. Physiological differences explain the co-existence of different regeneration strategies in Mediterranean ecosystems. *New Phytol.* 201, 1277,1288.

Voicu M.C., Zwiazek J.J., 2011. Diurnal and seasonal changes of leaf lamina hydraulic conductance in bur oak (*Quercus macrocarpa*) and trembling aspen (*Populus tremuloides*). *Trees* 25, 485-495

Voicu M.C., Zwiazek J.J., Tyree M.T., 2008. Light response of hydraulic conductance in bur oak (*Quercus macrocarpa*) leaves. *Tree Physiol.* 28,1007-1015

Wang X., Du T., Huang J., Peng S., Xiong D., 2018. Leaf hydraulic vulnerability triggers the decline in stomatal and mesophyll conductance during drought in rice. *J. Exp. Bot.* 69, 4033–4045.

Weigelt A., Mommer L., Andraczek K., Iversen C.M., Bergmann J., Bruelheide H., et al., 2021. An integrated framework of plant form and function: The belowground perspective. *New Phytol.* (in press doi:10.1111/nph.17590).

West A.G., Dawson T.E., February E.C., Midgley G.F., Bond W.J., Aston T.L., 2012. Diverse functional responses to drought in a Mediterranean-type shrubland in South Africa*. New Phytol*. 195, 396–407.

Wright I.J., Reich P.B., Westoby M., Ackerly D.D., Baruch Z., Bongers F., et al., 2004. The worldwide leaf economics spectrum. *Nature* 428, 821-7.

Xiong D., Nadal M., 2020. Linking water relations and hydraulics with photosynthesis. *Plant J.* 101, 800–815.

Xiong D., Flexas J., Yu T., Peng S., Huang J., 2017. Leaf anatomy mediates coordination of leaf hydraulic conductance and mesophyll conductance to CO_2 in *Oryza*. *New Phytol.* 213, 572-583.

Xiong D., Douthe C., Flexas J., 2018. Differential coordination of stomatal conductance, mesophyll conductance, and leaf hydraulic conductance in response to changing light across species. *Plant Cell. Environ.* 41, 436–450.

Zhao S.L., Gupta S.C., Huggins D.R., Moncrief J.F., 2001. Tillage and nutrient source effects on surface and subsurface water quality at corn planting. *J. Environ. Qual. 30, 998-1008.*

Zimmermann M.H., Sperry J.S., 1983. Anatomy of the palm Rhapis excels, IX. Xylem structure of the leaf insertion. *J. Arnold Arboret.* 64, 599-609.

Zweifel R., Sterck F., Braun S., et al., 2021. Why trees grow at night. *New Phytol.* 231, 2174-2185.